A reaction engineering approach to homogenously catalysed glycerol hydrochlorination

Cesar Augusto de Araujo Filho

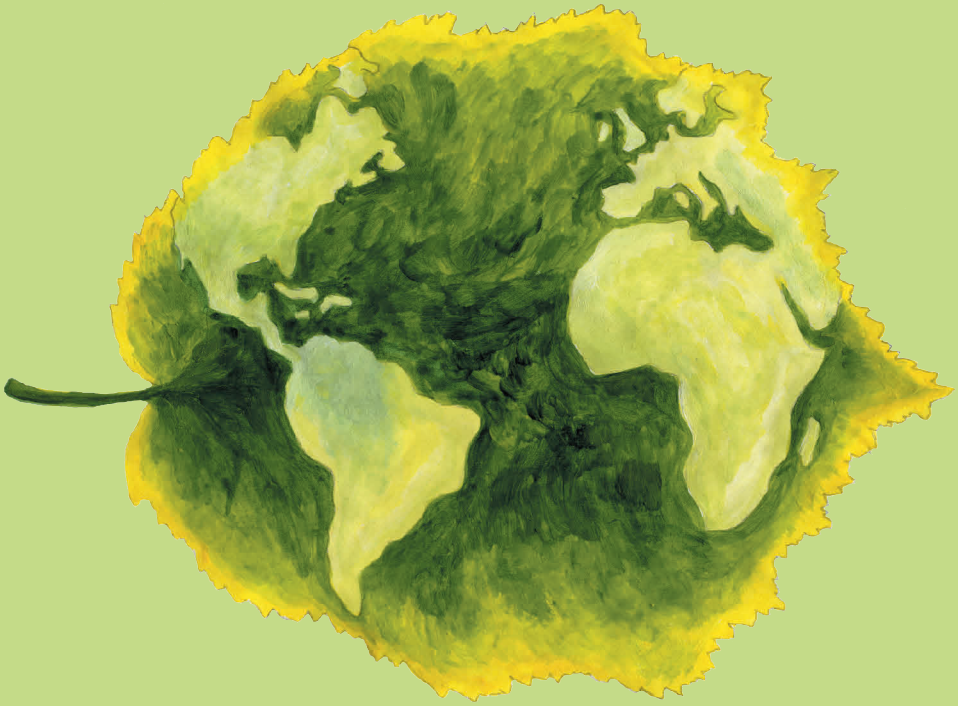

Laboratory of Industrial Chemistry and Reaction Engineering
Johan Gadolin Process Chemistry Centre
Faculty of Science and Engineering / Chemical Engineering
Åbo Akademi University
2016

Front cover art by: Olga Yu. Makeeva-Araujo

A reaction engineering approach to homogenously catalysed glycerol hydrochlorination

Cesar Augusto de Araujo Filho

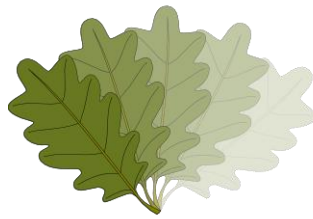

Laboratory of Industrial Chemistry and Reaction Engineering
Johan Gadolin Process Chemistry Centre
Faculty of Science and Engineering / Chemical Engineering
Åbo Akademi University
2016

Supervised by:

Professor Tapio O. Salmi
Laboratory of Industrial Chemistry and Reaction Engineering
Johan Gadolin Process Chemistry Centre
Åbo Akademi University
Åbo/Turku, Finland

and

Professor Jyri-Pekka Mikkola
Laboratory of Industrial Chemistry and Reaction Engineering
Johan Gadolin Process Chemistry Centre
Åbo Akademi University
Åbo/Turku, Finland
Technical Chemistry
Department of Chemistry
Chemical-Biological Centre
Umeå University
Sweden

Reviewers

Professor Juan García Serna
Departemento de Ingeniería Química y Tecnología del Medio Ambiente
University of Valladolid
Valladolid, Spain

and

Emeritus Professor Alírio Egídio Rodrigues
Department of Chemical Engineering
University of Porto
Porto, Portugal

Opponent

Professor Juan García Serna
Departemento de Ingeniería Química y Tecnología del Medio Ambiente
University of Valladolid
Valladolid, Spain

ISBN 978-952-12-3369-2
Painosalama Oy – Turku, Finland 2016

To my family

"'But I don't want to go among mad people', Alice remarked.
'Oh, you can't help that', said the Cat: 'we're all mad here. I'm mad. You're mad.'
'How do you know I'm mad?' said Alice.
'You must be,' said the Cat, 'or you wouldn't have come here.'"

Lewis Carrol, Alice's Adventures in Wonderland

Preface

The present work was carried out at the Laboratory of Industrial Chemistry and Reaction Engineering, Department of Chemical Engineering at Åbo Akademi University between 2012 and 2016. The research is part of the activities of the Johan Gadolin Process Chemistry Centre (PCC).

The financial support of the Graduate School of Chemical Engineering (GSCE), Academy of Finland and the Rector of Åbo Akademi is gratefully acknowledged.

I would like to express my deepest gratitude to Professor Tapio Salmi for the uncountable discussions and all the contributions he did to this work. Your everlasting energy and excitement towards work and life motivated me several times through this journey. It has been an honour to be your student. I would like to thank Professor J.-P. Mikkola for his insightful and original ideas with which he contributed to this work. Your creativity and ability to "think outside the box" really inspires me. Doctor Kari Eränen is gratefully acknowledged for his help and endless patience with experiments and analysis issues. Thanks Kari for being so kind and helpful, even when I ran at your office far too many times. I am sincerely grateful to Professor Johan Wärnå for his guidance and teaching on numerical modelling. It has been a privilege to learn and work with such a high-level scientist. I would like to express my gratitude to Professor Dmitry Yu. Murzin. Your fascinating lectures made a great impact on me; thanks for sharing your vast knowledge with such a passion and class.

Through these years, I had the opportunity to meet and work with several great people in the laboratory. I would like to thank all my colleagues for providing such a fruitful work environment. Naturally, I was able to develop a closer friendship with few people whom I dearly regard. I would like to thank Atte Aho, Ikenna Anungwon, Claudio Carletti, Stefan Haase, Alexey Kirilin, Ekaterina Korotkova, Gerson Martin, Elena Privalova, Bartosz Rozmysłowicz, Sabrina Schmidt, Olga Simakova, Martina Stekrova, Anton Tokarev and Pasi Tolvanen for the pleasure of your companies and joyful memories lived alongside.

I would like to thank my parents, Cesar and Nazinha, and my two brothers, Caio and Thiago, for all the support you gave me ever since I existed. The distance from you was always hard to deal with, but you always held me up during the hardest moments. *Obrigado por todo o amor que vocês me deram, sem ele eu não teria chegado até aqui*.

Finally, I would like to thank my wife Olga. Words cannot define how important you were for me to finish this journey. Thanks for all the love and support you gave me. You always believed in me more than I believed in myself and it is impossible to describe extension of my gratitude to you.

Åbo, March 2016
Cesar Augusto de Araujo Filho

Abstract

A reaction engineering approach to homogeneously catalysed glycerol hydrochlorination

Cesar Augusto de Araujo Filho

Doctoral Thesis, Laboratory of Industrial Chemistry and Reaction Engineering,
Johan Gadolin Process Chemistry Centre, Faculty of Science and Engineering/Chemical Engineering, Åbo Akademi, 2016.

Keywords: glycerol, hydrochlorination, reaction engineering, kinetics, gas-liquid reaction, mass transfer, solubility, semi-batch, reactive distillation, bubble column, fluid dynamics.

The production of biodiesel through transesterification has created a surplus of glycerol on the international market. In few years, glycerol has become an inexpensive and abundant raw material, subject to numerous plausible valorisation strategies. Glycerol hydrochlorination stands out as an economically attractive alternative to the production of biobased epichlorohydrin, an important raw material for the manufacturing of epoxy resins and plasticizers.

Glycerol hydrochlorination using gaseous hydrogen chloride (HCl) was studied from a reaction engineering viewpoint. Firstly, a more general and rigorous kinetic model was derived based on a consistent reaction mechanism proposed in the literature. The model was validated with experimental data reported in the literature as well as with new data of our own.

Semi-batch experiments were conducted in which the influence of the stirring speed, HCl partial pressure, catalyst concentration and temperature were thoroughly analysed and discussed. Acetic acid was used as a homogeneous catalyst for the experiments. For the first time, it was demonstrated that the liquid-phase volume undergoes a significant increase due to the accumulation of HCl in the liquid phase. Novel and relevant features concerning hydrochlorination kinetics, HCl solubility and mass transfer were investigated. An extended reaction mechanism was proposed and a new kinetic model was derived. The model was tested with the experimental data by means of regression analysis, in which kinetic and mass transfer parameters were successfully estimated. A dimensionless number, called Catalyst Modulus, was proposed as a tool for corroborating the kinetic model.

Reactive flash distillation experiments were conducted to check the commonly accepted hypothesis that removal of water should enhance the glycerol hydrochlorination kinetics. The performance of the reactive flash distillation experiments were compared to the semi-batch data previously obtained. An unforeseen effect was observed once the water was let to be stripped out from the liquid phase, exposing a strong correlation between the HCl liquid uptake and the presence of water in the system. Water has revealed to play an important role also in the HCl dissociation: as water was removed, the dissociation of HCl was diminished, which had a retarding effect on the reaction kinetics. In order to obtain a further insight on the influence of water on the hydrochlorination reaction, extra semi-batch

experiments were conducted in which initial amounts of water and the desired product were added. This study revealed the possibility to use the desired product as an ideal “solvent” for the glycerol hydrochlorination process.

A co-current bubble column was used to investigate the glycerol hydrochlorination process under continuous operation. The influence of liquid flow rate, gas flow rate, temperature and catalyst concentration on the glycerol conversion and product distribution was studied. The fluid dynamics of the system showed a remarkable behaviour, which was carefully investigated and described. High-speed camera images and residence time distribution experiments were conducted to collect relevant information about the flow conditions inside the tube. A model based on the axial dispersion concept was proposed and confronted with the experimental data. The kinetic and solubility parameters estimated from the semi-batch experiments were successfully used in the description of mass transfer and fluid dynamics of the bubble column reactor.

In light of the results brought by the present work, the glycerol hydrochlorination reaction mechanism has been finally clarified. It has been demonstrated that the reactive distillation technology may cause drawbacks to the glycerol hydrochlorination reaction rate under certain conditions. Furthermore, continuous reactor technology showed a high selectivity towards monochlorohydrins, whilst semi-batch technology was demonstrated to be more efficient towards the production of dichlorohydrins. Based on the novel and revealing discoveries brought by the present work, many insightful suggestions are made towards the improvement of the production of αγ-dichlorohydrin on an industrial scale.

Referat

Reaktionstekniskt studium av homogent katalyserad hydroklorering av glycerol

Cesar Augusto de Araujo Filho

Doktorsavhandling, Laboratoriet för teknisk kemi och reaktionsteknik,
Johan Gadolin Processkemiska Centret, Fakulteten för naturvetenskaper och teknik /Kemiteknik,
Åbo Akademi, 2016.

Nyckelord: glycerol, hydroklorering, reaktionsteknik, kinetik, gas-vätskereaktion, massöverföring, löslighet, halvkontinuerlig reaktor, reaktiv destillation, bubbelkolonn, fluidmekanik.

Framställning av biodiesel via transesterifiering av fettsyraestrar ger ett överskott av glycerol på den internationella marknaden. Under de senaste åren har glycerol blivit en förmånlig och lättillgänglig råvara, som kan förädlas med många strategier. Hydroklorering av glycerol är ett ekonomiskt attraktivt alternativ för framställning av biobaserad epiklorhydrin, som är utgångsämnet för produktion av epoxihartser och mjukgörare.

Hydroklorering av glycerol med gasformigt klorväte (HCl) studerades ur en reaktionsteknisk synvinkel. En allmännare och mera rigorös kinetisk modell utvecklades på basis av en konsistent reaktionsmekanism som tidigare föreslagits i litteraturen. Modellen verifierades med experimentella data från litteraturen samt egna reaktionskinetiska data.

Experiment genomfördes i en halvkontinuerlig reaktor, där effekten av omrörarhastigheten, partialtrycket av HCl, katalysatorkoncentrationen och temperaturen analyserades och diskuterades grundligt. Ättiksyra användes som homogen katalysator för experimenten. För första gången demonstrerades att vätskefasens volym signifikant ökar p.g.a. ackumulering av HCl i vätskefasen. Nya och relevanta fenomen i hydrokloreringens kinetik, löslighet av HCl och massöverföring undersöktes. En utvidgad reaktionsmekanism föreslogs och en ny kinetisk modell utvecklades. Modellen testades med experimentella data med hjälp av icke-linjär regressionsanalys, varvid kinetiska och massöverföringsparametrar framgångsrikt kunde estimeras. Ett dimensionslöst tal, katalysatormodul föreslogs som verktyg för bekräfta den kinetiska modellen.

Reaktiva flashdestillationsexperiment genomfördes för att kontrollera den hittills allmänt accepterade hypotesen om att avlägsnandet av vatten skulle påskynda hydroklorerings-kinetiken av glycerol. Prestandan av reaktiva flashdestillationsexperiment jämfördes med tidigare data från halvkontinuerliga experiment. En överraskande effekt observerades då vattnet förångades ur vätskefasen; en stark korrelation mellan lagringen av HCl och vattenkoncentrationen i vätskefasen bekräftades. Det visade sig att vatten även spelar en viktig roll i dissociationen av HCl: då vattnet avlägsnades, minskade dissociationen av HCl, vilket hade en bromsande effekt på reaktionskinetiken.

För att få en djupare insikt i vattnets inverkan på hydrokloreringsprocessen utfördes ytterligare halvkontinuerliga experiment, i vilka varierande begynnelsemängder av vatten och den önskade produkten αγ–diklorhydrin tillsattes. Denna undersökning avslöjade möjligheten att använda den önskade produkten som ett idealt lösningsmedel för hydroklorering av glycerol.

En bubbelkolonnreaktor som arbetade enligt medströmsprincipen användes för att undersöka hydroklorering av glycerol i kontinuerlig drift. Inverkan av vätskans strömningshastighet, temperatur och katalysatorkoncentration på omsättningen av glycerol och produkt-fördelningen studerades. Systemets fluidmekanik visade ett synnerligen intressant beteende, som studerades noggrant och beskrevs kvalitativt och kvantitativt. Bilder togs med en höghastighetskamera och uppehållstidsfördelningar studerades experimentellt för att samla relevant information om strömningsbetingelserna i kolonnreaktorn. En modell baserad på den axiella dispersionens princip utvecklades och jämfördes med experimentella data. De kinetiska och gaslöslighetsparametrar som hade estimerats utgående från halvkontinuerliga experiment användes med framgång för att beskriva massöverföringen och strömnings-betingelserna i bubbelkolonnreaktorn.

På basis av resultaten av detta arbete kunde reaktionsmekanismen för hydroklorering av glycerol äntligen klargöras. Det blev demonstrerat att reaktiv destillationsteknologi möjligen försämrar hydrokloreringens hastighet under vissa betingelser. Den kontinuerliga reaktorteknologin gav en hög selektivitet för monoklorhydriner, medan den halvkontinuerliga teknologin visade sig vara effektivare för framställning av diklorhydriner. På basis av de nya och avslöjande iakttagelser som gjordes i detta arbete, kunde flera förslag presenteras med tanke på förbättrad produktion av αγ – diklorhydrin i industriell skala.

Resumo

Uma abordagem de engenharia de reações sobre a hidrocloração do glicerol homogeneamente catalisada

César Augusto de Araújo Filho

Tese de doutorado, Laboratório de Química Industrial e Engenharia de Reações.
Centro de Processos Químicos Johan Gadolin, Faculdade de Ciências e Engenharia/Engenharia Química, Universidade Åbo Akademi, 2016.

Palavras-chave: glicerol, hidrocloração, engenharia de reações, cinética, reações gás-liquido, transferência de massa, solubilidade, semi-batelada, destilação reativa, coluna de bolhas, fluido dinâmica.

A produção de biodiesel por meio da transesterificação de ácidos graxos gerou um excedente de glicerol no mercado internacional. Em alguns anos, o glicerol tornou-se matéria-prima economicamente acessível e abundante, sujeito à inúmeras estratégias de valorização. A hidrocloração do glicerol se destaca como uma alternativa economicamente atrativa para produção de epicloridrina derivada de biomassa, matéria-prima importante para a manufatura de resinas epóxi e plastificantes.

A hidrocloração do glicerol utilizando cloreto de hidrogênio (HCl) gasoso foi investigada a partir de uma perspectiva da engenharia de reações. Pela primeira vez, um modelo cinético geral e rigoroso foi deduzido, baseado em consistente mecanismo de reação proposto na literatura. O modelo foi validado com dados experimentais disponíveis na literatura bem como dados obtidos pelo nosso grupo de pesquisa.

Realizaram-se experimentos em reator semi-batelada, nos quais a influência da velocidade de agitação, pressão parcial de HCl, concentração de catalisador e temperatura foram amplamente analisados e discutidos. Utilizou-se ácido acético como catalisador homogêneo em todos os experimentos. Pela primeira vez, demonstrou-se aumento significativo do volume da fase líquida devido ao acúmulo de HCl. Novas e relevantes características relacionadas à cinética de hidrocloração, solubilidade do HCl e transferência de massa foram investigadas. Um mecanismo de reação estendido foi proposto e um novo modelo cinético deduzido. Testou-se referido modelo com dados experimentais por meio de regressão não-linear, na qual se estimou, com sucesso, parâmetros cinéticos e de transferência de massa. Um número adimensional, chamado Módulo do Catalisador, foi proposto como ferramenta para corroborar o modelo cinético.

Experimentos em reator de destilação reativa *flash* foram feitos de modo a verificar a hipótese comumente aceita, na qual a retirada de água do sistema deve promover a cinética de hidrocloração do glicerol. A performance do reator de destilação reativa *flash* foi comparada aos dados obtidos

previamente no sistema semi-batelada. Observou-se efeito inesperado, uma vez que se permitiu que a remoção da água da fase liquida, expondo forte correlação entre o acúmulo de HCl e a presença de água no sistema. Revelou-se importante papel desempenhado pela água na dissociação de HCl: à medida que a água era removida, a dissociação de HCl diminuía, o que provocava efeito retardatário na cinética de reação. Visando ampliar conhecimentos sobre a influência da água no processo de hidrocloração, uma série extra de experimentos semi-batelada foram feitos, nos quais se adicionou várias quantidades iniciais de água e do produto desejado. Tal estudo revelou a possibilidade do uso de produto desejado αγ-dicloridrina como "solvente" ideal no processo de hidrocloração do glicerol.

Para investigar o processo de hidrocloração de glicerol de modo contínuo, utilizou-se uma coluna de bolhas operada de forma concorrente. A influência da vazão de liquido, vazão de gás, temperatura e concentração de catalisador na conversão de glicerol e na formação dos produtos foi analisada. A fluido dinâmica do sistema apresentou comportamento notável, o qual foi investigado e descrito cuidadosamente. Imagens obtidas por meio de câmera de alta velocidade e experimentos de distribuição de tempo de residência foram feitos de modo a coletar informações relevantes sobre as condições de fluxo dentro do reator. Um modelo baseado no conceito de dispersão axial foi desenvolvido e testado com dados experimentais. Os parâmetros cinéticos e de solubilidade, estimados com base nos dados obtidos no reator semi-batelada, foram usados com sucesso na descrição da transferência de massa e fluido dinâmica do reator de coluna de bolhas.

Sob a luz dos resultados da presente tese, o mecanismo da reação de hidrocloração do glicerol foi clarificado. Demonstrou-se que a destilação reativa pode comprometer a taxa de hidrocloração do glicerol sob certas condições. Ademais, a tecnologia de reatores contínuos testada constatou alta seletividade com relação à monocloridrinas, enquanto a tecnologia semi-batelada demonstrou maior eficiência na produção de dicloridrinas. Baseado nas novas e reveladoras descobertas contidas na presente tese, diversas sugestões perspicazes são feitas no sentido de aperfeiçoar a produção de αγ-dicloridrina em escala industrial.

List of Publications

I. **C. A. de Araujo Filho**, T. Salmi, A. Bernas and J.-P. Mikkola, "Kinetic model for homogeneously catalysed halogenation of glycerol," *Industrial & Engineering Chemistry Research,* vol. 52, no. 4, pp. 1523-1530, 2013.

II. **C. A. de Araujo Filho**, K. Eränen, J.-P. Mikkola and T. Salmi, "A comprehensive study on the kinetics, mass transfer and reaction engineering aspects of solvent-free glycerol hydrochlorination," *Chemical Engineering Science,* vol. 120, pp. 88-104, 2014.

III. **C. A. de Araujo Filho**, K. Eränen, J.-P. Mikkola and T. Salmi. "A comparative study of reactive flash distillation vs. semi-batch reactor technologies for the glycerol hydrochlorination with gaseous HCl", accepted, *Industrial & Engineering Chemistry Research,* 2016.

IV. **C. A. de Araujo Filho**, J. Wärnå, D. Mondal, S. Haase, K. Eränen, J.-P. Mikkola and T. Salmi, "Dynamic modelling of homogeneously catalysed glycerol hydrochlorination in bubble column reactor", accepted*, Chemical Engineering Science,* 2016.

Author's contribution to articles I-IV

I. Cesar de Araujo Filho carried out the modelling work and wrote the article.

II-IV Cesar de Araujo Filho conducted the experiments, carried out the modelling work and wrote the article.

Other publications related to the topic

I. **C. A. de Araujo Filho**, T. Salmi, A. Bernas, J.-P. Mikkola. Fine chemicals from glycerol: modelling of homogeneously catalysed halogenation. 20th International Congress of Chemical and Process Engineering, Prague, Czech Republic, August 2012. *Oral Presentation.*

II. **C. A. de Araujo Filho**, J.-P. Mikkola, T. Salmi. Valorisation of biodiesel by-product: Chlorination of glycerol for production of epichlorohydrin. 9th European Congress on Chemical Engineering, The Hague, Netherlands, April 2013. *Poster presentation.*

III. **C. A. de Araujo Filho**, J.-P. Mikkola, T. Salmi. Solvent-free synthesis of dichlorohydrins from glycerol: kinetic modelling of a new reaction mechanism. 10th Congress of Catalysis Applied to Fine Chemicals, Turku, Finland, June 2013. *Poster presentation.*

IV. **C. A. de Araujo Filho**, J.-P. Mikkola, T. Salmi. Glycerol upgrading: Kinetic study of the production of value-added dichlorohydrins from biodiesel waste. 4th International Workshop Cost Action, Valence, Spain, September 2013. *Poster presentation.*

V. **C. A. de Araujo Filho**, T. Salmi, J.-P. Mikkola. Modelling of reaction kinetics and mass transfer of solvent-free hydrochlorination of glycerol. 4th International Congress on Green Process Engineering, Sevilla, Spain. April 2014. *Oral Presentation.*

VI. **C. A. de Araujo Filho**, T. Salmi, J.-P. Mikkola. Comparison of reactor designs on the mass transfer and kinetics of glycerol hydrochlorination. European Symposium on Chemical Reaction Engineering, Munich, Germany. October 2015. *Oral Presentation.*

Table of Contents

1. Introduction

1.1. Glycerol availability and applications

During the past fifteen years, the scientific community has turned its attention to the development of more sustainable and environmentally friendly technologies, focusing on the use of biomass and waste as alternative energy sources to fossil fuels [1]. In this sense, the transesterification reaction has been extensively applied as a route to produce diesel-like fuel from vegetable oils, animal fats and bio waste raw materials [2] (Figure 1.1).

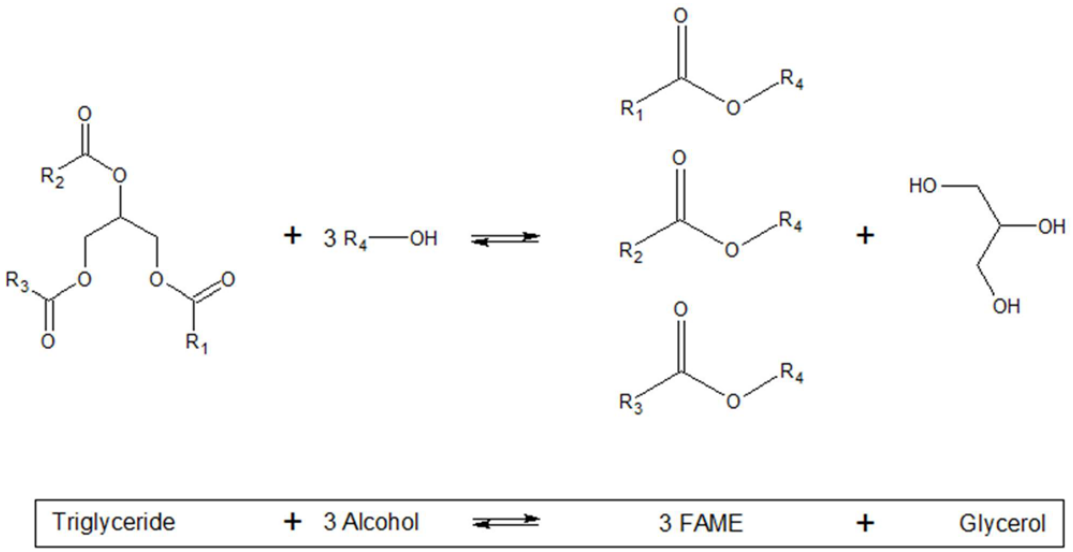

Figure 1.1. Transesterification reaction of triglyceride with alcohol producing Fatty Acid Methyl Esters (FAME, biodiesel) and glycerol. R_1, R_2, R_3 and R_4 represent alkyl groups.

Glycerol is a by-product of the transesterification reaction, constituting approximately 10% in weight of the crude biodiesel produced nowadays [3, 4]. For this reason, the global market supply of glycerol has become rather saturated, causing companies, such as Dow and Procter and Gambler, to shut down their glycerol production units [5]. On the other hand, the glycerol originating from biomass is of low-quality and requires expensive purification techniques to be used in the production of pharmaceuticals, cosmetics and alimentary [6], as these were the niche applications in the past [7, 8] (Figure 1.2).

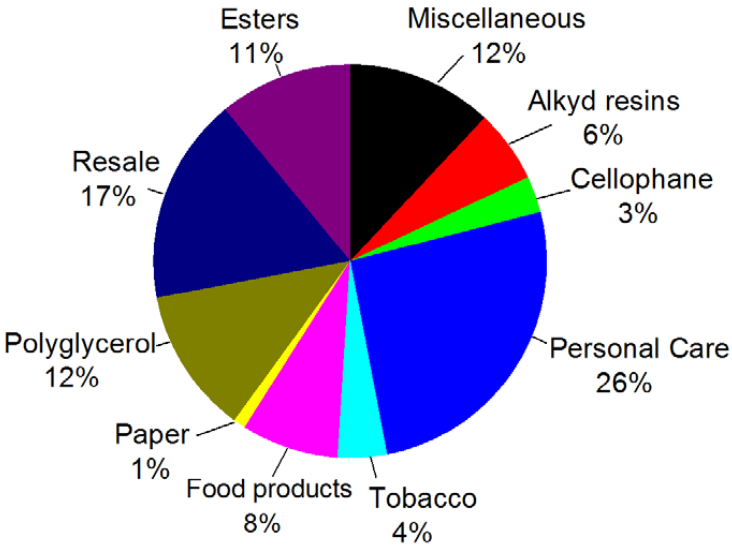

Figure 1.2. Glycerol market in 1995 [6].

With the start-up of many biodiesel production plants worldwide, a common practice has been to burn the crude glycerol on-site, to provide energy for the production units [9, 10]. However, this process suffers many disadvantages related to the low energy density of glycerol, high viscosity and high auto-ignition temperatures [9].

Recently, a paper published by Tuck and co-workers in *Science* [11] provided an interesting discussion of the use of biomass "waste", such as glycerol and bagasse, as raw material for the production of value-added chemicals; they compared the economic aspects of glycerol conversion to epichlorohydrin with its conversion to transportation fuel and electricity. As it turned out, the conversion to fine chemicals may be up to 10-fold more economically attractive than burning and 3-fold more than the conversion to biofuel. Such an analysis concluded that glycerol has a high potential to become a platform chemical of the future, once a bio-based focused economy is mature. Indeed, several research groups around the world have been studying different glycerol upgrading alternatives [7, 8, 12] (Figure 1.3). Among the main reactions investigated, there is the production of light olefins from glycerol [13], particularly towards acrolein [14], aiming to obtain bio-based plastics, chemical intermediates and organic solvents. The production of ethers from glycerol has attracted significant attention due to its excellent properties as gasoline and diesel fuel additives [15]. Glycerol carbonate can be produced with high yields by lipase catalysed reaction of renewable glycerol with dimethyl carbonate; glycerol carbonate is a high value-added intermediate, which can be used for the production glycidol and polyglycerol [12, 16]. Steam reforming and aqueous-phase reforming have been investigated as a way to produce hydrogen and syngas from glycerol [17, 18, 19, 20]. The production of high added-value metabolites from glycerol algae fermentation has recently attracted the attention of several biotechnology research groups due to its potential large-scale applicability in producing chemicals, biopolymers and pigments [21, 22]. In addition, the production of propylene glycol [23, 24], and 1,3-propanediol [25, 26] from glycerol have also been revisited, once the market availability of glycerol had increased exponentially.

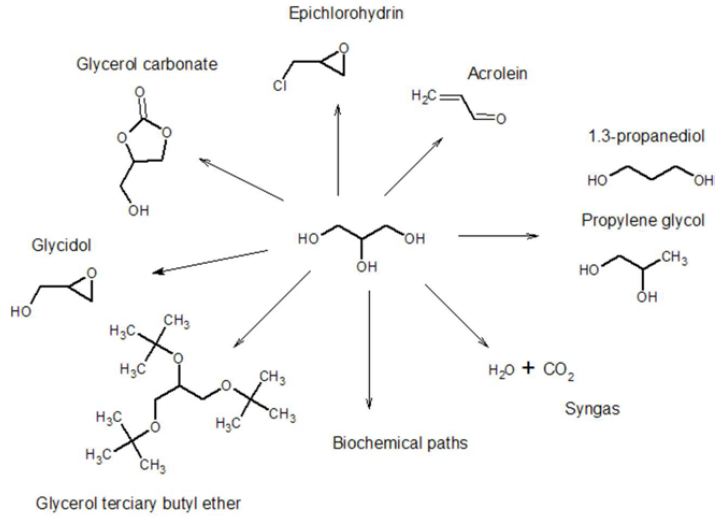

Figure 1.3. Possible glycerol conversion pathways.

Our research aims to investigate the glycerol hydrochlorination to produce dichlorohydrins, as this is the first step for the production of bio-based epichlorohydrin [27] (Figure 1.4), an important building block for the production of epoxy resins and plasticizers [28, 29, 30]. The Asian-Pacific region constitutes the largestarket for epichlorohydrin and it concentrates the main industrial production plants in the world. Solvay has commissioned the construction of an epichlorohydrin plant based on renewable glycerol with capacity of 100,000 ton/year in Thailand [11]. In addition, Solvay, Dow Chemicals and COSER have operating plants in China, using the bio-based epichlorohydrin concept [30].

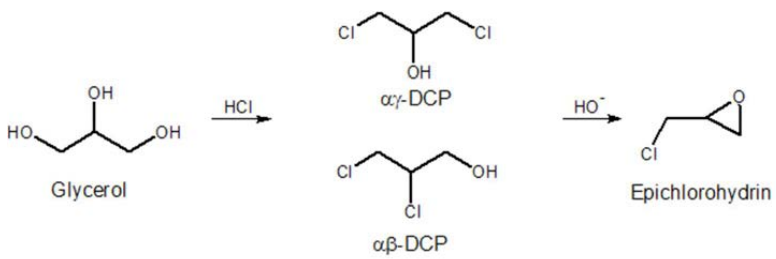

Figure 1.4. Reaction steps involved in the production of epichlorohydrin from glycerol.

The classic reaction route for the 1-chloro-2,3-epoxypropane (epichlorohydrin) synthesis consists of the halogenation of propylene using allyl chloride, yielding a mixture of ca. 70% of 1,2-dichloro-2-propanol (αβ-DCP) and 30% of 1,3-dichloro-2-propanol (αγ-DCP) [31]. However, this process has a number of serious drawbacks, such as low atom-efficiency [32], expensive raw material and waste treatment. Furthermore, the product composition is not favourable for carrying out the next reaction step, which involves the dehydrochlorination with an inorganic Brønsted base [33]; the main product, i.e. αβ-DCP, is ten times less reactive than αγ-DCP to give epichlorohydrin [27, 34].

On the other hand, glycerol hydrochlorination using HCl is able to produce very high yields of αγ-DCP, with a selectivity which is mainly steered by the reaction time [35, 36, 37].

Even though the first reports of the glycerol hydrochlorination reaction date back to the 1930's and 40's [38, 39, 40, 41], its relevance remained hindered due to the elevated price of glycerol. It was only after the biodiesel production boom caused the surplus of glycerol in the international market, that many research groups have begun revisiting this exciting area [30].

1.2. Glycerol hydrochlorination: a brief literature review

Glycerol hydrochlorination is a parallel-consecutive reaction (see Figure 1.5), usually carried out in the presence of low molecular weight organic acid catalysts, e.g. acetic, propionic and malonic acids, in the temperature range of 70-120ºC. The HCl can be introduced in the system either in gaseous form or as an aqueous solution of hydrochloric acid [30]. It is experimentally observed that, the first chlorination can take place in either of the OH positions, however, the second chlorination can only proceed via the 3-chloro-1,2-propanediol (α-MCP) compound. One molecule of water is produced for each chlorine atom added.

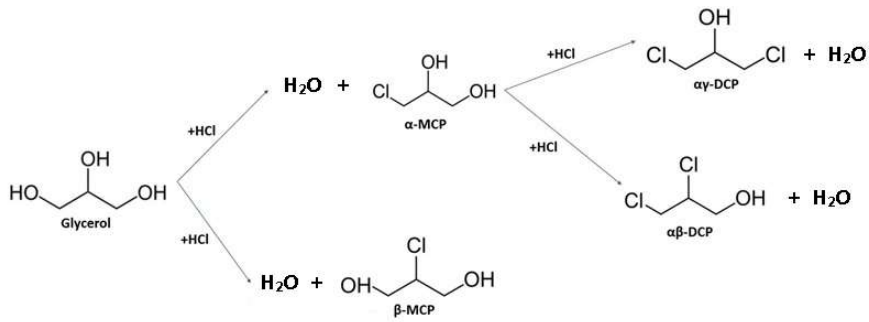

Figure 1.5. Overview of the glycerol hydrochlorination process: reactants and products.

Tesser et al. (2007) [35], Santacesaria et al. (2010) [29] and Vitiello et al. [42] (2014) have performed an extensive homogeneous catalyst screening, analysing the yields and selectivities of twenty-seven organic acids for the glycerol hydrochlorination using gaseous HCl. No correlation was observed between the catalyst pKa values and its selectivity and activity, as confirmed by the detailed study of Tesser et al. (2011) [43] .

Lee et al. (2008a) [44] screened heterogeneous catalysts for glycerol hydrochlorination, by analysing the yields and selectivities using heteropolyacids as catalyst and aqueous solutions of hydrochloric acid as chlorinating agent. The hydrochlorination reaction was much slower and the yields and selectivities reported were considerably lower than those obtained by the use of simple organic acids. In addition, no heterogeneous reaction mechanism was proposed.

A literature study revealed that, in recent years, four reaction mechanisms were proposed for explaining the glycerol hydrochlorination using an organic acid as catalyst. Bell et al. (2008) [28] suggested a reaction mechanism which involves an esterification reaction between glycerol and the organic acid, followed by the formation of an acetoxonium cation and further chlorination; even though this explains the regioselectivity of the chlorination, the formation of the acetoxonium cation is highly unlikely to occur (curiously, the proposed mechanism was based on literature sources dating to the year of 1862 [45]). No kinetic model was provided to verify the validity of such mechanism. Luo et al. (2009) [46] proposed a simple mechanism based on the esterification of glycerol and the organic acid followed by the chlorination step; surprisingly, there is no mention at all about the formation of the 2-chloro-1,3-propanediol (β-MCP), and therefore, the mechanism is clearly incomplete and does not correspond to the full reality. In the following year, Luo et al. (2010) [47] proposed a new reaction mechanism in which the formation of β-MCP is taken into account, however, it assumes that β-MCP reacts further to form αβ-DCP; this contradicts the experimental observations that β-MCP remains unreacted and does not consider the steric effects present in the molecule, once again, their model did not correspond to reality. Tesser et al. (2007) [35] have proposed the most consistent and reliable mechanism available in the literature at that point. The mechanism of Tesser et al. (2007) [35] involves the esterification of glycerol with the organic acid catalyst, followed by the formation of an epoxide ring cation and the final hydrochlorination steps. The mechanism explains the regioselectivity of the chlorine addition, why β-MCP did not react further and the absence of a tri-chlorinated product. A kinetic model was derived based on the assumption of a rate-determining step and a good fit of the experimental data was achieved. It is important to remind that, none of the proposed reaction mechanisms in the literature took into account the non-catalytic hydrochlorination experimentally observed by Lee et al. (2008b) [48] and Dmitriev and Zanaveskin (2011) [49].

A common agreement among many literature sources is that the presence of water exerts a negative effect on glycerol hydrochlorination. This effect was first reported by Britton and Heindel (1940) [39, 50], who were convinced that glycerol hydrochlorination was a reversible reaction. Their statement was later on refuted by Gerrard (1976) [51] and Tesser et al. (2007) [35] who have explained that, although the hydrochlorination of alcohols has intermediate steps, the addition of the chlorine group is, in practice, irreversible. Furthermore, Dmitriev and Zanaveskin (2011) [49] have also observed the negative effect of water on the hydrochlorination kinetics when studying glycerol hydrochlorination with hydrochloric acid solutions and acetic acid as the catalyst; their explanation for such a phenomenon was attributed to solvation issues involving water and organic molecules. Hughes and Ingold [52, 53] studied the influence of solvent polarity on elimination and substitution reactions; they have found that, for reactions that depend upon the interaction of ions of different charges, an increase in solvent polarity causes a decrease in the reaction rate. Following the mechanism proposed by Tesser et al. [35], glycerol hydrochlorination fits precisely to this description. Therefore, the solvent polarity is also a plausible explanation for the lower hydrochlorination kinetics in the presence of aqueous solutions. Lee et al. (2008b) [48] reports that the use of silica gel beads improved the yields and selectivity of the glycerol hydrochlorination; such effect was assumed to be caused by the water absorption into the silica, which enhanced the observed reaction rate. Finally, Santacesaria et al. [30] presented a comparative study of the kinetic constants estimated both using HCl gas and hydrochloric acid solutions, in the presence of acetic acid as the catalyst; it was concluded that the activation energies reported for HCl solutions were higher than for the case in

which gaseous HCl was used. Few authors [29, 35, 36] were convinced that the removal of water would enhance the glycerol hydrochlorination kinetics, in a similar way as the removal of water enhances the rate of esterification reactions [54, 55]; however, this assumption was not confirmed by experimental data.

The literature concerning glycerol hydrochlorination was lacking a unified investigation of the effects of temperature, catalyst concentration and partial pressure on the reaction kinetics. Furthermore, a continuous reactor for glycerol hydrochlorination has not been fully investigated, even though this class of apparatus would be highly interesting for industrial applications due to its higher throughput capacity.

1.3. Goal and scope of the research

The approach of our research was to study the glycerol hydrochlorination process from a more detailed and rigorous viewpoint than those given by the existing literature, focusing on the reaction engineering aspects. The final goal is to provide an answer to the question: which reactor technology should be used for glycerol hydrochlorination? Semi-batch, reactive distillation and continuous technologies were investigated.

Initially, our research focused on the development of a more generalized approach to the kinetic model of glycerol hydrochlorination, based on the reaction mechanism proposed by Tesser et al. (2007) [35]. The derived model was confronted with the experimental results reported in [35] and with data of our own in **Publication I**. It represented a more formal and rigorous approach for the interpretation of the reaction mechanism. This kinetic model constituted the backbone for the development of a more complete one presented in **Publication II**. A semi-batch study of the glycerol hydrochlorination was carried out in **Publication II** to evaluate the influence of temperature, catalyst concentration and HCl partial pressure on the reaction kinetics and the liquid-phase uptake of HCl. It was found that the liquid-phase volume increased significantly along the reaction time and that the non-catalytic reaction pathway was very prominent at elevated temperatures. The kinetic model proposed in **Publication I** was modified in order to account for the non-catalytic reaction and new kinetic equations were derived. A more rigorous description of the mass balances was done, taking into account the HCl mass transfer, the effect of temperature and partial pressure on the HCl solubility and the liquid-phase volume increase. Kinetic, solubility and mass transfer parameters were estimated by regression analysis and the experimental data were described by the model in an excellent manner.

In order to validate the hypothesis that water removal would enhance the glycerol hydrochlorination reaction, experiments under reactive flash distillation conditions were performed and reported in **Publication III**. The idea was to compare the results obtained with the semi-batch data reported in **Publication II**. It was noticed that the stripping of water from the reaction mixture caused the HCl concentration in the liquid-phase to decrease, for it was observed that the HCl liquid uptake is very dependent on the water concentration. The experiments provided clear evidence that changes in the water composition could compromise the reaction rate. For this reason, additional experiments were

conducted with the intention to get further insight on the influence of the initial liquid-phase composition on the product distribution and the HCl uptake. The investigation provided evidence that the desired product, i.e. αγ-DCP, may serve as a great "solvent" for the hydrochlorination reaction, improving considerably the glycerol conversion to hydrochlorinated products.

Finally, to evaluate the performance of a continuous tubular reactor for the solvent-free glycerol hydrochlorination, experiments were conducted in a continuous bubble column operated co-currently. The results are reported in **Publication IV**. The effect of the liquid flow rate, gas flow rate, temperature and catalyst concentration were evaluated and compared to the semi-batch results reported in **Publication II**. Residence time distribution (RTD) experiments and high-speed camera images were used to characterize the flow inside the reactor. The kinetic and solubility parameters estimated in the semi-batch experiments were used for modelling the fluid dynamics and mass transfer phenomena happening during the transient conditions. The axial dispersion model was successfully applied to describe the flow inside the tube over a wide range of operating conditions.

The different reactor technologies used were crucial for revealing important aspects of the glycerol hydrochlorination, providing relevant insights on the kinetics and mass transfer phenomena happening in the process. Figure 1.6 summarizes the most relevant aspects investigated by each reactor technology used in this research.

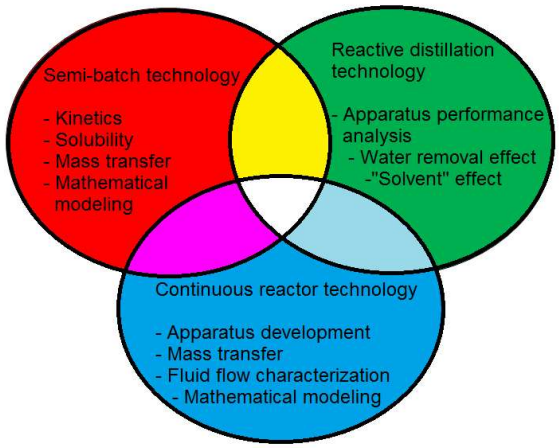

Figure 1.6. Overview of the reactor technologies used and the most relevant aspects investigated by each one.

2. Kinetic model – the primary approach

Examining the literature which provides mechanisms and kinetic models for the homogeneously catalysed glycerol hydrochlorination, the famous group of Professor Santacesaria from University of Naples stood out as proposing the most consistent reaction mechanism. They suggest [35] that an esterification step, followed by the formation of an epoxide intermediate are the key elements in the reaction mechanism. However, their approach to the kinetic model was focused mainly on the assumption of a rate-determining step. At this point, we aimed to re-interpret their reaction mechanism by applying the quasi-steady state hypothesis to the reaction intermediates, expanding the treatment of the kinetic equations to more general cases [56, 57].

2.1. Reaction mechanism for glycerol hydrochlorination

Figure 2.1 depicts the reaction mechanism for the homogeneously catalysed glycerol hydrochlorination using a mild organic acid as catalyst proposed in ref. [35].

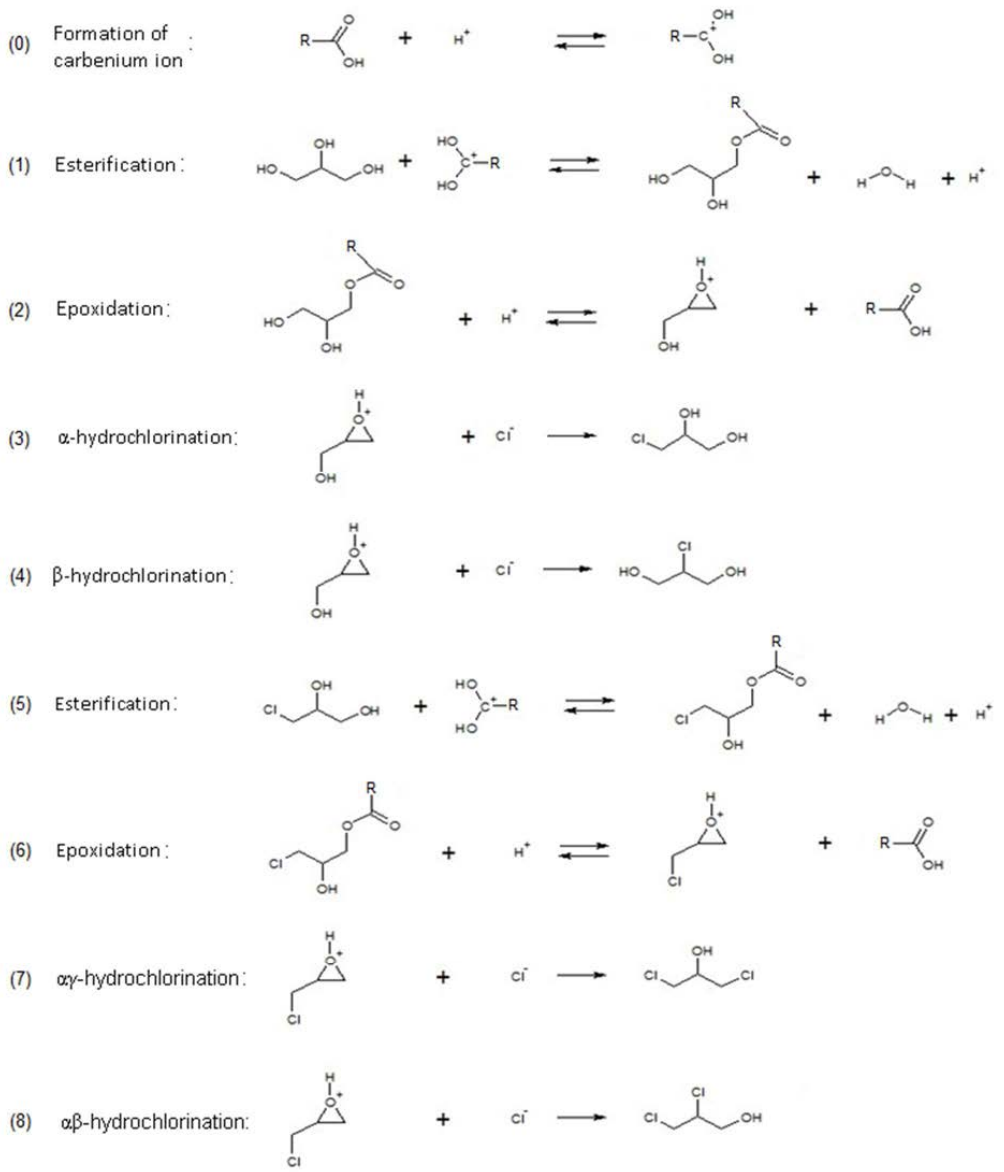

Figure 2.1. Mechanism of the homogeneously catalysed glycerol hydrochlorination.

In step (0), it is assumed that the catalyst (cat) is protonated by the H^+ originating from HCl. Such equilibrium is considered to be stablished in the first moments of the reaction; therefore this step is considered to be in quasi-equilibrium. Step (1) corresponds to esterification, producing water (W) and the ester intermediate E_1. The following step (2) implies the formation of an epoxide ring (I_1^+) which is chlorinated in steps (3) and (4). The nucleophilic addition of chlorine to the epoxide intermediate (I_1^+) should preferably take place in the least substituted carbon [58], reason why α-MCP is produced in much larger quantities than β-MCP. The production of αγ and αβ-DCP follows the same logic as explained in steps (1)-(4). Actually, it can be noticed that step (1) is analogous to step

(5), step (2) to step (6), step (3) to step (7) and step (4) to step (8). β-MCP is unable to form an epoxide ring, as depicted in steps (2) and (6), because it does not have two vicinal OH groups to do so. This is the reason why it is observed that β-monochlorohydrin remains unreacted throughout the hydrochlorination process.

In order to facilitate the derivation of the kinetic equations, the reaction mechanism depicted in Figure 2.1 is presented in the form of four different reaction routes, as illustrated in Figure 2.2.

Step and step number		*Stoichiometric numbers* (N) *of reaction routes* $1-4$			
		N_1	N_2	N_3	N_4
$cat + H^+ = catH^+$	(0)	1	1	1	1
$A + catH^+ = E_1 + W + H^+$	(1)	1	1	0	0
$E_1 + H^+ = I_1^+ + cat$	(2)	1	1	0	0
$I_1^+ + Cl^- \rightarrow \alpha$	(3)	1	0	0	0
$I_1^+ + Cl^- \rightarrow \beta$	(4)	0	1	0	0
$\alpha + catH^+ = E_1 + W + H^+$	(5)	0	0	1	1
$E_2 + H^+ = I_2^+ + cat$	(6)	0	0	1	1
$I_2^+ + Cl^- \rightarrow \alpha\gamma$	(7)	0	0	0	0
$I_2^+ + Cl^- \rightarrow \alpha\beta$	(8)	0	0	1	1

Overall reactions:

$N_1: A + H^+Cl^- \rightarrow \alpha + W$

$N_2: A + H^+Cl^- \rightarrow \beta + W$

$N_3: \alpha + H^+Cl^- \rightarrow \alpha\gamma + W$

$N_4: \alpha + H^+Cl^- \rightarrow \alpha\beta + W$

Figure 2.2. Illustration of the 4 different catalytic routes for the catalytic glycerol hydrochlorination

It is important to emphasize that, at this point, all treatment given to the reaction mechanism and kinetic model is mostly based on the information available in the literature, therefore only catalytic routes for the glycerol hydrochlorination are hereby treated. In Chapter 3, it is discussed that a parallel non-catalytic reaction pathway was evidenced in our semi-batch experiments. This important observation leads to an addition of an extra reaction step to the mechanism depicted in Figure 2.1.

The reaction mechanism is able to explain the experimental observation that water exerts a retarding role on the glycerol hydrochlorination kinetics, because water appears on the right-hand side of equilibrium steps (1) and (5). It provides evidence that, although the overall reaction is irreversible, it is constituted by reversible elementary steps that may affect the overall reaction rate.

2.2. Kinetic model

The principle of quasi-steady state implies that the net reaction rates of intermediates is zero [56, 57], because they rapidly react further. Thus, generation rates for the intermediates can be written as

$$r_{E_1} = r_1 - r_2 = 0 \tag{2.1}$$
$$r_{E_2} = r_5 - r_6 = 0 \tag{2.2}$$
$$r_{I_1^+} = r_2 - r_3 - r_4 = 0 \tag{2.3}$$
$$r_{I_2^+} = r_6 - r_7 - r_8 = 0 \tag{2.4}$$

The proton transfer step (0) is assumed to be in quasi-equilibrium, giving

$$K_0 = \frac{c_{catH}}{c_{cat} c_H} \tag{2.5}$$

The mass balance for the catalyst is

$$c_{cat0} = c_{cat} + c_{catH} \tag{2.6}$$

where c_{cat0} is the initial concentration of the catalyst. Substituting eq. (2.6) in eq. (2.5), the effective catalyst concentration becomes

$$c_{cat} = \frac{c_{cat0}}{1 + K_0 c_H} \tag{2.7}$$

In general, acids are not eager to accept an additional proton (H^+); therefore, K_0 is considered to be small and the approximation $c_{cat} \approx c_{cat0}$ is presumed.

For the sake of comprehensiveness, the following abbreviations are introduced: $a_1 = k_1 c_A c_{catH}$, $a_{-1} = k_{-1} c_W c_H$, $a_2 = k_2 c_H$, $a_{-2} = k_{-2} c_{cat}$, $a_3 = k_3 c_{Cl}$, $a_{-3} = k_{-3} c_\alpha$, $a_4 = k_4 c_{Cl}$, $a_{-4} = k_{-4} c_\beta$, $a_5 = k_5 c_\alpha c_{catH}$, $a_{-5} = k_{-5} c_W c_H$, $a_6 = k_6 c_H$, $a_{-6} = k_{-6} c_{cat}$, $a_7 = k_7 c_{Cl}$, $a_{-7} = k_{-7} c_{\alpha\gamma}$, $a_8 = k_8 c_{Cl}$, $a_{-8} = k_{-8} c_{\alpha\beta}$. Hence, rewriting and rearranging equations (2.1)-(2.4) we arrive at

$$a_1 - (a_{-1} + a_2) c_{E_1} + a_{-2} c_{I_1^+} = 0 \tag{2.8}$$
$$a_2 c_{E_1} - (a_{-2} + a_3 + a_4) c_{I_1^+} + a_{-3} + a_{-4} = 0 \tag{2.9}$$
$$a_5 - (a_{-5} + a_6) c_{E_2} + a_{-6} c_{I_2^+} = 0 \tag{2.10}$$
$$a_6 c_{E_2} - (a_{-6} + a_7 + a_8) c_{I_2^+} + a_{-7} + a_{-8} = 0 \tag{2.11}$$

According to Tesser et al. (2007), the equilibria of the effective chlorination reaction steps (3), (4), (7) and (8) are assumed to be strongly shifted towards the products, and therefore it is reasonable to assume that $a_{-3} = a_{-4} = a_{-7} = a_{-8} = 0$. Solving c_{E_1} from equation (2.8) gives

$$c_{E_1} = \frac{c_{I_1^+}(a_{-2} + a_3 + a_4)}{a_2} \tag{2.12}$$

After inserting eq. (2.12) in eq. (2.9) the concentration of intermediate I_1^+ can be obtained,

$$c_{I_1^+} = \frac{a_1 a_2}{a_{-1}a_{-2} + (a_{-1} + a_2)(a_3 + a_4)} \tag{2.13}$$

The rates of reaction steps (3) and (4) are given by

$$r_3 = k_3 c_{I_1^+} c_{Cl} \tag{2.14}$$
$$r_4 = k_4 c_{I_1^+} c_{Cl} \tag{2.15}$$

After substituting eq. (2.13) in eq. (2.14) and (2.15) we arrive at the rate expressions,

$$r_3 = \frac{K_0 k_1 k_2 k_3 c_{cat} {c_H}^2 c_A c_{Cl}}{k_{-1}k_{-2}c_{cat}c_H c_W + (k_{-1}c_W + k_2)(k_3 + k_4)c_H c_{Cl}} \tag{2.16}$$
$$r_4 = \frac{K_0 k_1 k_2 k_4 c_{cat} {c_H}^2 c_A c_{Cl}}{k_{-1}k_{-2}c_{cat}c_H c_W + (k_{-1}c_W + k_2)(k_3 + k_4)c_H c_{Cl}} \tag{2.17}$$

Introducing the following notation: $k_3' = K_0 K_1 K_2 k_3$, $k_4' = K_0 K_1 K_2 k_4$, $\alpha' = (k_3 + k_4)/k_{-2}$, $\beta' = K_2(k_3 + k_4)/k_{-1}$, equations (2.16) and (2.17) can be written as

$$r_3 = \frac{k_3' c_{cat} c_A c_H c_{Cl}}{c_{cat}c_W + (\alpha' c_W + \beta')c_{Cl}} \tag{2.18}$$
$$r_4 = \frac{k_4' c_{cat} c_A c_H c_{Cl}}{c_{cat}c_W + (\alpha' c_W + \beta')c_{Cl}} \tag{2.19}$$

As discussed previously, there is an analogy between the reaction steps of the mechanism displayed in Figure 2.1, and therefore, there is no need for a separate derivation of the reaction rates for the reaction steps (7) and (8). In fact, by introducing the following notation $k_7' = K_0 K_5 K_6 k_7$, $k_8' = K_0 K_5 K_6 k_8$, $\gamma' = (k_7 + k_8)/k_{-6}$, $\delta' = K_6(k_7 + k_8)/k_{-5}$, it can be analogously written

$$r_7 = \frac{k_7' c_{cat} c_\alpha c_H c_{Cl}}{c_{cat}c_W + (\gamma' c_W + \delta')c_{Cl}} \tag{2.20}$$
$$r_8 = \frac{k_8' c_{cat} c_\alpha c_H c_{Cl}}{c_{cat}c_W + (\gamma' c_W + \delta')c_{Cl}} \tag{2.21}$$

At this point, it is assumed that, due to the continuous feeding of HCl to the system, the liquid-phase is always saturated with HCl. Furthermore, because HCl is a strong acid, it is considered to be fully dissociated in the reaction mixture. In fact, as discussed in Chapters 3 and 4, these considerations are not necessarily true, but at this stage of the research development, these were commonly accepted assumptions [35, 43]. A very small amount of H^+ reacts with the catalyst to produce the species $catH^+$, although this equilibrium is assumed to prevail at the very beginning of the reaction. Hence, the reaction mechanism consumes equivalent amounts of H^+ and Cl^-. For this reason, it is reasonable to write that $c_H = c_{Cl} = c_{HCl}$. Hence, the reaction rates (2.18)-(2.21) may be condensed to

$$r_3 = \frac{k_3' c_{cat} c_A {c_{HCl}}^2}{D_{34}} \tag{2.22}$$

$$r_4 = \frac{k_4' c_{cat} c_A {c_{HCl}}^2}{D_{34}} \tag{2.23}$$

$$r_7 = \frac{k_7' c_{cat} c_\alpha {c_{HCl}}^2}{D_{78}} \tag{2.24}$$

$$r_8 = \frac{k_8' c_{cat} c_\alpha {c_{HCl}}^2}{D_{78}} \tag{2.25}$$

where $D_{34} = c_{cat}c_W + (\alpha' c_W + \beta')c_{HCl}$ and $D_{78} = c_{cat}c_W + (\gamma' c_W + \delta')c_{HCl}$.

Water appears on the right hand-side of equilibrium steps (1) and (5), and consequently, water concentration appears on the denominators of the reaction rates (2.22)-(2.25). This explains quantitatively the experimentally observed fact that water has a negative effect on the hydrochlorination kinetics. In fact, the reaction mechanism strongly suggests that the removal of water would enhance the hydrochlorination kinetics.

Interestingly, the catalyst concentration appears both in the numerator and denominator of the reaction rates, because the catalyst appears on the right-hand sides of equilibrium steps (2) and (6). Thus, it suggests that the catalyst might also play a somewhat suppressing role in the hydrochlorination kinetics. Such an assumption was later on confirmed as experiments at different catalyst concentrations were carried out (Chapter 3).

2.3. Mass balances and numerical considerations

According to the reaction stoichiometry (Figure 1.5), the generation and consumption rates for all the components in the reaction system can be written as follows

$$r_A = -r_3 - r_4 \tag{2.26}$$

$$r_\alpha = r_3 - r_7 - r_8 \tag{2.27}$$

$$r_\beta = r_4 \tag{2.28}$$

$$r_{\alpha\gamma} = r_7 \tag{2.29}$$

$$r_{\alpha\beta} = r_8 \tag{2.30}$$

$$r_{HCl} = -r_3 - r_4 - r_7 - r_8 \tag{2.31}$$

$$r_W = r_3 + r_4 + r_7 + r_8 \tag{2.32}$$

For the perfectly backmixed semi-batch reactor, in which HCl is continuously fed, the general mass balance for the components in the liquid-phase can be written as [59] (All symbols are explained in Notation)

$$N_i A_{GL} + r_i V_L = \dot{n}_i + \frac{dn_i}{dt} \tag{2.33}$$

where N_i denotes the gas-liquid molar flux, $A_{GL}$is the gas-liquid interfacial area and V_L is the liquid-phase volume. The semi-batch reactor operated under full reflux conditions prevented all the components, except HCl, to escape from the liquid-phase. Thus, the term $\dot{n}_i$, which expresses the flow of liquid across the system boundaries, is set to zero. Assuming that the HCl mass transfer is very rapid, the liquid-phase is considered to be saturated with HCl at all times. Furthermore, the liquid-phase volume is taken as constant throughout the reaction (as assumed by Tesser et al. [35]). Therefore, equation (2.33) can be simplified to

$$\frac{dc_i}{dt} = r_i \tag{2.34}$$

for all the liquid-phase components.

The family of equations (2.34) constitutes a system of non-linear ordinary differential equations (ODE) which was solved in situ during the nonlinear regression analysis with the software MODEST [60]. The objective function was defined as

$$Q = \sum_k \left(c_{iexp,t} - c_{i,t}\right)^2 \tag{2.35}$$

where $c_{iexp,t}$ is the experimentally recorded concentration of the compound i ($i = A, \alpha, \beta, \alpha\beta, \alpha\gamma$) at time t and $c_{i,t}$ is the concentration estimated by the model. The backward difference method was implemented in a stiff ODE solver. Both Simplex and Levenberg-Marquardt optimization algorithms were used to minimize the objective function. The overall goodness of the regression analysis was checked by the degree of explanation which was defined as

$$R^2 = 1 - \frac{\sum_k \left(c_{iexp,t} - c_{i,t}\right)^2}{\sum_k \left(c_{iexp,t} - c_{iav,t}\right)^2} \tag{2.36}$$

where $c_{iav,t}$ is the average value of the experimentally recorded concentrations.

2.4. Parameter estimation and model validation

The article of Tesser et al. [35] reports the molar fractions of glycerol, α-MCP, β-MCP, αγ-DCP and αβ-DCP for five experiments performed at different temperatures, in which malonic acid was used as the catalyst. Such data was implemented in the parameter estimation subroutine previously described. The liquid-phase concentration of HCl was set constant to 10% by mole and the catalyst concentration was 8% by mol. The fit of the model to the experimental data is presented in Figure 2.3 and the results of the parameter estimation are summarized in Table 2.1.

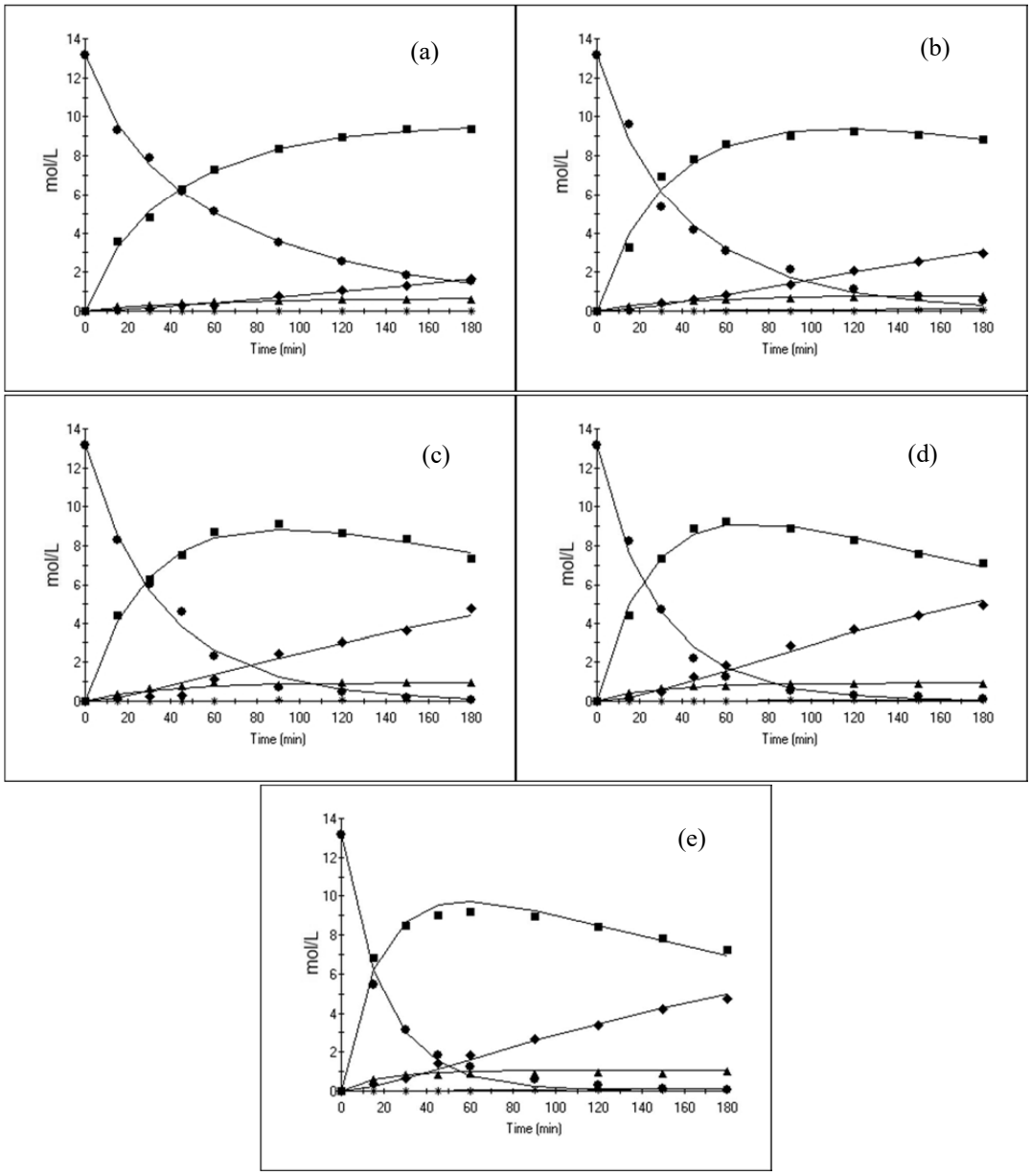

Figure 2.3. Results of the parameter estimation analysis using the data available in literature [35] for the solvent-free glycerol hydrochlorination. (a) 80ºC, (b) 90ºC, (c) 100ºC, (d) 110ºC, (e) 120ºC. Symbols: (●) glycerol, (■) α-MCP, (▲) β-MCP, (*) αβ-DCP, (◆) αγ-DCP. Catalyst concentration: 8% malonic acid.

Table 2.1. Kinetic parameters estimated at different reaction temperatures.

	$T = 80°C$	$T = 90°C$	$T = 100°C$	$T = 110°C$	$T = 120°C$
$k'_3(L \cdot mol^{-1} \cdot min^{-1})$	$9.36 \cdot 10^{-4}$	$3.98 \cdot 10^{-3}$	$1.26 \cdot 10^{-2}$	$4.30 \cdot 10^{-2}$	$1.70 \cdot 10^{-1}$
$k'_4(L \cdot mol^{-1} \cdot min^{-1})$	$5.45 \cdot 10^{-5}$	$2.64 \cdot 10^{-4}$	$1.01 \cdot 10^{-3}$	$3.30 \cdot 10^{-3}$	$1.54 \cdot 10^{-2}$
$k'_7(L \cdot mol^{-1} \cdot min^{-1})$	$1.81 \cdot 10^{-4}$	$5.48 \cdot 10^{-4}$	$1.25 \cdot 10^{-3}$	$2.23 \cdot 10^{-3}$	$2.89 \cdot 10^{-3}$
$k'_8(L \cdot mol^{-1} \cdot min^{-1})$	$6.55 \cdot 10^{-7}$	$5.03 \cdot 10^{-6}$	$5.75 \cdot 10^{-6}$	$3.29 \cdot 10^{-5}$	$7.77 \cdot 10^{-5}$
$\beta'(mol.L^{-1})$	0.57	2.05	6.33	17.50	50.70
$\delta'(mol.L^{-1})$	1.43	2.62	4.06	6.91	10.30
$R^2(\%)$	99.89	99.33	99.51	99.59	99.13

The model showed an excellent fit to the experimental data, with a degree of explanation exceeding 99% for all the temperatures. The Arrhenius plots displayed in Figure 2.4 explained the temperature dependence of the kinetic parameters.

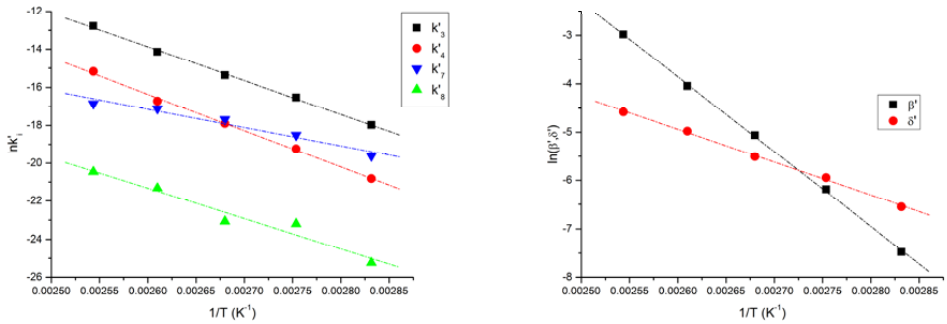

Figure 2.4. Arrhenius plots for the reaction constants and parameters β' and δ'.

Activation energies and pre-exponential factors were estimated, as shown in Table 2.2.

Table 2.2. Activation energies and pre-exponential factors for the glycerol hydrochlorination using malonic acid.

	r_3	r_4	r_7	r_8
$E_a(kJ/mol)$	147.5	159.4	80.7	132.1
$\ln(A/L \cdot mol^{-1} \cdot min^{-1})$	32.3	33.5	8.1	20.0

The parameter estimation was also carried out with our own data from solvent-free glycerol hydrochlorination experiments using 11% by mole of acetic acid as catalyst at 105ºC. The results of the parameter estimation and the model fitting are depicted in Table 2.3 and Figure 2.5, respectively. The model fitting corresponds to two separate experiments performed under same reaction conditions. A similar fit was observed, with a 97% degree of explanation (Figure 2.5).

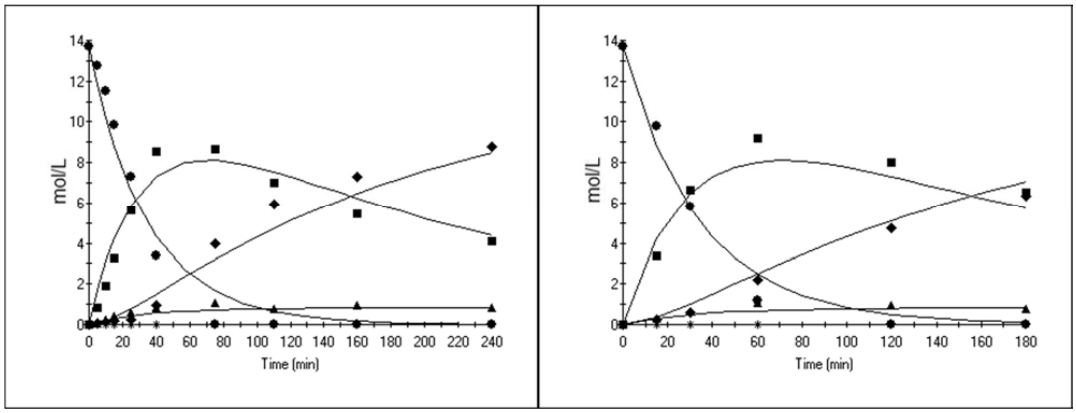

Figure 2.5. Semi-batch glycerol hydrochlorination at 105ºC and 11% acetic acid. Symbols: (●) glycerol, (■) α-MCP, (▲) β-MCP, (*) αβ-DCP, (◆) αγ-DCP.

Table 2.3. Estimated kinetic parameter for glycerol hydrochlorination performed at 105ºC and 11% by moles of acetic acid.

$k_3'(L \cdot mol^{-1} \cdot min^{-1})$	$2.16 \cdot 10^{-2}$
$k_4'(L \cdot mol^{-1} \cdot min^{-1})$	$1.39 \cdot 10^{-3}$
$k_7'(L \cdot mol^{-1} \cdot min^{-1})$	$1.01 \cdot 10^{-3}$
$k_8'(L \cdot mol^{-1} \cdot min^{-1})$	$1.29 \cdot 10^{-9}$
$\beta'(mol.L^{-1})$	17.4
$\delta'(mol.L^{-1})$	1.91
$R^2(\%)$	97.00

The reaction mechanism and many underlying mass balance assumptions applied for solving this model were mainly based on the observations reported in literature. In fact, as will be discussed in Chapter 3, many of these assumptions are refuted and an improved description of the semi-batch system is provided. Notwithstanding, the kinetic model presented hereby constitutes the backbone of a more realistic model that is presented later on. In fact, in the review article published by Santacesaria et al. (2013) [30], the present kinetic model was described as the most general and rigorous description of the glycerol hydrochlorination reaction.

3. Semi-batch technology and extended kinetic model

Aiming to further develop the kinetic model presented in Chapter 2, an extensive experimental study was performed under semi-batch conditions for the solvent-free glycerol hydrochlorination. The influence of stirring speed, temperature, catalyst concentration and HCl partial pressures were evaluated and many relevant effects, previously not reported or poorly reported by the literature, were noticed and described. The reaction mechanism, kinetic model and mass balances proposed in Chapter 2 were updated in order to account for the new experimental observations. Parameter estimation was carried out in which kinetic and mass transfer parameters were described. In addition, a new concept, named Catalyst Modulus, was derived from the kinetic equation and tested with the experimental data obtained.

3.1. Materials and methods

3.1.1. Experimental apparatus

The reactor consisted of a 250 mL glass jacketed container, provided with a PTFE coated radial flow impeller (Bohlender GmbH). A gas sinter provided fine bubbling of the gas phase into the liquid. Hydrogen chloride gas (AGA, 99.8%) was used as reactant and argon (99.999%) was employed as the diluting gas for the experiments performed under different HCl partial pressures. The gas flows were measured and controlled by rotameters. A condenser operating at -4ºC was attached to one of the necks of the reactor to prevent the evaporation of any volatile compounds that would eventually escape from the liquid-phase and attempt to leave the reaction vessel. In such a construction, only gaseous HCl was allowed to leave the system. Finally, the unreacted HCl gas leaving the reactor was conducted to neutralization bottles containing a concentrated solution of sodium hydroxide in order to be neutralized. A manometer was connected to the reactor in order assure that the inner gauge pressure of all experiments was zero. Figure 3.1 depicts an overview of the reactor setup used for the semi-batch experiments.

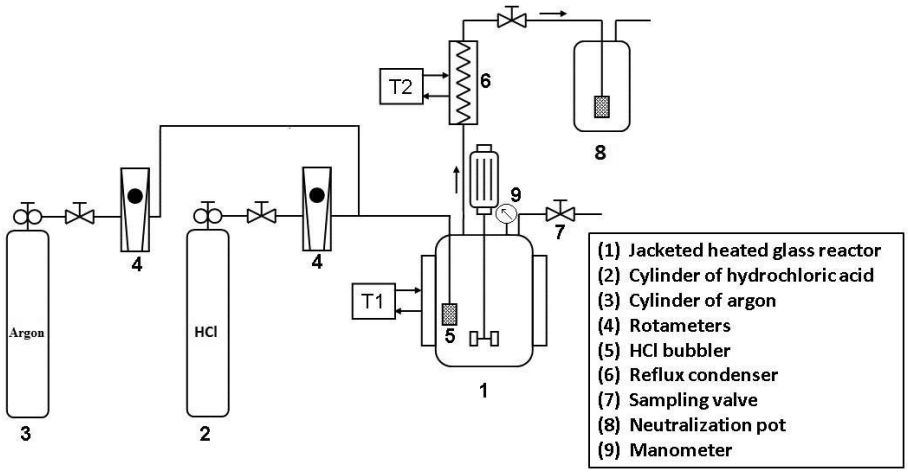

Figure 3.1. Overview of semi-batch glycerol hydrochlorination apparatus.

3.1.2. Experimental procedure

Firstly, glycerol and acetic acid (J.T. Baker, >99%) were consecutively loaded to the reactor. The liquid mixture was subject to heating, vigorous stirring and continuous bubbling of argon until the reaction temperature was reached. At this point, the gas flow of HCl was switched on and this was considered to be "time zero". Samples were withdrawn, ca. 2 mL, by means of a plastic syringe and they were immediately quenched to -4ºC.

3.1.3. Analytical methods

The analytical methods described here were applied for all experiments presented in Chapters 3, 4 and 5.

The mass fractions of glycerol and its chlorinated derivatives (GCD compounds) were analysed by means of gas chromatograph (Hewlett Packard 6890 Series) equipped with a capillary column (J&W Scientific, HP-5, 30 m x 0.32 mm x 0.25 mm) and a flame ionization detector (FID). Helium was used as a carrier gas. The samples were first diluted at a ratio of 1:20 and the injection volume was 1 μL. The initial temperature of the column was 50ºC and it was increased to 280ºC at a rate of 10ºC/min and held at this temperature for 10 minutes. The injector temperature was 270ºC and the detector temperature was 300ºC. It ought to be emphasized that this method only provided the value of mass fractions for glycerol, α-MCP, β-MCP, αγ-DCP and αβ-DCP, as the other compounds, including acetic acid, remained invisible to the column.

The mass fractions of HCl in the liquid bulk phase were analysed by means of an automatic titrator (751 GPD Titrino, Metrohm) using a standard solution of sodium hydroxide 0.2 M (Merck S.A.). For each sample, two titrations were carried out and an average was used as the final value.

3.2. Change of liquid volume

For all experiments, a significant increase in mass and volume of the reaction mixture was noticed (Figure 3.2). Even though this effect was pronounced, no source in the literature had referred to it. The reason for such an increase is due to the significant accumulation of HCl in the liquid-phase.

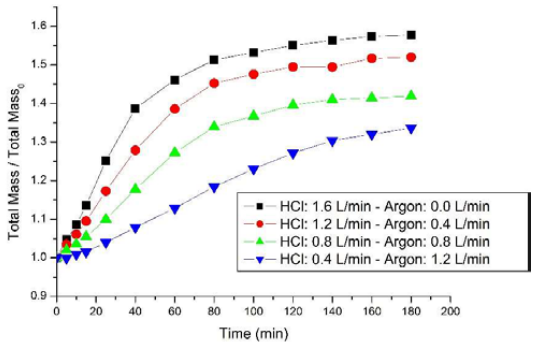

Figure 3.2. Estimated mass increase of the liquid-phase during the semi-batch glycerol hydrochlorination under different partial pressures of HCl

In order to have a more realistic description of our reaction system and, therefore, estimate reliable kinetic parameters, a dynamic and ideal model for the liquid-phase volume was proposed as follows

$$V^L(t) = \frac{m_{GCD}}{\rho_{GCD}} + \frac{m_{cat}}{\rho_{cat}} + \frac{m_W + m_{HCl}}{\rho_W} \tag{3.1}$$

where ρ_i is the density of the pure compound i at the reaction temperature. The abbreviation GCD stands for "**G**lycerol and **C**hlorinated **D**erivatives", primarily mentioned in Section 3.1.3. Figure 3.3 illustrates the concepts of GCD compounds and bulk liquid-phase. The distinction between these two groups arises from the fact that the mass fractions of HCl, obtained by titration analysis, and the mass fractions of GCD compounds, obtained by gas chromatographic analysis, are calculated on different basis.

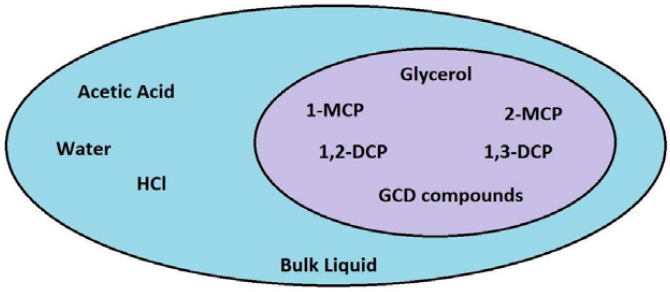

Figure 3.3. The liquid bulk phase comprises all the components present in the liquid, meanwhile the GCD compounds is a subset of the bulk liquid that comprises glycerol, α-MCP, β-MCP, αβ-DCP and αγ-DCP. It is important to emphasize that this distinction is merely conceptual; indeed, the liquid phase is assumed to be constituted by a single homogeneous phase.

Equation (3.1) may be considered a rough approximation of the liquid-phase volume, since it does not take into account the interactions between the molecules in the liquid mixture and does not consider the densities of each individual compound. In fact, it has been found that the densities of α-MCP and αγ-DCP differ considerably from that of glycerol at room temperature [61]. However, (3.1) represents a reasonably convenient way to describe the volume increase of the liquid-phase due to the accumulation of HCl and the production of water in the system. It definitely represents an improvement over the erroneous assumption of constant volume previously considered. In addition, density correlations for glycerol, acetic acid and water are reliable and well documented in the literature [62].

The mass of acetic acid and GCD compounds were calculated as

$$m_{cat} = m_{cat}^{0} \tag{3.2}$$

$$m_{GCD_i} = \frac{m_{gly}^{0} MM_{GCD_i}}{MM_{gly}} x'_{GCD_i} \tag{3.3}$$

where m_i^0 is the initial mass of compound i, x'_{GCD_i} is the molar fraction of GCD compound i calculated from the GC analysis and MM_i is the molar mass of compound i.

Assuming that all the water produced remains in the liquid-phase due to complete reflux, the amount of water was estimated from the stoichiometric molar balance

$$n_w = n_\alpha + n_\beta + 2\left(n_{\alpha\beta} + n_{\alpha\gamma}\right) \tag{3.4}$$

The mass fractions of HCl in the bulk liquid-phase were determined by titration. For the liquid-phase, the following mass balance is written

$$m_{HCl} = w_{HCl}\left(\sum m_{GCD} + m_{cat} + m_w + m_{HCl}\right) \tag{3.5}$$

Rewriting and rearranging eq. (3.5) in order to isolate the term m_{HCl} we obtain

$$m_{HCl} = \frac{w_{HCl}}{1 - w_{HCl}}\left(\sum m_{GCD} + m_{cat} + m_w\right) \tag{3.6}$$

Hence, the liquid-phase mass (Figure 3.2) can therefore be calculated from

$$m^L(t) = \sum_i m_{GCD_i}(t) + m_{cat}(t) + m_w(t) + m_{HCl}(t) - m_s(t) \tag{3.7}$$

where $m_s(t)$ represents the sum of the samples withdrawn until time 't'. Equation (3.7) was able to predict the final mass of the liquid-phase with an error within the range of 0.12-3.76%, with an average value of 1.2% error.

The liquid-phase volume increase plays a decisive impact when calculating the concentrations of compounds in the reaction system. Figure 3.4 clearly illustrates the importance of this effect when estimating the catalyst concentration for the experiments conducted under different partial pressures of HCl. Even though the amount of acetic acid is considered constant throughout the reaction time, its concentration decreases significantly due to the liquid volume increase.

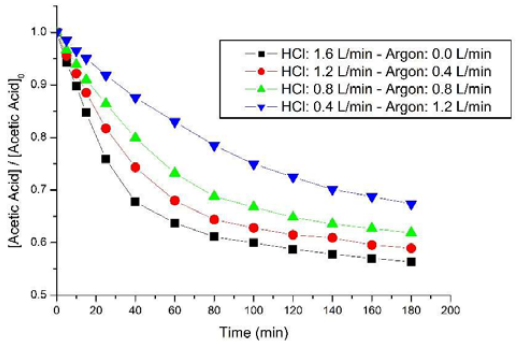

Figure 3.4. Concentration of acetic acid for experiments conducted under different HCl partial pressures

3.3. Experimental results

3.3.1. External mass transfer effect

Lee et al. (2008b) [48] has demonstrated that the stirring rate might have a significant effect on the glycerol hydrochlorination rate. Thus, in order to ensure the experiments were conducted in the absence of external mass transfer limitations, a first set of experiments was performed in which the stirring speed was varied; Figure 3.5 depicts the glycerol concentration profiles obtained for experiments carried out under different stirring speeds.

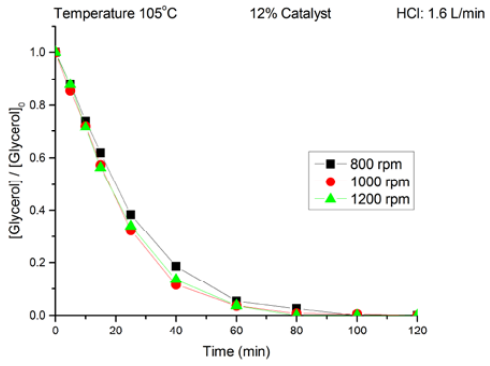

Figure 3.5. Influence of different stirring speeds on the conversion of glycerol.

It is noticed that for stirring speeds exceeding 1000 rpm, the external mass transfer limitations are surmounted; even the stirring speed of 800 rpm gave almost the same hydrochlorination rates as 1000 and 1200 rpm. Actually, 1000 rpm was selected as the stirring speed for all semi-batch and reactive distillation experiments.

3.3.2. Effect of HCl partial pressure

The influence of the partial pressure of hydrogen chloride on the glycerol conversion and the HCl uptake was evaluated by means of four experiments in which the gaseous stream of HCl was diluted with argon. In order to maintain a constant volumetric flow of 1.6 L/min, the HCl and argon flows were adjusted accordingly. The results obtained are displayed in Figure 3.6.

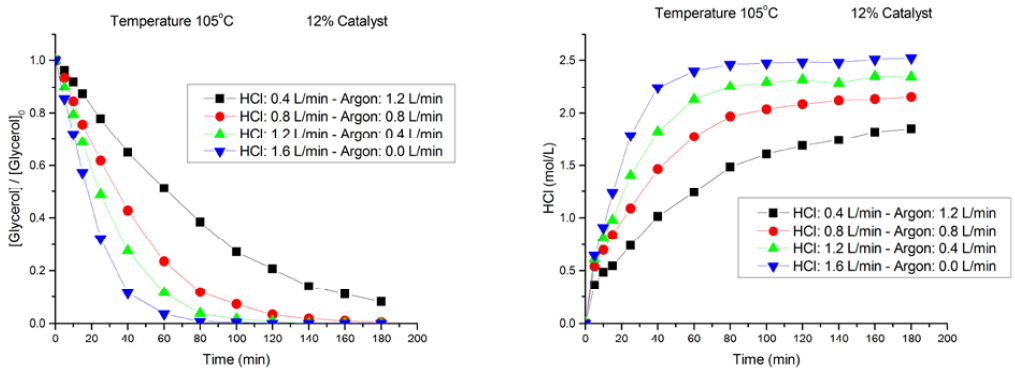

Figure 3.6. Glycerol conversion and HCl liquid uptake for semi-batch experiments performed at different HCl partial pressures.

The results reveal that the partial pressure of HCl has a significant effect both on the glycerol conversion and the HCl uptake, as previously reported in the literature [28, 43, 48]. As expected, an increase on the HCl partial pressure promotes the glycerol conversion and enhances HCl liquid uptake.

3.3.3. Catalyst concentration effect

The influence of the initial catalyst concentration on the semi-batch glycerol hydrochlorination was investigated over a wide range of concentrations (0, 3, 6, 9, 12, 15, 20 and 50% by mole). The results obtained for the glycerol consumption and the HCl uptake are depicted in Figure 3.7.

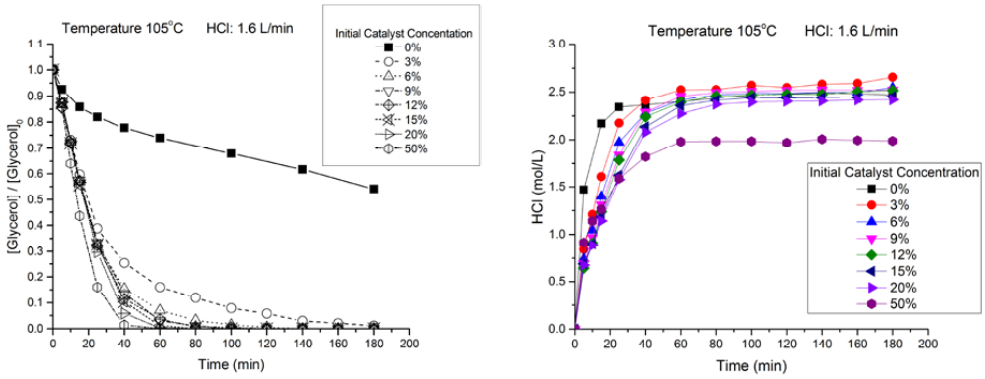

Figure 3.7. Effect of the catalyst concentration on the glycerol conversion and the HCl liquid uptake.

Surprisingly, there was significant glycerol conversion in the experiment performed in the absence of catalyst. For this reason, a series of non-catalysed experiments at different temperatures was carried out later on. Nevertheless, it is observed that the catalytic reaction route is much more preferred than the non-catalytic one; for instance, at 3% of the catalyst concentration, a significant increase in the glycerol conversion was observed compared to 0% catalyst. Interestingly, for the catalytic experiments, an increase in the catalyst concentration would not produce a significant increase in glycerol conversion, even at the absurdly high catalyst concentration of 50%. Such a particular effect of the catalyst concentration in the glycerol hydrochlorination rate is in agreement with the kinetic treatment derived in Chapter 2, in which the catalyst concentration appeared both in the numerator and denominator of the rate equations (2.22)-(2.25). The catalyst concentration did not affect considerably the HCl liquid uptake, except for the experiment at 50% catalyst, which showed a much lower HCl uptake compared to the other ones.

3.3.4. Temperature effect on catalysed experiments

The influence of the reaction temperature on the catalysed experiments was investigated and the results of glycerol concentration and HCl liquid uptake are depicted in Figure 3.8.

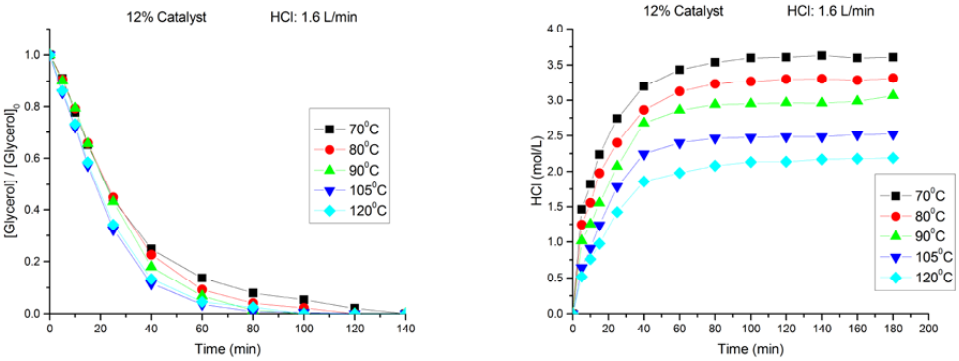

Figure 3.8. Effect of temperature on the glycerol conversion and HCl liquid uptake in semi-batch glycerol hydrochlorination.

The observed effect of temperature on glycerol conversion is not substantially strong for catalysed experiments. Indeed, an increase of the temperature caused a slight enhancement in the glycerol conversion kinetics, up until the temperature of 105ºC. However, at 120ºC, the glycerol conversion is nearly identical to at 105ºC. This can be attributed to the compensation effect of temperature, which diminishes the solubility of gaseous HCl in the liquid-phase as the temperature increases [63]. Therefore, an increase of the reaction rate due to temperature is partially compensated by a decrease on HCl solubility in the reaction mixture.

3.3.5. Temperature effect on non-catalysed experiments

The influence of the reaction temperature on the non-catalytic experiments was investigated thoroughly. The experimental results are presented in Figure 3.9.

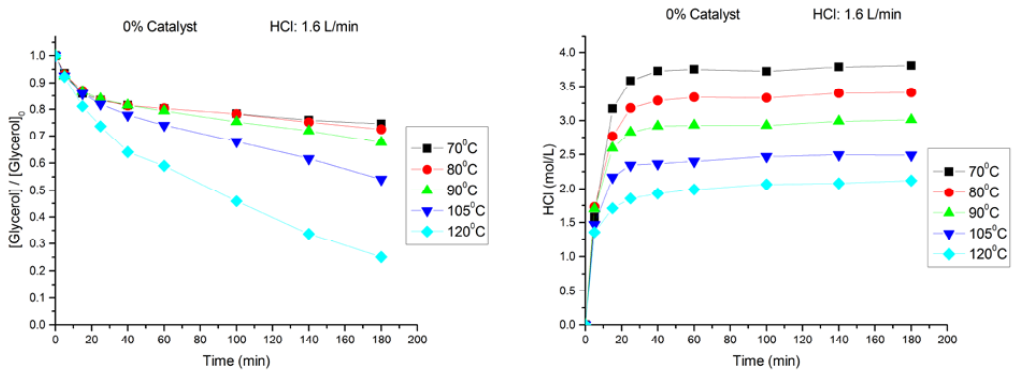

Figure 3.9. Effect of temperature in the glycerol conversion and HCl liquid uptake for the non-catalytic solvent-free glycerol hydrochlorination in semi-batch conditions.

The non-catalytic reaction route is substantially temperature sensitive, and results in a remarkable glycerol conversion at temperatures of 105ºC and 120ºC. However, it should be noted that, the production of αγ-DCP and αβ-DCP was virtually nil in these experiments. The HCl liquid uptake is similar to the one observed in the catalytic experiments (Figure 3.8).

3.4. Reaction mechanism and rate equations

Based on the insights brought by the semi-batch experiments, the reaction mechanism proposed in Chapter 2 was extended to correspond to the reality. For this reason, the formation of the epoxide intermediate I_1^+ is assumed to occur in parallels, via catalytic and non-catalytic reaction pathways, as displayed in Figure 3.10.

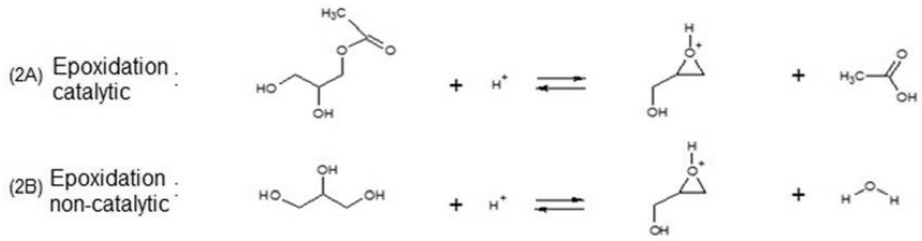

Figure 3.10. Proposed non-catalytic reaction step.

As only small traces of αγ-DCP and αβ-DCP were present in the non-catalytic experiments, these compounds were ignored by the non-catalytic reaction route. Indeed, Dmitry and Zanaveskin (2011) [49] reported a similar observation when studying the non-catalytic glycerol hydrochlorination with hydrochloric acid.

In addition, the production of αβ-DCP was extremely low for all the experiments, often presenting a random oscillatory behaviour due to its trace-like nature [28, 29, 43, 46, 47]. Thus, the formation rate of 1,2-DCP is assumed negligible. Luo et al. (2009) [46] had the same approach when studying the glycerol hydrochlorination in the presence of hydrochloric acid and acetic acid as catalyst. In practice, this implies that reaction step 8 in the reaction mechanism is zero. Finally, the modified reaction mechanism for the glycerol hydrochlorination is depicted in Figure 3.11.

Step and step number		*Stoichiometric numbers* (N) *of reaction routes* $1-6$					
		N_1	N_2	N_3	N_4	N_5	N_6
$cat + H^+ = catH^+$	(0)	1	0	1	0	1	1
$A + catH^+ = E_1 + W + H^+$	(1)	1	0	1	0	0	0
$E_1 + H^+ = I_1^+ + cat$	$(2A)$	1	0	1	0	0	0
$A + H^+ = I_1^+ + W$	$(2B)$	0	1	0	1	0	0
$I_1^+ + Cl^- \rightarrow \alpha$	(3)	1	1	0	0	0	0
$I_1^+ + Cl^- \rightarrow \beta$	(4)	0	0	1	1	0	0
$\alpha + catH^+ = E_1 + W + H^+$	(5)	0	0	0	0	1	1
$E_2 + H^+ = I_2^+ + cat$	(6)	0	0	0	0	1	1
$I_2^+ + Cl^- \rightarrow \alpha\gamma$	(7)	0	0	0	0	1	0
$I_2^+ + Cl^- \rightarrow \alpha\beta$	(8)	0	0	0	0	0	1
Overall reactions:							
$N_1, N_2: A + H^+Cl^- \rightarrow \alpha + W$							
$N_3, N_4: A + H^+Cl^- \rightarrow \beta + W$							
$N_5: \alpha + H^+Cl^- \rightarrow \alpha\gamma + W$							
$N_6: \alpha + H^+Cl^- \rightarrow \alpha\beta + W$							

Figure 3.11. Extended reaction mechanism explaining both catalytic and non-catalytic reaction routes.

Routes 2 and 4 correspond to the non-catalytic pathway. It could be noted that, the reaction pathways for the production of αγ-DCP and αβ-DCP were not modified, thence, the reaction rates r_7 and r_8 (eq.

(2.24) and (2.25)) remains unchanged. However, the production of α-MCP and β-MCP are assumed to occur via a non-catalytic route too, and therefore, new reaction rate expressions were derived. The derivation of the kinetic equations for the updated kinetic model is analogous to that used in Chapter 2: the quasi-steady state hypothesis was applied on the reaction intermediates (E_1 and I_1^+) and a system of equation is solved to give explicit expressions for the hydrochlorination reaction rates. For the interested reader, the complete derivation of such equations is presented in the Appendix of **Publication II**. Finally, the reaction rates r_3 and r_4 for the glycerol hydrochlorination taking into account both catalytic and non-catalytic reaction routes are presented as follow

$$r_3 = \frac{k_3' c_A c_{HCl}^2 (c_{cat0} + \kappa')}{c_{cat0} c_W + \alpha_{HCl} c_{HCl} + \alpha_W c_W} \tag{3.8}$$

$$r_4 = \frac{k_4' c_A c_{HCl}^2 (c_{cat0} + \kappa')}{c_{cat0} c_W + \alpha_{HCl} c_{HCl} + \alpha_W c_W} \tag{3.9}$$

The impact of the non-catalytic reaction pathway is accounted for by parameters κ' and α_W.

3.5. Mass balances and numerical strategy

All the components, except unreacted gaseous HCl, are prevented to leave the reaction mixture due to the presence of the reflux condenser. Therefore, the semi-batch mass balance (2.33) is reduced to

$$\frac{dn_i}{dt} = r_i V^L \tag{3.10}$$

where i=A, α-MCP, β-MCP and αγ-DCP.

The HCl mass transfer was described by the double film theory [59, 64]. It is assumed that, no reactions occur in the liquid film, because this system belongs to the category of slow reactions in the classification of gas-liquid reactions. Therefore, the mass balance for the HCl in the liquid-phase can be written as

$$\frac{dn_{HCl}^L}{dt} = k_G A_{GL} \left(\frac{P_{HCl}}{RT_0} - K_{HCl} c_{HCl}^L \right) + r_{HCl} V^L \tag{3.11}$$

where k_G is the mass transfer coefficient, A_{GL} is the gas-liquid interfacial area, T_0 is the room temperature and K_{HCl} is the distribution coefficient, which is the ratio between the HCl concentration in the gas bulk phase and the HCl equilibrium concentration in the liquid-phase.

It should be recalled that, the liquid-phase volume that appears in equations (3.10) and (3.11) is described by the dynamic equation (3.1). The generation and consumption rates of components are the same as described in eqs. (3.8), (3.9), (2.24).

The software Modest [60] described in Chapter 2 was used for solving the ODE system of eqs. (3.10) and (3.11). The objective function was defined as

$$Q = \sum_i \left(n_{iexp,t} - n_{i,t}\right)^2 \tag{3.12}$$

The degree of explanation was calculated as follows

$$R^2 = 1 - \frac{\sum\left(n_{iexp,t} - n_{i,t}\right)^2}{\sum\left(n_{iexp,t} - n_{iav,t}\right)^2} \tag{3.13}$$

to check the quality of the fit.

3.6. Modelling results

3.6.1. Solubility of HCl

An analysis of the distribution coefficient (K_{HCl}) was performed prior to the implementation of the parameter estimation process. For this purpose, the liquid-phase concentration of HCl at $t = 180$ minutes was considered to be the equilibrium concentration of HCl in the liquid-phase. The dependency of K_{HCl} with HCl partial pressure at 105ºC was described by the empirical relation $K_{HCl} = a(P_{HCl})^b$ (Figure 3.12).

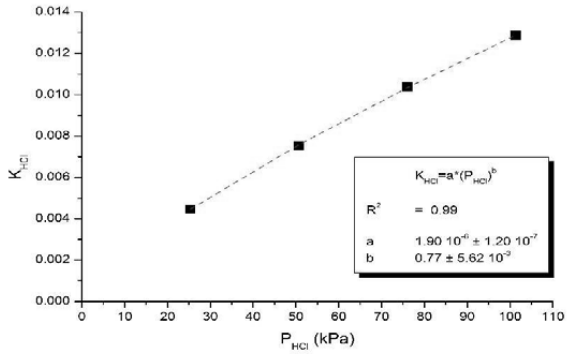

Figure 3.12. Influence of HCl partial pressure on the distribution coefficient K_{HCl} at 105ºC (data from Figure 3.6b).

Interestingly, Figure 3.12 indicates that the HCl dissolution in the reaction mixture cannot be fully explained by a linear Henry law dependence [51, 63].

The temperature influence on the HCl equilibrium concentration in the liquid-phase was evaluated in terms of the equation $ln(c^*_{L,HCl}) = A + {}^{B}/_{T}$, which has widespread applications in the literature for describing the dissolution of HCl and Cl_2 in various organic solvents and water [65] (Figure 3.13).

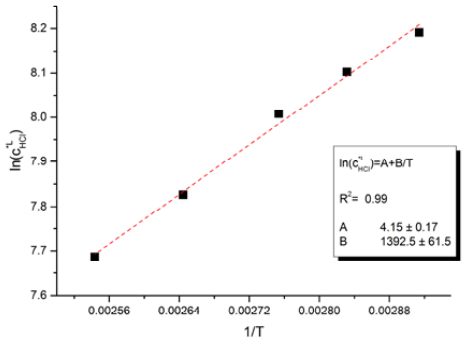

Figure 3.13. Temperature influence on the HCl equilibrium concentration in the reaction mixture.

Hence, the dependence of K_{HCl} with the reaction temperature is described as

$$K_{HCl} = \frac{c^*_{G,HCl}}{c^*_{L,HCl}} = \frac{P_{HCl}}{RT_0} exp\left(-A - \frac{B}{T}\right) \tag{3.14}$$

The equations relating K_{HCl} variations with partial pressure and temperature were inserted in the parameter estimation subroutine. Although the liquid-phase character changes considerably as the reaction proceeds, K_{HCl} and $k_G A_{GL}$ were assumed constant throughout the reaction time.

3.6.2. Kinetic results

The first sets of experiments to be regressed were the ones performed at 105ºC, because that is the temperature at which most experiments were conducted. The data fitting results are collected in Figure 3.14.

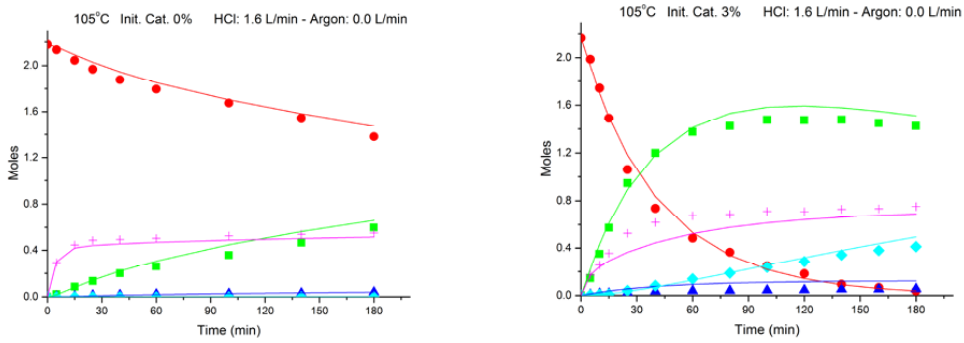

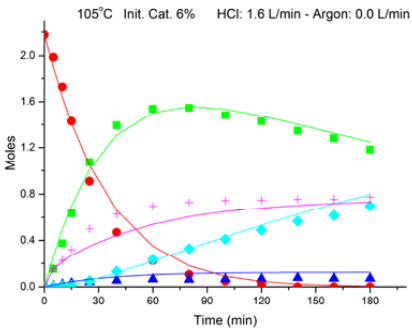
105°C Init. Cat. 6% HCl: 1.6 L/min - Argon: 0.0 L/min
Moles
Time (min)

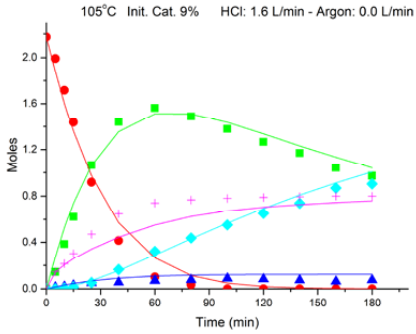
105°C Init. Cat. 9% HCl: 1.6 L/min - Argon: 0.0 L/min
Moles
Time (min)

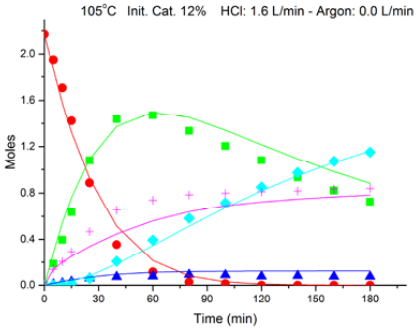
105°C Init. Cat. 12% HCl: 1.6 L/min - Argon: 0.0 L/min
Moles
Time (min)

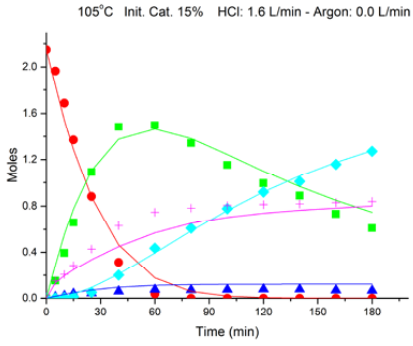
105°C Init. Cat. 15% HCl: 1.6 L/min - Argon: 0.0 L/min
Moles
Time (min)

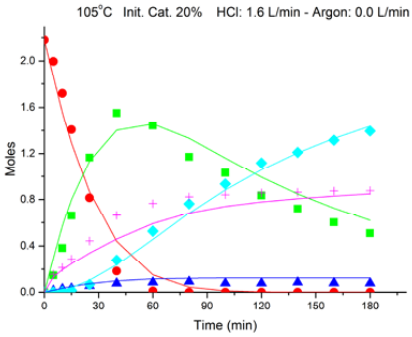
105°C Init. Cat. 20% HCl: 1.6 L/min - Argon: 0.0 L/min
Moles
Time (min)

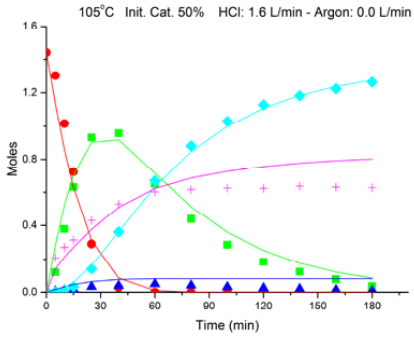
105°C Init. Cat. 50% HCl: 1.6 L/min - Argon: 0.0 L/min
Moles
Time (min)

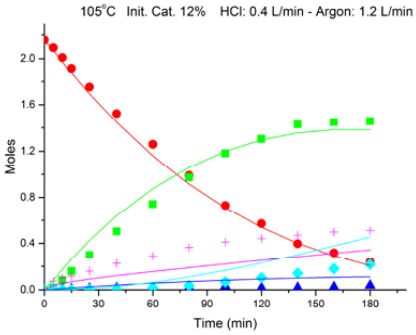
105°C Init. Cat. 12% HCl: 0.4 L/min - Argon: 1.2 L/min
Moles
Time (min)

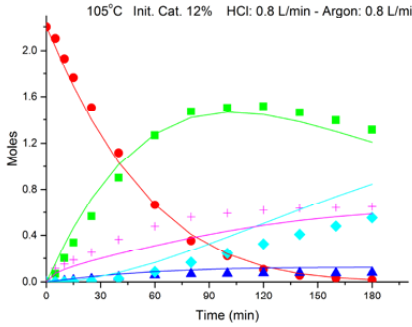
105°C Init. Cat. 12% HCl: 0.8 L/min - Argon: 0.8 L/min
Moles
Time (min)

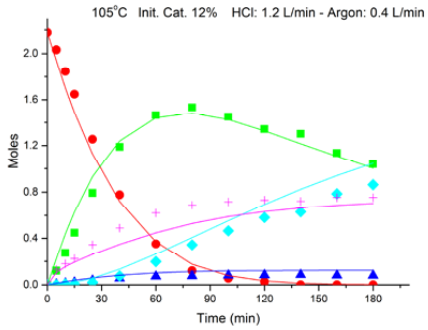

Figure 3.14. Data fitting for the experiments performed at 105ºC at different catalyst concentrations and HCl partial pressures (moles of compounds in liquid phase). Symbols: (●) glycerol, (■) α-MCP, (▲) β-MCP, (◆) αγ-DCP, (┼) HCl.

The overall degree of explanation for the curves presented in Figure 3.14 is 97.8%, which is reasonably high, regarding the number of data sets used for the regression. The estimated kinetic and mass transfer parameters are presented in Table 3.1.

Table 3.1. Kinetic and mass transfer parameters estimated at 105ºC.

Parameter	*Value*	*Standard Error (%)*
$k_3'(L \cdot mol^{-1} \cdot min^{-1})$	$3.63 \cdot 10^{-6}$	15.1
$k_4'(L \cdot mol^{-1} \cdot min^{-1})$	$2.19 \cdot 10^{-7}$	16.8
$k_7'(L \cdot mol^{-1} \cdot min^{-1})$	$7.63 \cdot 10^{-7}$	10.4
$\kappa'\ (mol \cdot m^{-3})$	7.80	28.8
$\alpha_{HCl}\ (mol \cdot m^{-3})$	990.97	54.5
$\delta'\ (mol \cdot m^{-3})$	3992.66	69.4
$\alpha_W\ (mol \cdot m^{-3})$	1240.39	28.2
γ'	1.05	32.0
$k_G A_{GL}\ (m^3 \cdot s^{-1})$	$5.60 \cdot 10^{-5}$	2.5

For the sake of simplicity, the parameters α_W, α_{HCl}, γ' and δ' estimated at 105ºC were assumed constant for the temperatures studied. The data fitting of the kinetic model for the experiments at 70ºC, 80ºC, 90ºC and 120ºC is displayed in Figure 3.15.

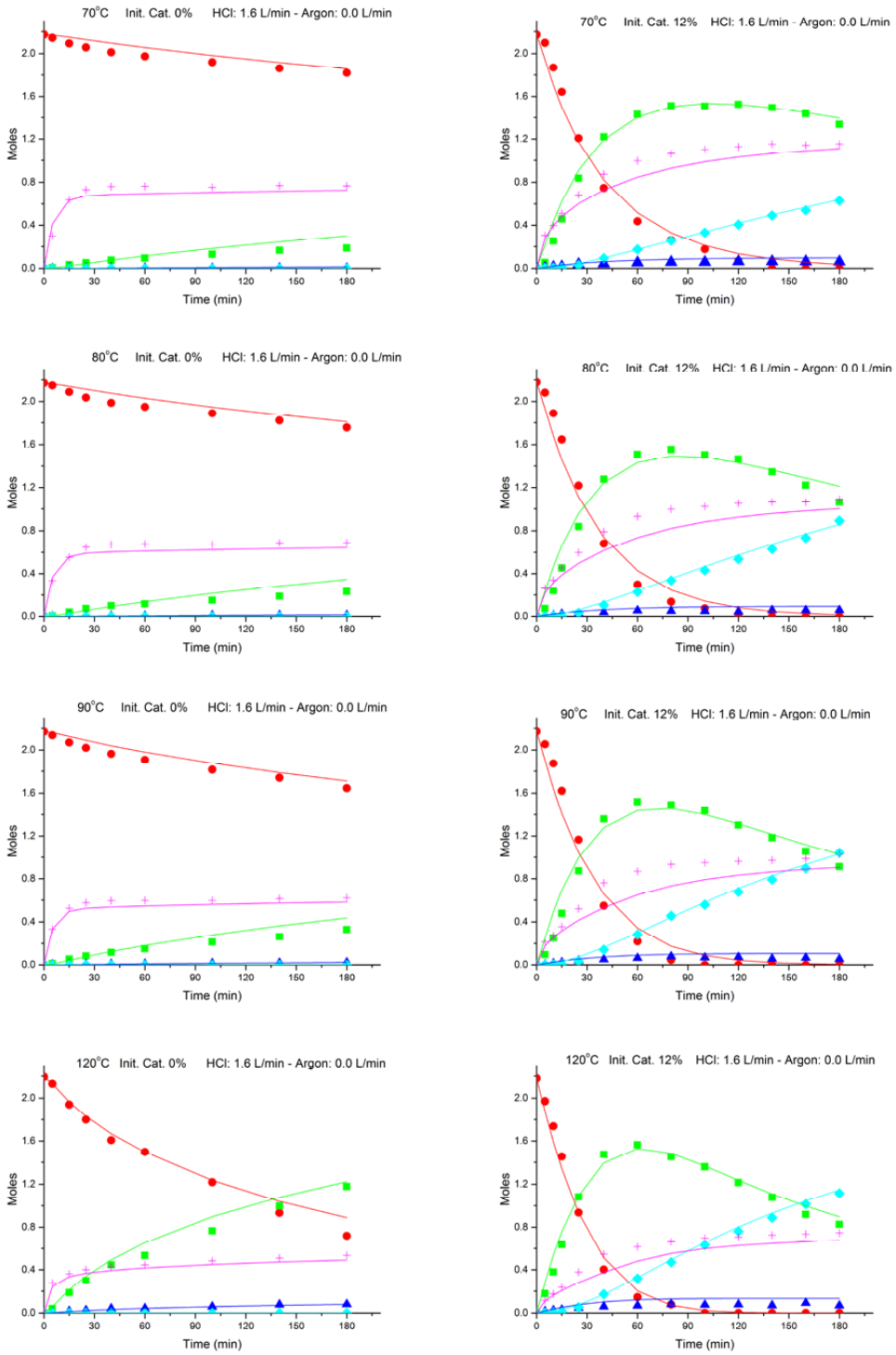

Figure 3.15. Kinetic model data fitting for the catalysed and non-catalysed experiments performed at 70ºC, 80ºC, 90ºC and 120ºC (moles of compounds in liquid phase).

The explanation degrees for the curves presented in Figure 3.15 are 99.1%, 98.6%, 98.3% and 98.1% for the temperatures of 70ºC, 80ºC, 90ºC and 120ºC, respectively. The results of the parameter estimation for these experiments are summarized in Table 3.2.

Table 3.2. Kinetic and mass transfer parameters estimated for the temperatures of 70ºC, 80ºC, 90ºC and 120ºC.

Temperature	*Parameter*	*Value*	*Error* (%)
70℃	$k_3'(m^3 \cdot mol^{-1} \cdot s^{-1})$	$6.45 \cdot 10^{-7}$	7.1
	$k_4'(m^3 \cdot mol^{-1} \cdot s^{-1})$	$3.08 \cdot 10^{-8}$	23.1
	$k_7'(m^3 \cdot mol^{-1} \cdot s^{-1})$	$1.90 \cdot 10^{-7}$	5.6
	$\kappa'\ (mol \cdot m^{-3})$	6.30	17.1
	$k_G A_{GL}\ (m^3 \cdot s^{-1})$	$6.30 \cdot 10^{-5}$	6.4
80℃	$k_3'(m^3 \cdot mol^{-1} \cdot s^{-1})$	$1.10 \cdot 10^{-6}$	10.4
	$k_4'(m^3 \cdot mol^{-1} \cdot s^{-1})$	$5.00 \cdot 10^{-8}$	29.5
	$k_7'(m^3 \cdot mol^{-1} \cdot s^{-1})$	$3.30 \cdot 10^{-7}$	5.9
	$\kappa'\ (mol \cdot m^{-3})$	6.38	16.6
	$k_G A_{GL}\ (m^3 \cdot s^{-1})$	$5.81 \cdot 10^{-5}$	7.8
90℃	$k_3'(m^3 \cdot mol^{-1} \cdot s^{-1})$	$1.81 \cdot 10^{-6}$	12.9
	$k_4'(m^3 \cdot mol^{-1} \cdot s^{-1})$	$9.40 \cdot 10^{-8}$	28.6
	$k_7'(m^3 \cdot mol^{-1} \cdot s^{-1})$	$5.13 \cdot 10^{-7}$	5.9
	$\kappa'\ (mol \cdot m^{-3})$	7.69	13.9
	$k_G A_{GL}\ (m^3 \cdot s^{-1})$	$5.55 \cdot 10^{-5}$	8.2
120℃	$k_3'(m^3 \cdot mol^{-1} \cdot s^{-1})$	$5.18 \cdot 10^{-6}$	12.6
	$k_4'(m^3 \cdot mol^{-1} \cdot s^{-1})$	$3.40 \cdot 10^{-7}$	19.1
	$k_7'(m^3 \cdot mol^{-1} \cdot s^{-1})$	$9.09 \cdot 10^{-7}$	4.4
	$\kappa'\ (mol \cdot m^{-3})$	23.78	12.2
	$k_G A_{GL}\ (m^3 \cdot s^{-1})$	$5.39 \cdot 10^{-5}$	6.0

The Arrhenius plots for the kinetic constants k_3', k_4' and k_7' are depicted in Figure 3.16. Table 3.3 presents the estimated values for the activation energies and pre-exponential factors.

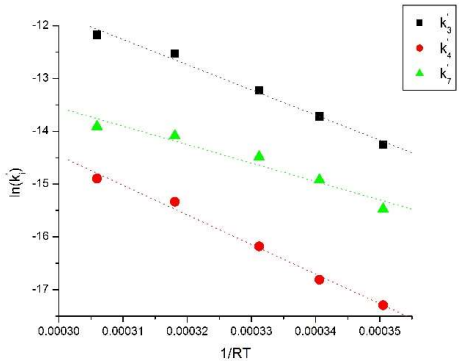

Figure 3.16. Arrhenius plot for the reaction constants k_3', k_4' and k_7' .

Table 3.3. Activation energies and pre-exponential factors for the reactions constants $k_3^{'}$, $k_4^{'}$ and $k_7^{'}$.

	$E_a(kJ/mol)$	lnA	R^2
k_3'	47.8	2.55	0.99
k_4'	56.1	2.37	0.99
k_7'	35.0	−3.06	0.95

The activation energies listed in Table 3.3 are in good agreement with the ones estimated by Luo et al. (2010) [47] when studying glycerol hydrochlorination using hydrochloric acid and acetic acid as catalyst.

By manipulating eqs. (3.8) and (3.9) so that the catalyst concentration is set to zero, it is possible to calculate the pure non-catalysed reaction constants (k_3'' and k_4''), which are defined as follows

$$k_3'' = k_3'\kappa' \tag{3.15}$$
$$k_4'' = k_4'\kappa' \tag{3.16}$$

Figure 3.17 presents the Arrhenius plots for the pure non-catalysed reaction constants.

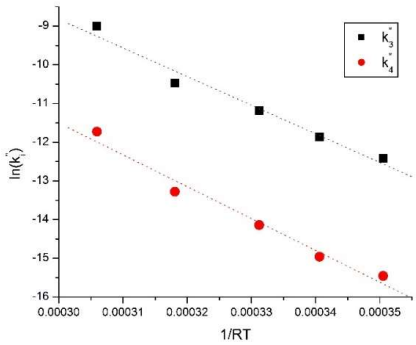

Figure 3.17. Arrhenius plots for the non-catalysed reaction rates.

Table 3.4 displays the activation energies and pre-exponential factors of parameters k_3'' and k_4''.

Table 3.4. Activation energies and pre-exponential factors for the non-catalysed glycerol hydrochlorination reaction

	$E_a(kJ/mol)$	lnA	R^2
k_3''	74.0	13.37	0.97
k_4''	82.3	13.19	0.98

As expected, the activation energies estimated for the non-catalysed glycerol hydrochlorination reaction are much higher than the ones calculated for catalytic process.

3.6.3. Catalyst Modulus

In order to corroborate the validity of the kinetic model presented in this Chapter, a novel concept named Catalyst Modulus (Ψ) was developed. Suppose that, hypothetically, the catalyst concentration could reach infinite. In this case, one could assume that the reaction rate for the formation of the desired product (r_7) would be maximum at this condition. The Catalyst Modulus is defined as the ratio between the real reaction rate and this maximum reaction rate. Mathematically it can expressed as

$$\Psi = \frac{r_7}{\lim\limits_{c_{cat0}\to+\infty} r_7} = \frac{\dfrac{k_7' c_{cat0} c_\alpha c_{HCl}^2}{c_{cat0} c_w + (\gamma' c_w + \delta') c_{HCl}}}{\lim\limits_{c_{cat0}\to+\infty} \dfrac{k_7' c_{cat0} c_\alpha c_{HCl}^2}{c_{cat0} c_w + (\gamma' c_w + \delta') c_{HCl}}} \tag{3.17}$$

Solving (3.17), the Catalyst Modulus can be calculated as

$$\Psi = \frac{c_{cat0} c_w}{c_{cat0} c_w + (\gamma' c_w + \delta') c_{HCl}} \tag{3.18}$$

Rearranging (3.18) in a more convenient way

$$\frac{1}{\Psi} = 1 + s\frac{1}{c_{cat0}} \tag{3.19}$$

where $s = c_{HCl}(\gamma' c_w + \delta')/c_w$.

Equation (3.19) was used for calculating the Catalyst Modulus for the series of experiments at different catalyst concentrations. Indeed, even though a variation of Ψ was observed at the beginning of each experiment, its value readily stabilized. By plotting the reciprocal of the stable value of Ψ and the reciprocal of the experimental value c_{cat0} a straight line is obtained. The data fitting is presented in Figure 3.18.

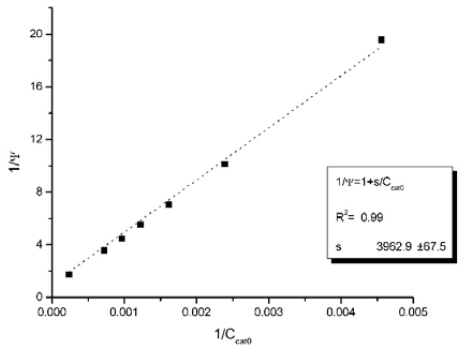

Figure 3.18. Reciprocal value of the calculated Catalyst Modulus plotted against the reciprocal value of the experimental catalyst concentration.

Figure 3.18 reveals an excellent fit of equation (3.19). The Catalyst Modulus is a theoretical parameter derived from our kinetic equations; the excellent agreement of this parameter when confronted with experimental data suggests that we are on the right path to comprehend the kinetics of glycerol hydrochlorination.

4. Reactive flash distillation technology

Experimental and mathematical evidences suggest that water exerts a negative effect on the glycerol hydrochlorination kinetics; thus, it has been claimed that the removal of water from the system might promote hydrochlorination. Santacesaria et al. (2010) [29] is the only literature source providing data on glycerol hydrochlorination under the conditions similar to reactive distillation. However, they report molar fractions of components in these experiments, but do not compare with their previously obtained results from semi-batch operation [35]. Indeed, by collecting the results presented in both articles, it is not completely clear whether the removal of water increases the reaction rate. For this reason, catalytic and non-catalytic reaction experiments under stripping conditions, i.e. reactive flash distillation, at different temperatures were carried out to compare their performances with the semi-batch data previously obtained (Chapter 3). In addition, the same analysis was extended to experiments by using a non-volatile catalyst, i.e. adipic acid. Finally, intending to investigate the influence of the initial liquid-phase composition on the hydrochlorination kinetics and HCl uptake, further semi-batch experiments were conducted by adding water or αγ-DCP.

4.1. Materials and methods

4.1.1. Reaction apparatus

The apparatus used for the reactive flash distillation experiments was very similar to the one used in the semi-batch experiments (Figure 3.1). The main difference was that the condenser was detached from the reactor and the volatile compounds were no longer returned to the reaction mixture. In fact, they were conducted outwards the reactor, where they would be condensed and collected. The unreacted and uncondensed HCl gas was bubbled into neutralization bottles, located past the condenser. Figure 4.1 gives a schematic overview of the reactive flash distillation setup.

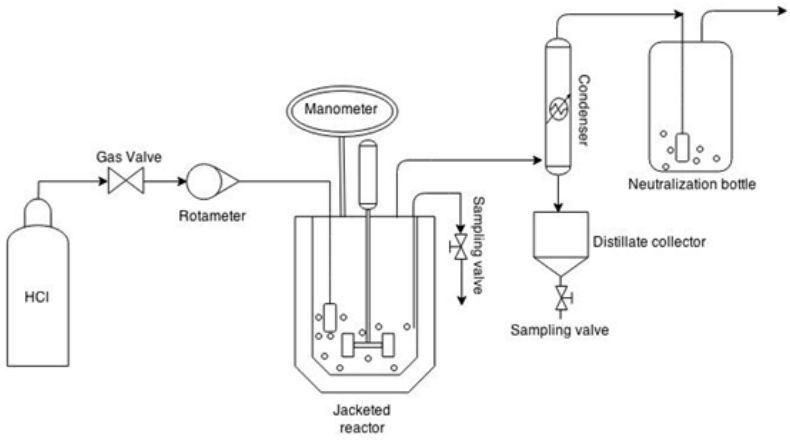

Figure 4.1. Overview of reactive flash distillation apparatus.

4.1.2. Reaction procedure

Firstly, glycerol was added to the reactor, being subject to vigorous stirring and heating until the reaction temperature was attained. Meanwhile, acetic acid was heated under stirring in a separate vessel; once acetic acid reached the reaction temperature, it was promptly weighted and added to the reactor. Immediately after this, the HCl gas flow was switched on and this moment was set to be "time zero". For the experiment performed using adipic acid as catalyst, glycerol and adipic acid were loaded together to the reactor, since the boiling point of adipic acid is too high to allow its evaporation under the reaction conditions.

4.1.3. Remarks on analysis

The analytical methods used for detecting the HCl mass fractions in the bulk liquid and GCD mole fractions were the same as described in Chapter 3. Nevertheless, under reactive flash distillation conditions, volatile compounds escape the reaction mixture and the liquid-phase volume cannot be estimated from equation (3.1). Therefore, the analytical results presented here are not calculated on volumetric basis, e.g. mol/L.

4.2. Distillate analysis results

The concentrations of the GCD compounds were extremely low in the distillate, under all reaction conditions studied. Indeed, the boiling points of these compounds are much higher than the studied temperature range (70-120ºC) and it is unlikely to consider they would evaporate in a large extent. Table 4.1 summarizes the atmospheric boiling points for the most abundant compounds present in the reaction system [62, 66] .

Table 4.1. Atmospheric boiling point of compounds present in the system.

	$T(°C)$
$Glycerol$	290
$\alpha - MCP$	213
$\alpha\gamma - DCP$	174
$Adipic\ acid$	338
$Acetic\ acid$	117
$Water$	100
HCl	−85

It is reasonable to assume that, mostly water, HCl and acetic acid are stripped from the liquid-phase under the studied reaction conditions. Figure 4.2 shows the cumulative mass of distillate for the catalytic and non-catalytic experiments conducted at different temperatures.

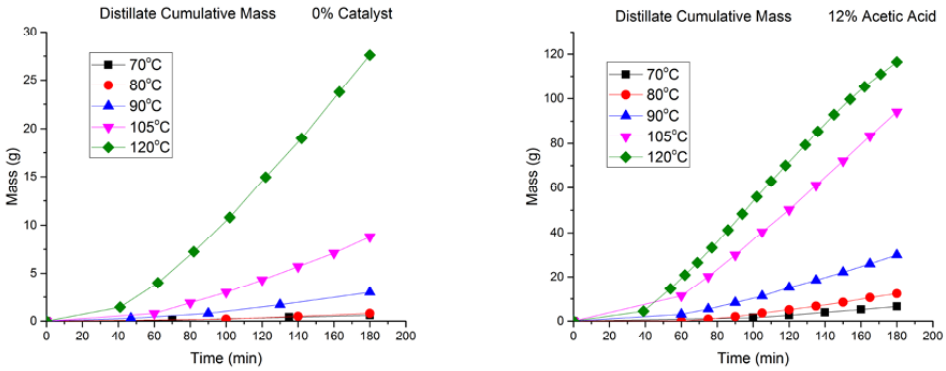

Figure 4.2. Cumulative mass of distillate collected for both catalytic (right) and non-catalytic (left) experiments performed at different temperatures.

The accumulated mass of distillate increases with temperature for both sets of experiments. In fact, at temperatures above 100ºC this increase is very sharp, strongly suggesting that water is the major component being condensed. As more water is produced in the catalytic experiments, the amount of liquid collected in the distillate is significantly higher. The HCl mass fractions in the distillate were analysed and the results are presented in Figure 4.3.

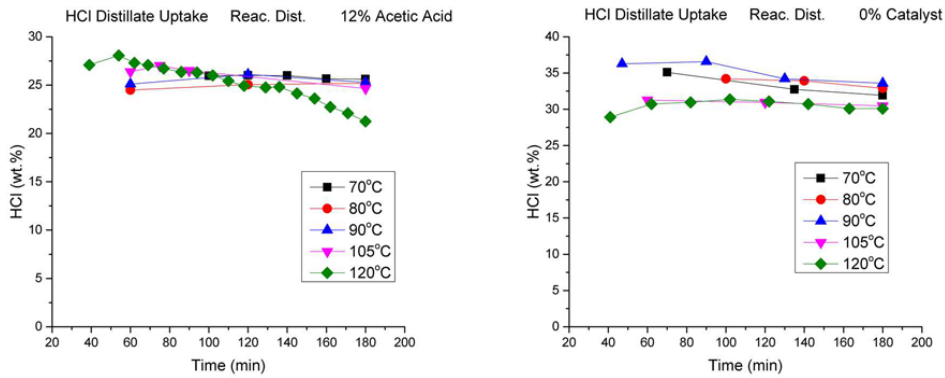

Figure 4.3. HCl uptake in distillate samples.

Interestingly, the HCl content in the distillate samples was very high for both sets of catalytic and non-catalytic experiments. At first, these results seemed quite intriguing because, as shown in Table 4.1, the boiling point of HCl is much lower than the condenser temperature (-4ºC). A reasonable explanation is that, the mechanism by which HCl is transferred to the distillate is not by condensation, but, by absorption. The liquid film of water condensed on the surface of the tube absorbs the HCl gas passing in the vicinity, therefore, dragging it to the condensed liquid. This provides strong evidence that the presence of water is crucial for the solubility of gaseous HCl.

4.3. Reactor analysis

In general, the effect of the reaction temperature on the glycerol consumption for experiments conducted under reactive flash distillation mode shows a nearly identical behaviour to that observed in the semi-batch conditions, as displayed in Figure 4.4.

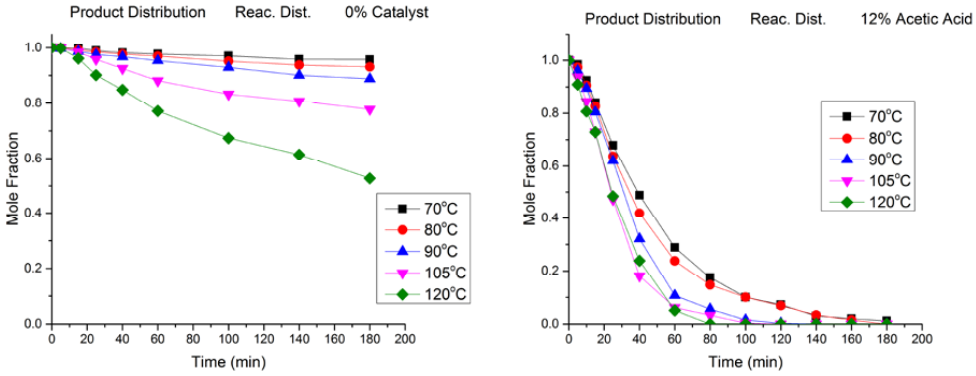

Figure 4.4. Glycerol mole fractions for non-catalytic and catalytic reactive flash distillation experiments conducted at different temperatures.

The HCl liquid uptake for the corresponding experiments presented in Figure 4.4 showed an unforeseen behaviour, which is depicted in Figure 4.5.

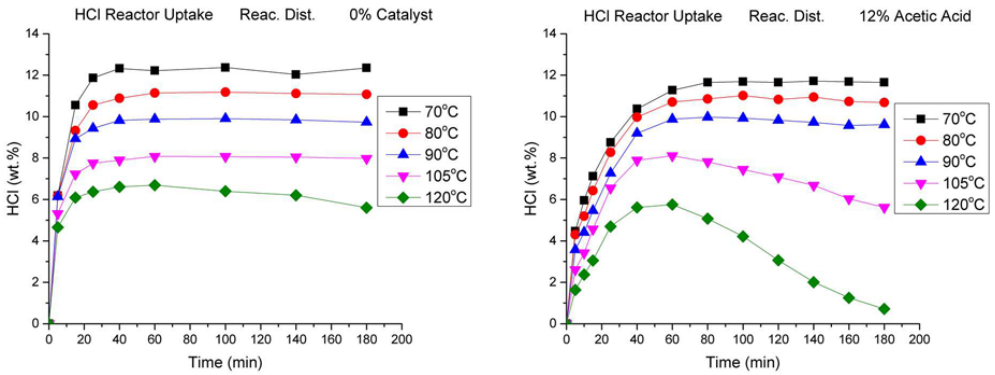

Figure 4.5. HCl liquid uptake for catalytic and non-catalytic reactive flash distillation experiments performed at different temperatures.

Surprisingly, for the experiments performed at temperatures close or exceeding the boiling point of water (100ºC), the HCl uptake goes through a maximum but declines thereafter. This implies that the presence of water plays a major role on the HCl uptake in the reaction mixture.

In fact, based on literature studies [51, 65, 67, 68], it was confirmed that the substitution of an OH group by a chlorine group in mono and di-alcohols, dramatically decreases the solubility of HCl. Furthermore, other references [51, 65, 69] suggest that, although HCl solubility may be high in glycerol, HCl is be present as a weak electrolyte, because the ability of glycerol to receive a proton is very limited (glycerol pKa=4.4 [70]).

Hence, it is reasonable to assume that, at the beginning of the reactive flash distillation experiments, glycerol is the seed that promotes HCl solubility and dissociation. Shortly after, as glycerol is consumed and water is produced, the solubility and dissociation of HCl is mainly promoted by water molecules. However, if the water is allowed to leave the liquid-phase, the reaction mixture becomes more concentrated with chlorohydrins, which have lower solubility to HCl, causing the HCl uptake to drop.

4.4. Comparison of reactive flash distillation and semi-batch technologies

4.4.1. Non-catalytic experiments

Figure 4.6 presents the product distribution and HCl liquid uptake for the experiments conducted in the absence of the catalyst.

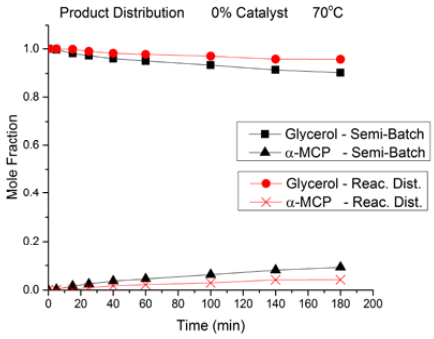
Product Distribution 0% Catalyst 70°C
Mole Fraction
Time (min)
Glycerol - Semi-Batch
α-MCP - Semi-Batch
Glycerol - Reac. Dist.
α-MCP - Reac. Dist.

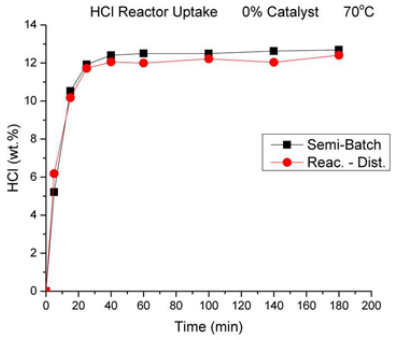
HCl Reactor Uptake 0% Catalyst 70°C
HCl (wt.%)
Time (min)
Semi-Batch
Reac. - Dist.

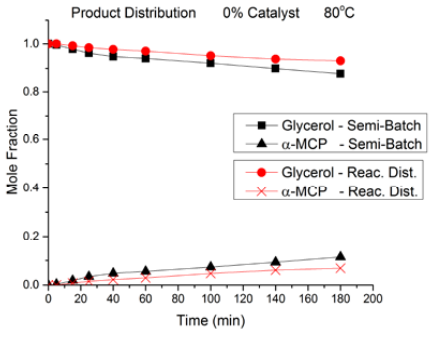
Product Distribution 0% Catalyst 80°C
Mole Fraction
Time (min)
Glycerol - Semi-Batch
α-MCP - Semi-Batch
Glycerol - Reac. Dist.
α-MCP - Reac. Dist.

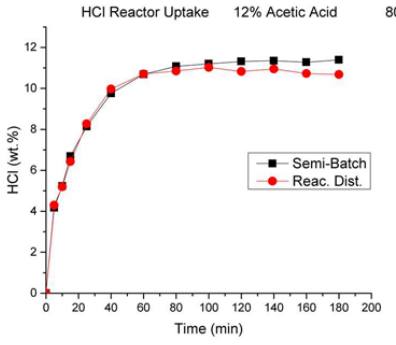
HCl Reactor Uptake 12% Acetic Acid 80°C
HCl (wt.%)
Time (min)
Semi-Batch
Reac. Dist.

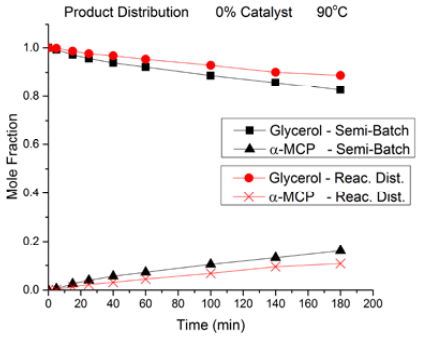
Product Distribution 0% Catalyst 90°C
Mole Fraction
Time (min)
Glycerol - Semi-Batch
α-MCP - Semi-Batch
Glycerol - Reac. Dist.
α-MCP - Reac. Dist.

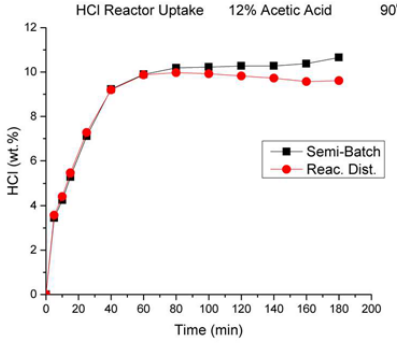
HCl Reactor Uptake 12% Acetic Acid 90°C
HCl (wt.%)
Time (min)
Semi-Batch
Reac. Dist.

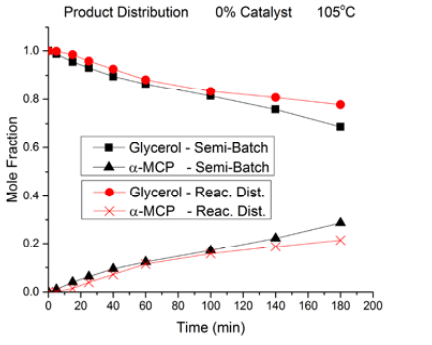
Product Distribution 0% Catalyst 105°C
Mole Fraction
Time (min)
Glycerol - Semi-Batch
α-MCP - Semi-Batch
Glycerol - Reac. Dist.
α-MCP - Reac. Dist.

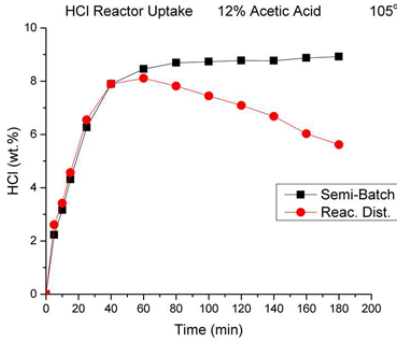
HCl Reactor Uptake 12% Acetic Acid 105°C
HCl (wt.%)
Time (min)
Semi-Batch
Reac. Dist.

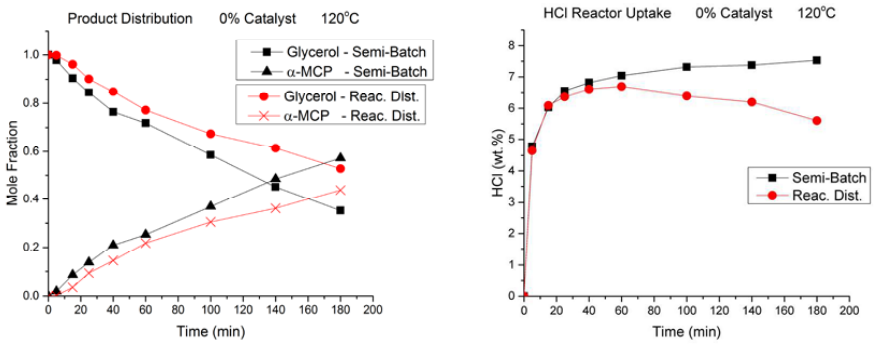

Figure 4.6. Product distribution and HCl uptake comparison for non-catalytic experiments performed in semi-batch and reactive flash distillation regimes.

Figure 4.6 reveals that, the glycerol consumption and HCl liquid uptake are higher for semi-batch than for reactive distillation experiments. The stripping of water in the reactive distillation experiments is assumed to be the cause of the observed effect. Under non-catalytic conditions, the HCl solubility and dissociation in the reaction mixture becomes seriously supressed by the evaporation of water, causing a diminishment in the observed hydrochlorination rate.

4.4.2. Acetic acid catalysed experiments

The product distribution and the liquid-phase uptake of HCl for semi-batch and reactive flash distillation experiments performed with 12% acetic acid are presented in Figure 4.7.

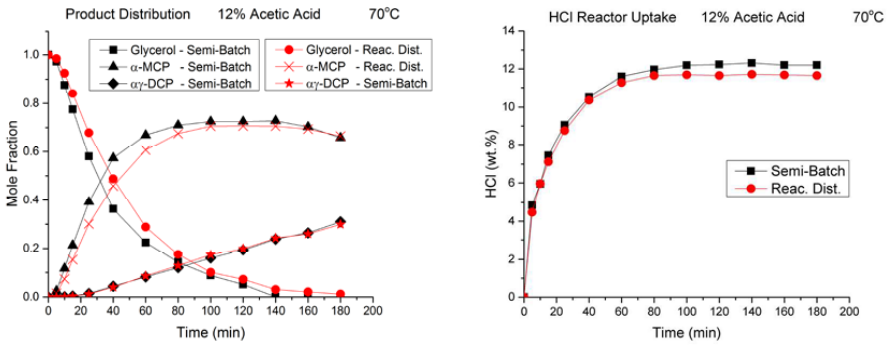

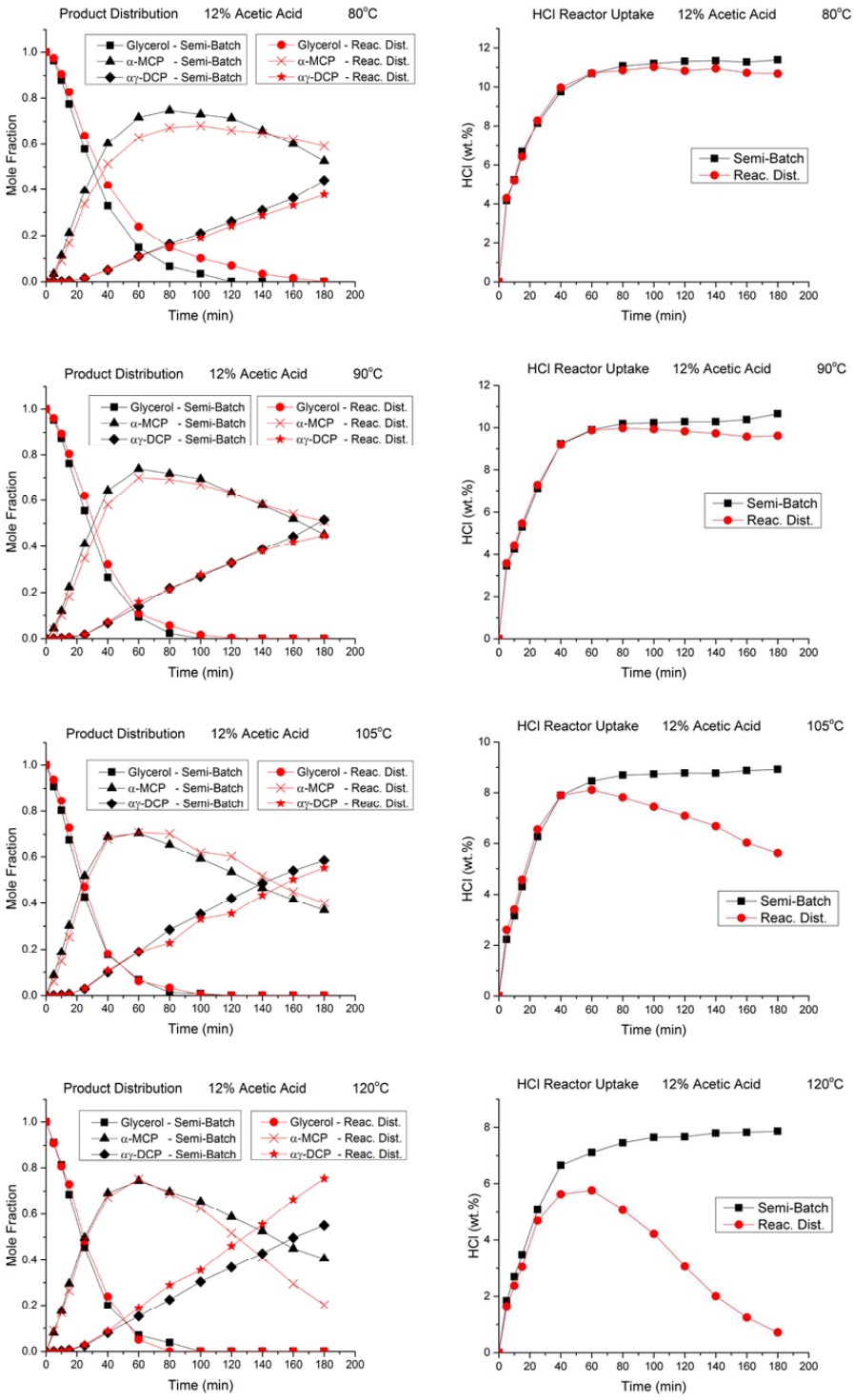

Figure 4.7. Product distribution and HCl liquid uptake for the acetic acid catalysed experiments performed in semi-batch and reactive flash distillation mode.

The differences between glycerol mole fractions observed in semi-batch and reactive flash distillation experiments suggest that, at temperatures under 100ºC, the first chlorination step is disfavoured in reactive distillation. However, as the temperature increases, this difference diminishes, until it becomes virtually nil for the experiments at 105ºC and 120ºC. On the other hand, the discrepancy between the liquid-phase uptake of HCl between semi-batch and reactive flash distillation increases sharply with temperature. This is evidence that the removal of water increases the glycerol hydrochlorination rate despite the decrease in HCl uptake.

In fact, the only experiment that showed a higher yield of the desired product (αγ-DCP) under reactive flash distillation conditions was the one at 120ºC. Even though the HCl uptake had decreased significantly in this experiment, due to the substantial water removal, the kinetic effect of water compensates the decrease of the HCl solubility and dissociation.

4.4.3. Non-volatile catalyst experiments

As the catalytic experiments presented were carried out in the presence of acetic acid, the issue of the catalyst volatility could be raised. In this sense, additional experiments were performed using adipic acid as the catalyst, aiming to evaluate the performances of the semi-batch and reactive flash distillation systems in which the catalyst would not evaporate at all. The results obtained are depicted in Figure 4.8.

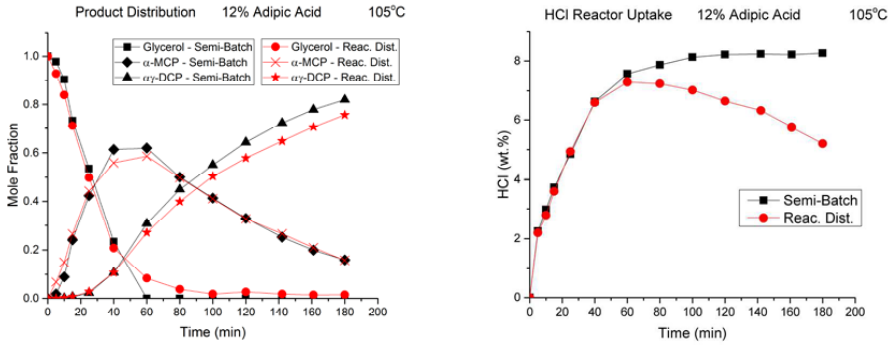

Figure 4.8. Product distribution and HCl liquid uptake for semi-batch and reactive flash distillation experiments performed using 12% of adipic acid as catalyst.

The observed product distribution and HCl uptake were very similar to the experiment carried out in the presence of acetic acid at 105ºC (Figure 4.7). Therefore, it might be assumed that the volatility of acetic acid did not influence significantly the experiments previously discussed. In fact, even though the catalyst might partially escape from the liquid-phase, it was shown in Chapter 3 that, the catalyst concentration does not influence very significantly the hydrochlorination kinetics (Figure 3.7).

4.5. Influence of the initial liquid composition

The somewhat unexpected phenomena observed in the reactive flash distillation experiments provided conclusive evidences that the glycerol hydrochlorination with gaseous HCl gas was strongly influenced by the presence of water. In order to get further insight on how the liquid-phase composition affects both the product distribution and the HCl uptake, four additional experiments were carried out with various amounts of water added. Semi-batch mode was chosen in order not to mix the effects observed with considerations concerning the evaporation of the liquid-phase compounds.

The results are presented in Figure 4.9. The experiments assigned with indexes (1)-(4) had different initial amounts of water added. Experiment (5) had αγ-DCP added in the same molar fraction as water was added in experiment (2). αγ-DCP does not react in the system and has a viscosity of approximately 70 times lower than that of glycerol at room temperature [66, 71]. The composition of each experiment is presented in Figure 4.9.

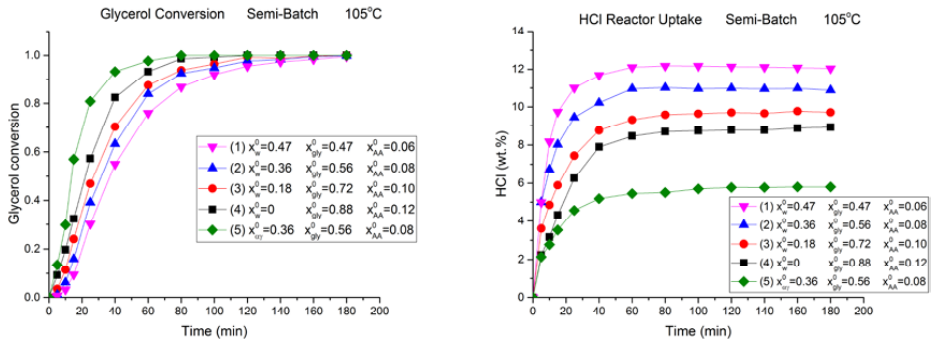

Figure 4.9. Effect of initial liquid-phase composition on glycerol conversion and HCl liquid uptake in semi-batch experiments.

As the initial amount of water in the liquid-phase increases, the HCl uptake also increases, evidencing that the presence of water really enhances the HCl uptake in the liquid-phase. The HCl uptake for experiment (5) is much lower because αγ-DCP has a significantly lower solubility of HCl than water and glycerol [51, 65].

Analysing the product distribution for experiments (1)-(4), it is noticed that the glycerol conversion rate is slower for increasing initial amounts of water added. Nevertheless, no conclusive remark can be made about this observation, because the catalyst concentration is also decreased.

By comparing experiments (2) and (5), which have exactly the same initial mole fractions of glycerol and catalyst, one can clearly see that the glycerol conversion is much faster for experiment (5). This might be attributed to the retarding role that water exerts in glycerol hydrochlorination.

Surprisingly, experiment (5) showed a faster performance even when compared to experiment (4), carried out in the absence of any additionally added compound. This can be explained by the

diminishment of the polarity of the liquid phase, caused by the excess of αγ-DCP. It has been summarized by Reichardt and Welton [72] and Amis [73] that, reactions which depend upon the interaction of ions of different charges (in our case, I_1^+ and Cl^-, I_2^+ and Cl^-) are positively affected by a diminishment of the solvent polarity. For the case of experiment (5), the HCl uptake is much lower than all the other experiments, therefore, the liquid phase polarity should be dramatically lower in that case. Such result may be of great industrial importance, because it suggests that the desired product (αγ-DCP) could be recycled to the reactor and be used as a "perfect solvent" for the glycerol hydrochlorination: it is produced by the system, it decreases the HCl consumption, it enhances the reaction rate and it does not require any additional separation unit downstream.

5. Continuous reactor technology

Continuous reactor technology is often preferred over batch/semi-batch operation due to its higher throughput capacity, lower operating costs, stable operation and easy to control. The performance of glycerol hydrochlorination in a continuous reactor apparatus was evaluated on a co-current isothermal bubble column reactor. A classic bubble column reactor was selected due to the simplicity of its construction, which allows a high liquid content and high interphase mass transfer rates. The influence of characteristic process parameters, such as liquid flow rate, gas flow rate, temperature and catalyst concentration was thoroughly investigated by a large set of experiments. Residence time distributions (RTD) and high-speed camera images were used to characterize the flow inside the reactor. The system presented interesting fluid dynamics, similar to vertical tubular absorbers. Axial dispersion model was used to describe the transient behaviour of the system. The kinetic and solubility parameters estimated in Chapter 3 were used in the modelling. Fluid dynamic and mass transfer parameters were successfully estimated based on the experimental data obtained in the laboratory-scale continuous reactor.

5.1. Materials and methods

5.1.1. Experimental setup

The experiments were conducted in a 66 cm long glass-jacketed bubble column reactor, vertically positioned. The internal diameter of the tube was 1.62 cm. Both the gaseous hydrogen chloride and the liquid phase were inserted from the bottom of the reactor. The liquid-phase flow was provided by a piston pump (Smartline 100, KNAUER GmbH). A rotameter controlled the gas inlet flow and a fine glass sinter (porosity P3, ISO 4793, max. pore size 16-40 μm) provided the bubbling of the gas phase into the liquid. A thermocouple was inserted from the top of the reactor to measure the temperature. Samples were withdrawn by means of a three-way valve placed at the reactor outlet and immediately quenched to -4ºC. The gas-liquid mixture leaving the column reactor was conducted to a separator, where the liquid was collected and the gas was bubbled into neutralization bottles containing concentrated solutions of sodium hydroxide. All the experiments were conducted at atmospheric pressure. An overview of the continuous bubble column system is depicted in Figure 5.1.

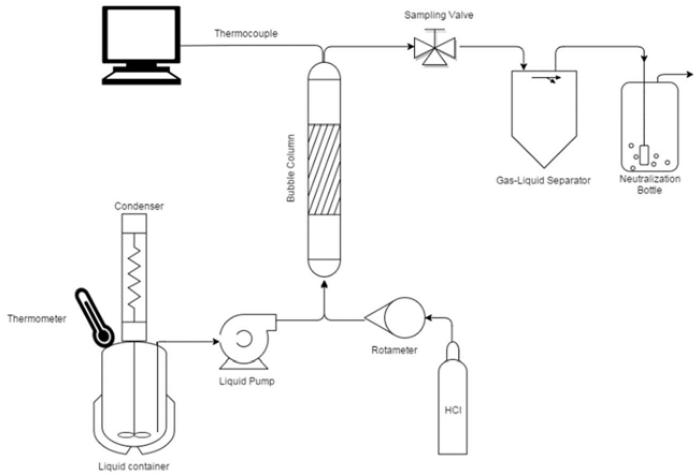

Figure 5.1. Schematic overview of the continuous bubble column system.

The high-speed camera used was a FastCam SA3 model produced by Photrom™. The pixel density in all pictures was 1024 x 1024 and the frame rate varied between 125-500 fps depending on the gas flow rate and light conditions.

5.1.2. Experimental procedure

Approximately 1.2 kg of a mixture containing the desired concentrations of glycerol and acetic acid was loaded to a three-necked round-bottom liquid container (Figure 5.1). The container was placed in a heating vessel, set at the reaction temperature, under vigorous stirring of the liquid phase. A thermometer was inserted through one of the necks of the container to monitor the liquid temperature. Catalyst evaporation was prevented by attaching a condenser at -4ºC to the liquid container. Meanwhile, the heating jacket of the reactor was set at the reaction temperature. When both the liquid container and the heating jacket had attained the desired temperature, the piston pump was started to fill the reactor. Once the reactor was ca. 80% filled, the HCl gas flow was switched on and this moment was set to be “time zero”.

The residence time distribution (RTD) in the column reactor was determined by step response experiments. At a certain reaction time (≈ 52 min), as the steady-state was presumed to be achieved, the tracer (αβ-DCP) was injected (ca. 1.5-2mL) in the liquid container. It should be noticed that, even though αβ-DCP is a product of the hydrochlorination reaction, its concentration was negligible before the tracer injection, because the selectivity towards this compound is close to zero under the experimental conditions (vide Chapters 3 and 4). More details about the use of αβ-DCP as a tracer for the RTD experiments are given in Section 5.4.5. The concentration of the tracer was measured at the reactor outlet and analysed off-line by gas chromatography.

5.2. Fluid dynamic regimes and flow visualization

Gaseous hydrogen chloride has a high solubility in glycerol and water, (Chapters 3 and 4), which has a huge impact on the fluid dynamics of glycerol hydrochlorination in bubble columns. In fact, the mass transfer rate of HCl to the liquid phase is so high that the fluid dynamics of the bubble column can be generally described as a vertical tubular absorber [74, 75]. The present system is located in a particular intersection, where the reaction engineering aspects of a bubble column reactor meet the high gas-liquid mass transfer rates of vertical tubular absorbers, which are commonly applied in refrigeration cycles. Figure 5.2 gives a general illustration of the flow regimes present in the bubble column.

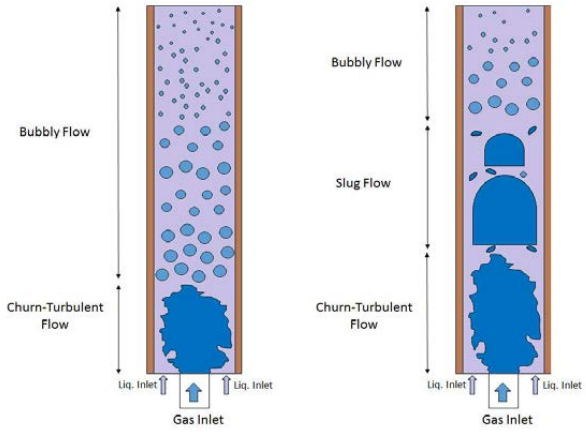

Figure 5.2. Overview of the flow regimes inside the bubble column reactor. (Left) Liquid flow: 6 mL/min, gas flow: 0.4-1.0 L/min. (Right) Liquid flow: 6 mL/min, gas flow: 1.2 L/min.

It was visually observed that the flow of HCl suffered a significant diminishment along the reactor. At the inlet, a churn-turbulent (approximately 6 cm long) regime was observed, where gas bubbles were large and intense mixing took place. Past this zone, the bubbles were small and finely dispersed. Taitel et al. [76] and Infante [74] described the churn-turbulent zone as an inlet effect, associated with the existence of slug flow further along the tube. However, at gas flow rates of 0.4-1.0 L/min, the HCl absorption at the inlet was so pronounced that the slug flow regime was completely suppressed. However, if the gas flow was increased to 1.2 L/min, the churn-turbulent zone expanded and Taylor bubbles started emerging from it, characterizing the establishment of the slug flow regime.

The formation of Taylor bubbles was an undesired phenomenon in our system. Because of their large dimensions, as they travel along the tube, they flush the column of liquid on top of them outwards. This effect causes the reactor to be partially emptied. Furthermore, it raises concerns involving the safe operation of the reactor, because this flushing is followed by a significant vibration of the reactor tube. Therefore, the formation of a slug flow regime was avoided. The elaboration of a detailed flow map was out of the scope of the present study, so, in practice, the experimental constraints applied to ensure the suppression of the slug flow were: liquid flow rate $\geq$ 6 mL/min and HCl flow rate $\leq$ 1.0 L/min.

In order to illustrate the very interesting fluid dynamics of the system, high-speed camera images were recorded at three different elevations of the reaction tube (inlet, middle and top positions). Figure 5.3 presents a sample of these images.

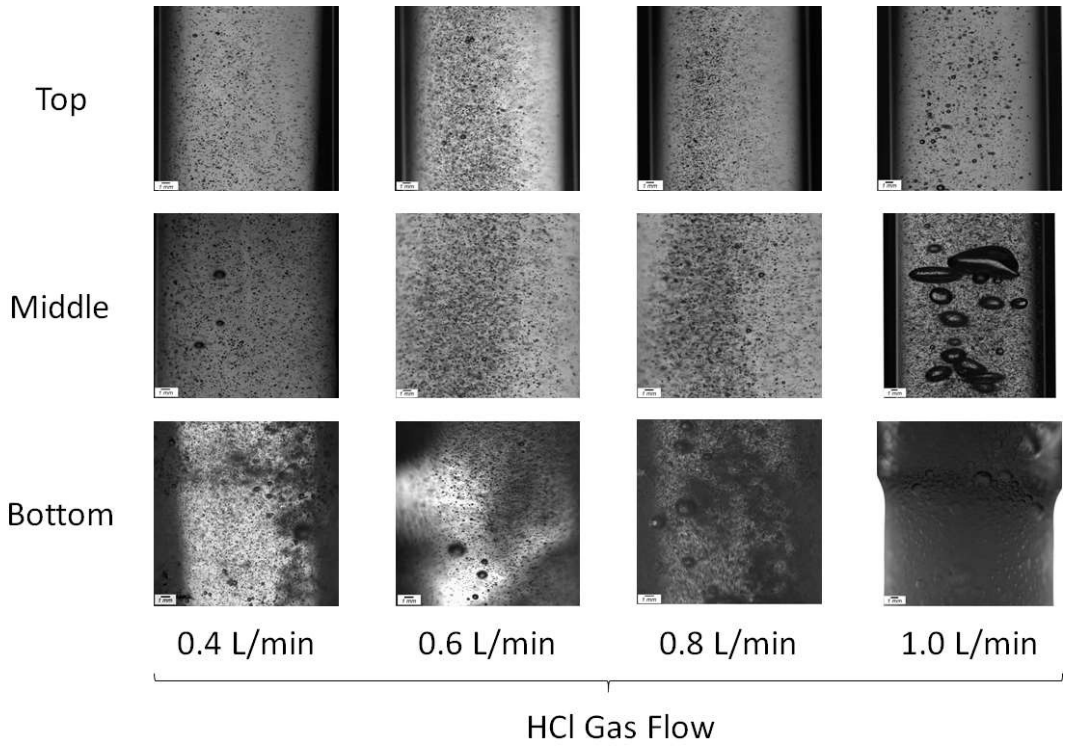

Figure 5.3. Experiments conducted at 105ºC, 3% of acetic acid (catalyst) and 6 mL/min of liquid-phase. Each image was recorded with a different focal depth, which was chosen according to the light conditions and ability to capture sharp images. A scale is provided in the corner of each image.

The froth formed at the bottom of the reactor increased with an increasing gas flow rate. In this region, the HCl absorption was so pronounced that gas bubbles shrink and disappear in a matter of few milliseconds. For gas flows of 0.4-0.8 L/min, the middle and top sections of the bubble column show a finely dispersed bubbly flow. However, at the HCl flow rate of 1.0 L/min, large wobbled bubbles begin to emerge from the churn-turbulent zone; these bubbles do not reach the top of the reactor, because they dissolve along the way. Nevertheless, they indicate the beginning of the flow regime transition to slug flow. Similar fluid dynamics has been reported by Rennie and Smith [77] who presented high-speed camera images of the breakdown of ammonia-air mixtures in an acid solution. Figure 5.4 depicts the coalescence happening in a Taylor bubble at the middle part of the reactor tube as the gas flow was switched to 1.2 L/min.

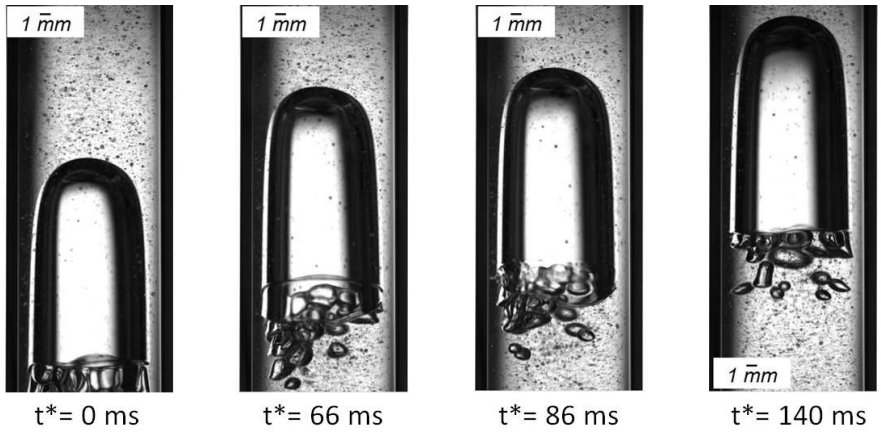

Figure 5.4. Coalescence in a Taylor bubble. Reaction conditions: 105ºC, 3% acetic acid, 6 mL/min liquid flow rate and 1.2 L/min gas flow rate. Image recorded from the middle section of the reactor.

An attempt was made to conduct a non-catalytic experiment at 105ºC, 6 mL/min of liquid flow and 0.8 L/min of gas flow. From 0 to 25 minutes of experiment, the fluid dynamics behaved just like a catalytic experiment under similar conditions. However, after 25 minutes, the slug flow regime was established and the experiment halted. The significant decline of the reaction rate caused by the absence of the catalyst was responsible for the accumulation of unreacted HCl at the churn-turbulent zone, causing the formation of Taylor bubbles [78, 79]. Thus, it is concluded that the hydrochlorination reaction itself influences the hydrodynamic regimes observed in the bubble column.

Another experiment at 105ºC, 6 mL/min of liquid flow and 0.8 L/min of gas flow was attempted. This time, αγ-DCP was added to the liquid phase, using the same composition as in experiment (5) in Figure 4.9. From 0 to 15 minutes of experiment, the fluid dynamics behaved "normally". However, the slug regime was stablished shortly after. The reason is attributed to the decrease in the HCl solubility in the liquid phase due to the addition of αγ-DCP to the liquid mixture, as previously evidenced by Figure 4.9. The accumulation of unreacted HCl caused the formation of the Taylor bubbles.

Due to the fluid dynamic limitations previously described, the conditions did not favour high conversions of glycerol. The desired product, αγ-DCP, was formed in very low amounts and the main hydrochlorination product detected in all the experiments was α-MCP. Certainly, many alternatives may be discussed that could possibly circumvent the low glycerol conversion in the system, such as changes to the reactor design or even addition of another reaction unit connected in series with the bubble column. However, due to time constraints and spatial limitations it was not feasible to do so within the timeframe of this study. Hopefully, these issues shall be addressed in future investigations.

5.3. Change of liquid volumetric flow rate

As discussed in Section 3.2, the liquid volume increased with time for the experiments conducted under semi-batch conditions (Figure 3.2). An analogous phenomenon was noticed when performing glycerol hydrochlorination in the bubble column: the outlet volumetric flow of the liquid increased. As in the semi-batch reactor, the main reason for such a change is due to the significant accumulation of HCl in the liquid phase. In that sense, an analogous form of equation (3.1) was used to describe the liquid volumetric flow at the outlet ($\dot{V}_L(L,t)$),

$$\dot{V}_L(L,t) = \frac{\sum \dot{m}_{GCD_i}}{\rho_{gly}} + \frac{\dot{m}_{cat}}{\rho_{cat}} + \frac{\dot{m}_w + \dot{m}_{HCl}}{\rho_w} \tag{5.1}$$

where $\dot{m}_i$ is the mass flow rate of compound i. The mass flow rates of the compounds were calculated analogously to equations (3.2), (3.3), (3.4) and (3.6),

$$\dot{m}_{cat} = MM_{cat}\dot{n}^0_{cat} \tag{5.2}$$

$$\dot{m}_{GCD_i} = MM_i x'_{GCD_i}\dot{n}^0_{gly} \tag{5.3}$$

$$\dot{m}_w = MM_w\left[MM_\alpha\dot{m}_\alpha + MM_\beta\dot{m}_\beta + 2\left(MM_{\alpha\gamma}\dot{m}_{\alpha\gamma} + MM_{\alpha\beta}\dot{m}_{\alpha\beta}\right)\right] \tag{5.4}$$

$$\dot{m}_{HCl} = \frac{w_{HCl}}{1 - w_{HCl}}\left(\sum \dot{m}_{GCD_i} + \dot{m}_{cat} + \dot{m}_w\right) \tag{5.5}$$

where $\dot{n}^0_{gly}$ and $\dot{n}^0_{cat}$ are the inlet molar flow rate of glycerol and acetic acid, respectively. By applying a mass balance on the liquid container, $\dot{n}^0_{gly}$ and $\dot{n}^0_{cat}$ are found to be

$$\dot{n}^0_{gly} = \frac{\dot{V}^0_L}{\frac{MM_{gly}}{\rho_{gly}}x^0_{gly} + \frac{MM_{cat}}{\rho_{cat}}x^0_{cat}}x^0_{gly} \tag{5.6}$$

$$\dot{n}^0_{cat} = \frac{\dot{V}^0_L}{\frac{MM_{gly}}{\rho_{gly}}x^0_{gly} + \frac{MM_{cat}}{\rho_{cat}}x^0_{cat}}x^0_{cat} \tag{5.7}$$

where $\dot{V}^0_L$ is the volumetric flow rate set by in the piston pump and x^0_i is the mole fraction of compound i inside the liquid container. The concentrations of the compounds at the outlet were estimated from

$$C_i(L,t) = \frac{\dot{n}_i}{\dot{V}_L(L,t)} \tag{5.8}$$

The formal treatment given to equation (5.1) is of practical importance when calculating the liquid-phase volumetric flow at the reactor outlet ($z = L$), but it is not useful in describing the liquid volumetric flow at different points inside the tube. As HCl is absorbed by the liquid phase, the total concentration of compounds increase, so does the liquid flow rate. Therefore, eq. (5.9) is proposed

for describing the liquid flow rate inside the reactor as a function of the total concentration of compounds, at any given time and position

$$\dot{V}_L(z,t) = \dot{V}_L^0 + b(C_T(z,t) - C_T^0) \tag{5.9}$$

where $C_T(z,t)$ is the sum of the concentrations of all compounds in the liquid phase at a given time t and position z. C_T^0 is the total concentration of compounds in the inlet flow and b is a fitting parameter. It is trivial to verify that (5.9) is true for $z = 0$. However, if (5.9) is valid, it should also give approximately the same values of liquid flow rate at the outlet as equation (5.1). By setting $z = L$ in (5.9), we are able to compare the results estimated by equation (5.1) and (5.9), which are presented by Figure 5.5.

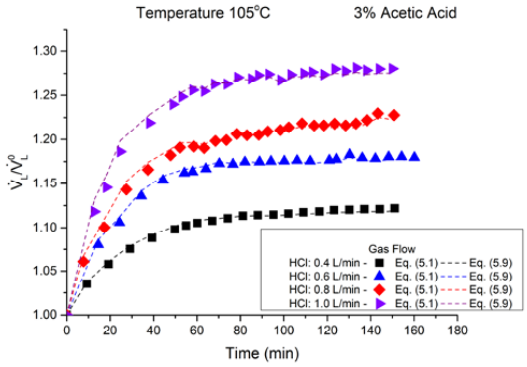

Figure 5.5. Ratio between the outlet and inlet liquid volumetric flows under transient conditions. The dots represent the values calculated by equation (5.1) and the dashed lines represent the values calculated by equation (5.9).

Figure 5.5 presents the transient effect of the liquid flow rate increase for experiments carried out at different HCl gas flow rates. We may conclude, from Figure 5.5, that equation (5.9) constitutes an excellent approximation of the liquid volumetric flow rate at the outlet at different times, as predicted by equation (5.1). As (5.9) holds true for the system boundaries, i.e. $z = 0$ and $z = L$, we assume that (5.9) is valid for all positions inside the reactor. The fitting parameter b was estimated individually for each experiment and inserted in the parameter estimation subroutine. It is important to point out that, for the experiments depicted in Figure 5.5, the flow rate increased monotonically until it reached the steady-state, showing an augment of 10-27% of the liquid flow rate compared to the inlet.

5.4. Experimental results

5.4.1. Effect of HCl gas flow rate

The influence of the HCl gas flow rate was evaluated by means of two sets of experiments carried out with different catalyst concentrations (3% and 12% catalyst). The steady-state results obtained are displayed in Figure 5.6.

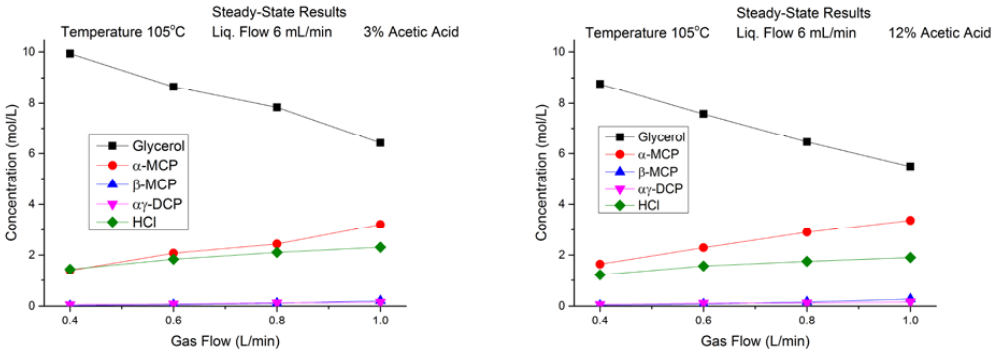

Figure 5.6. Outlet concentration of compounds at the steady-state, depicting the effects of HCl gas flow rates on product distribution and liquid uptake of HCl.

The HCl flow rate shows a significant impact on the glycerol conversion for both sets of experiments. It is observed that, the conversion of glycerol and the liquid uptake of HCl increase with the increase of HCl gas flow rate, similar to the effect of HCl partial pressure discussed in Chapter 3.

5.4.2. Effect of liquid flow rate

The effect of the liquid flow rate was investigated by four sets of experiments carried out at different temperatures. The steady-state results obtained are depicted in Figure 5.7.

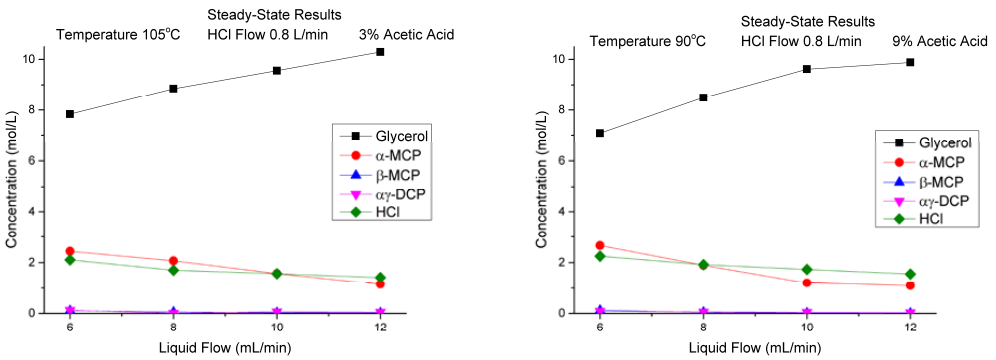

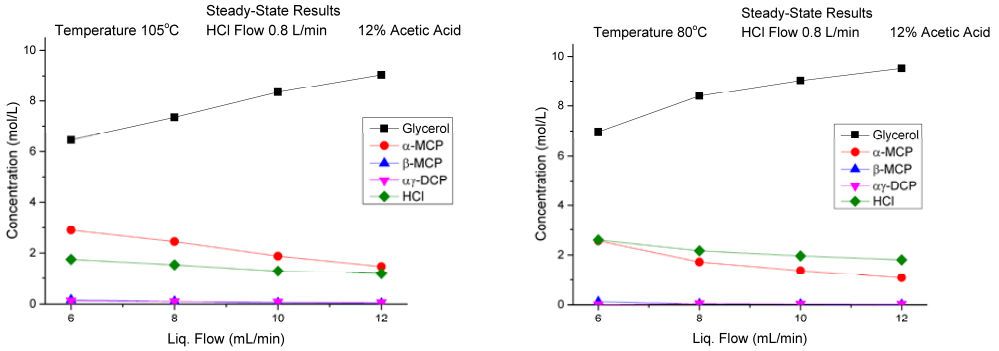

Figure 5.7. Outlet concentration of compounds at the steady-state, depicting the effects of liquid flow rate on product distribution and liquid uptake of HCl.

The liquid-flow rate strongly influences the product distribution. As the liquid flow rate increases, the conversion of glycerol and liquid uptake of HCl decrease, which is a natural consequence of the diminishment of the liquid residence time in the reactor.

5.4.3. Temperature effect

The effect of temperature on the glycerol conversion and product distribution was studied by two sets of experiments conducted at different catalyst concentrations, as displayed by Figure 5.8.

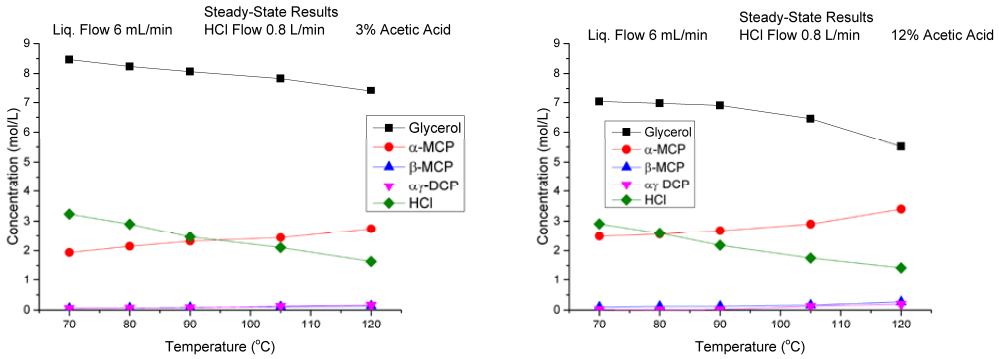

Figure 5.8. Outlet concentration of compounds at the steady-state, depicting the influence of temperature on product distribution and liquid uptake of HCl.

The results reveal that the hydrochlorination reaction is enhanced by an increase of the reaction temperature. As expected, the uptake of HCl in the liquid-phase diminished with the increase of temperature due to the decrease of the liquid-phase solubility of HCl, as discussed in Chapters 3 and 4.

5.4.4. Catalyst concentration effect

Four experiments were conducted at 105ºC, with the liquid flow rate of 6 mL/min, gas flow rate of 0.8 L/min and different catalyst concentrations (3, 6, 9 and 12%). The steady-state results obtained are shown in Figure 5.9.

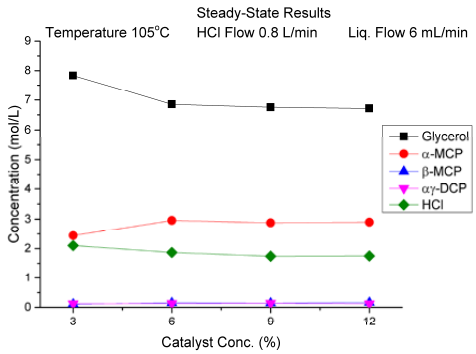

Figure 5.9. Outlet concentration of compounds at the steady-state, depicting the influence of catalyst concentration on product distribution and liquid uptake of HCl.

The catalyst concentration shows a minor effect on the outlet composition, in the range of 6-12% catalyst. This is in excellent agreement with the catalyst concentration effect observed in the semi-batch experiments, as discussed in Figure 3.7.

5.4.5. Residence time distribution experiments (RTD)

The liquid-phase properties are strongly affected by the HCl dissolution, which causes a decrease in the viscosity and density of the medium. Moreover, as discussed in Section 5.2, the glycerol hydrochlorination also affects the fluid dynamics of the system. Therefore, the generally accepted way to obtain realistic information about the residence time distribution (RTD) of the fluid elements in the reactor is to study it simultaneously in real reaction experiments.

αβ-DCP was selected as a tracer due to its chemical stability and natural affinity to the reaction mixture. As discussed in Chapters 3 and 4, the formation of αβ-DCP is so minor that it can be considered negligible. In any case, in order to suppress even more the production of αβ-DCP by the reaction route, most of the RTD experiments were conducted at the lowest catalyst concentration, i.e. 3% acetic acid. Due to the limitations of the apparatus design, pulse response RTD experiments could not be conducted, but step response RTD experiments were successfully carried out. The step response generated by the tracer injection was calculated from

$$F(t) = \frac{C_{\alpha\beta}}{C_{\alpha\beta}^{max}} \tag{5.10}$$

where $C_{\alpha\beta}^{max}$ is the asymptotic concentration of tracer at the outlet.

Even though the primary data obtained was based on $F(t)$ curves, the dispersion effects are better visualized by the $E(t)$ curves [80], which are obtained as follows

$$E(t_i) = \frac{dF(t_i)}{dt} = \frac{1}{2}\left(\frac{F(t_{i+1}) - F(t_i)}{t_{i+1} - t_i} + \frac{F(t_i) - F(t_{i-1})}{t_i - t_{i-1}}\right) \tag{5.11}$$

Figure 5.10 presents a summary of the $E(t)$ curves for all the liquid-phase RTD experiments performed.

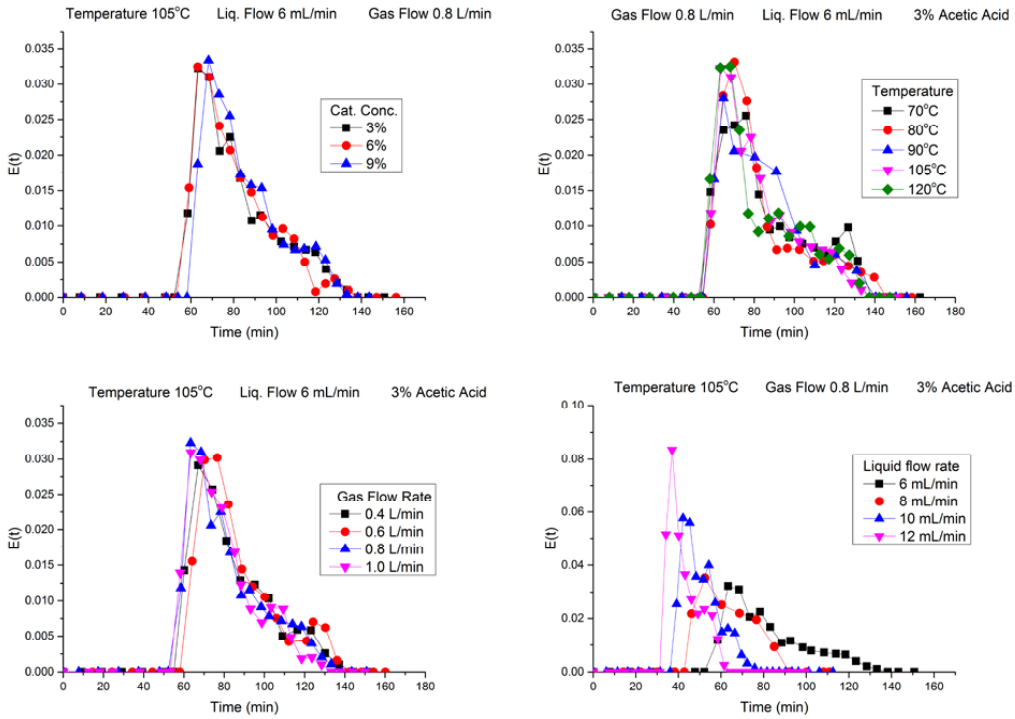

Figure 5.10. Summary of the liquid-phase E(t) curves obtained by the RTD experiments at different catalyst concentrations, temperatures, gas flow rates and liquid flow rates.

Figure 5.10 evidences that the flow pattern inside the reactor deviates significantly from plug flow, because the $E(t)$ curves are non-symmetrical and significant tailing can be observed. In fact, the $E(t)$ curves show a certain degree of bimodality, characteristic of systems in which channeling might occur. Interestingly, the effects of temperature, gas flow rate and catalyst concentration on the shape of the peaks is not pronounced. On the other hand, the increase in the liquid flow rate caused a narrowing of the peaks and diminishment of tailing, which is characteristic of the decrease of the liquid residence time [59, 80].

For the sake of simplicity, even though the system deviates considerably from the plug flow and the behaviour is asymmetric, the axial dispersion model was assumed as a first approximation for

describing the backmixing inside the reactor. The Péclet number (Pe) is hereby used as a measure of the degree of dispersion of the liquid phase,

$$Pe = \frac{uL}{D_L} = \frac{\dot{V}_L}{A}\frac{L}{D_L} \tag{5.12}$$

where u is the fluid velocity and L is the length of the tube, A is the cross sectional area of the tube and D_L is the dispersion coefficient. In the case of plug flow, the dispersion coefficient is assumed negligible, therefore $Pe \to \infty$. In the case of complete backmixing, the dispersion coefficient is too high, thus $Pe \to 0$. Indeed, it is generally accepted that, $Pe \geq 100$ represents small deviations from plug flow [59, 80]. The following relation is valid for closed-closed boundary condition systems [81] and was used for estimating the Péclet number,

$$\frac{\sigma^2}{\bar{t}^2} = \frac{2}{Pe} - \frac{2}{Pe^2}\left(1 - e^{-\frac{1}{Pe}}\right) \tag{5.13}$$

where σ^2 and $\bar{t}$ are the variance and the residence time, respectively, calculated from the $E(t)$ curves (Figure 5.10) as follows

$$\bar{t} = \int_0^\infty t \cdot E(t)\, dt - t_{inj} \tag{5.14}$$

$$\sigma^2 = \int_0^\infty \left(t - t_{inj} - \bar{t}\right)^2 E(t) dt \tag{5.15}$$

where t_{inj} is the time in which the tracer was injected. Table 5.1 collects the calculated Péclet numbers for the experiments displayed in Figure 5.10.

Table 5.1. Summary of Péclet numbers calculated for the RTD experiments.

$Liq.flow$: 6 mL/min $Gas\ flow$: 0.8 mL/min $Catalyst\ conc.$: 3%		$Temp.$: 105℃ $Gas\ flow$: 0.8 mL/min $Catalyst\ conc.$: 3%		$Temp.$: 105℃ $Liq.flow$: 6 mL/min $Catalyst\ conc.$: 3%		$Temp.$: 105℃ $Liq.flow$: 6 mL/min $Gas\ flow$: 0.8 mL/min	
$Temp.$	$Péclet$	$Liq.flow$	$Péclet$	$Gas\ flow$	$Péclet$	$Catalyst$	$Péclet$
70℃	3.64	6 mL/min	4.61	0.4 L/min	4.19	3%	4.61
80℃	3.23	8 mL/min	5.45	0.6 L/min	4.17	6%	4.45
90℃	3.99	10 mL/min	4.90	0.8 L/min	4.61	9%	5.11
105℃	4.61	12 mL/min	3.86	1.0 L/min	4.50		
120℃	3.59						

The values of Péclet number in Table 5.1 vary in a narrow range for all the studied reaction conditions. In general, they are in good agreement with commonly observed values of liquid-phase Péclet numbers in bubble columns [82, 83]. Nevertheless, the numerical interpretation of the Péclet number in our system is challenging, because the liquid flow rate inside the reactor is not constant, as discussed in Section 5.3; therefore the Péclet number calculated is somewhat an average of the local

Péclets along the reactor. Anyhow, given the wide range of variation in the reaction conditions investigated and the errors associated with the numerical differentiation of the original data, experimental sampling and gas chromatographic analysis, the Péclet number may be assumed constant, for all the studied reaction conditions. The corresponding value is attributed to the arithmetic average of Péclet numbers calculated in Table 5.1, i.e. $\overline{Pe} = 4.28$.

5.5. Mass balances and numerical strategies

An infinitesimal volume element of the bubble column is defined for the derivation of the mass balance. As gas and liquid flow co-currently upwards, the length coordinate z has its origin at the reactor inlet ($z = 0$) and ends at the reactor outlet ($z = L$). The system is isothermal and only axial concentration gradients are considered in the present approach. Figure 5.11 depicts the volume element, which is considered to represent any cross section inside the reactor.

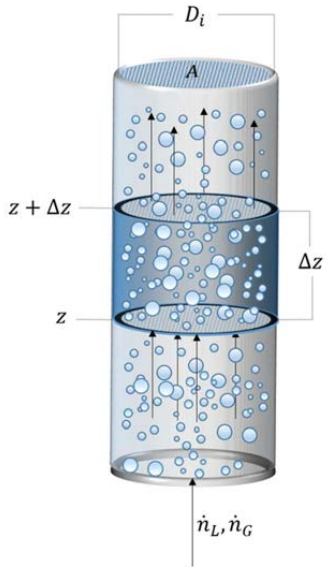

Figure 5.11. Scheme of a control volume inside the reactor.

The general mass balance for the liquid phase in the differential control volume is

$$\left[\dot{n}_{L,i} + \left(-D_L \frac{\partial C_{L,i}}{\partial z} A\varepsilon_L\right)\right]\Big|_z - \left[\dot{n}_{L,i} + \left(-D_L \frac{\partial C_{L,i}}{\partial z} A\varepsilon_L\right)\right]\Big|_{z+\Delta z} + N_i A_{GL} + r_i \Delta V_L = \frac{\partial (n_{L,i})}{\partial t} \tag{5.16}$$

Convective and dispersive transport effects are assumed to cross the system boundaries at points z and $z + \Delta z$. The double-film theory is assumed to describe the gas-liquid mass transfer of HCl; the mathematical treatment given to the term $N_i A_{GL}$ is the same as in Chapter 3. The rate of production/consumption of compounds in the volume element is $r_i \Delta V_L$. Both gas and liquid occupy the volume element, therefore the liquid volume element is defined as $\Delta V_L = \varepsilon_L A \Delta z$, where ε_L is the liquid holdup. Dividing all terms by $A\Delta z$ and letting $\Delta z \to 0$, eq. (5.16) becomes

$$\frac{\partial(\varepsilon_L C_{L,i})}{\partial t} = -\frac{1}{A}\frac{\partial(C_{L,i}\dot{V}_L)}{\partial z} + \frac{\partial}{\partial z}\left(D_L \varepsilon_L \frac{\partial C_{L,i}}{\partial z}\right) + k_{G_i} a \left(\frac{P_i}{RT_0} - K_i C_{L,i}\right) + r_i \varepsilon_L \tag{5.17}$$

where $a = A_{GL}/(A\Delta z)$ is the ratio between the interfacial area of mass transfer and the total volume of the volume element. For the sake of simplicity, the dispersion and liquid holdup are presumed to be constant along the time and position in the reactor. By doing so, we approximate that all reactor is subject to the same fluid dynamics conditions at all times and positions [84], even though it has been experimentally observed otherwise. Therefore, the dispersion and gas holdup used in the model represent an average of these fluid dynamic properties. This assumption has serious implications in the gas-phase mass balance, as will be discussed soon. Hence, the dynamic mass balance for the compounds in the liquid phase becomes

$$\frac{\partial(C_{L,i})}{\partial t} = -\frac{1}{A\varepsilon_L}\frac{\partial(C_{L,i}\dot{V}_L)}{\partial z} + D_L \frac{\partial^2 C_{L,i}}{\partial z^2} + \frac{k_{G_i} a}{\varepsilon_L}\left(\frac{P_i}{RT_0} - K_i C_{L,i}\right) + r_i \tag{5.18}$$

We assume that only HCl is present in the gas phase and its partial pressure remains constant throughout the reactor. Thus, for all compounds $P_i = K_i = 0$, except for HCl. Equation (5.18) is subject to the following initial and boundary conditions

$$C_{L,i} = C_{L,i}^0 \qquad \forall\, z \qquad t \leq 0 \qquad i = glycerol, acetic\ acid \tag{5.19}$$

$$\frac{dC_{L,i}}{dz} = \frac{\dot{V}_L^0 (C_{L,i} - C_{L,i}^0)}{A D_L \varepsilon_L} \qquad z = 0 \qquad t > 0 \qquad i = glycerol, acetic\ acid \tag{5.20}$$

$$\frac{dC_{L,i}}{dz} = 0 \qquad z = L \qquad t > 0 \qquad i = all\ compounds \tag{5.21}$$

Equation (5.19) sets the initial condition of the reactor, which is filled with glycerol and acetic acid before the reaction is started. Equations (5.20) and (5.21) are the classic Danckwerts inlet and outlet boundary conditions for closed-closed systems [85], respectively.

A mathematical description of the gas-phase mass balance could be drawn based on the same principles applied in deriving equation (5.18), reminding that no reactions take place in the gas phase, which is constituted only by gaseous HCl. However, the numerical solution of it becomes a very complex task in many different aspects. Firstly, there are no studies available in the literature concerning the properties of glycerol-HCl bubble columns; furthermore, the correlations available for bubble diameter, bubble rise velocity and $k_G a$ [86, 87] are unsuitable for the case of a viscous organic liquid, i.e. glycerol, and a soluble gas, i.e. HCl, at high temperatures and in presence of electrolytes [88]. Furthermore, the absorption of HCl at the inlet zone is so pronounced that it creates a very steep

local decline in the gas holdup, which produces substantial numerical challenges when coupling the gas and liquid mass balances. In the present approach, the liquid holdup is assumed constant throughout the reactor. For this reason, the mass balance for the gas phase was excluded. The presence of the gas phase in the system is accounted for by the fluid dynamic parameter ε_L and the mass transfer term, i.e. $k_G a$, in equation (5.18). This assumption leads to a simplified approach towards the role of the gas-phase in the reactor; on the other hand, it avoids the use of literature correlations for the estimation of gas phase properties, e.g. bubble diameter and bubble rise velocity, which would likely not be valid for such an uncommon bubble column system. The accuracy and reliability of this approach is tested when confronting the experimental data with the model.

Even though the fluid dynamic parameters are averaged along the reactor column, the mass transfer term $k_G a$ may be assumed to vary along the reactor length and time to compensate for the lack of a rigorous gas-phase mass balance. The churn-turbulent zone, at the inlet, is characterized by the presence of large bubbles; which, in general, are considered to have smaller $k_G a$. As gaseous HCl is absorbed along the tube, smaller bubbles are formed, which are characterized by higher $k_G a$ values [87]. Furthermore, the gas flow rate is well-known to have a significant influence on the mass transfer term. Therefore, in order to take into account such important mass transfer features, eq. (5.22) is proposed for describing the dependence of the mass transfer parameter $k_G a$ along the reactor length and position,

$$k_G a(z,t) = \omega_0 + \omega_1 \left(\dot{V}^0_{HCl,G}\right)^{\omega_2} \left(\frac{C_{HCl,L}(z,t)}{C^{sat}_{HCl,L}}\right) \tag{5.22}$$

where ω_0, ω_1 and ω_2 are fitting parameters and $C^{sat}_{HCl,L}$ is the HCl saturation concentration in the liquid phase (as described in Chapter 3, Figure 3.13). The inlet gas flow rate of HCl, i.e. $\dot{V}^0_{HCl,G}$, is used in eq. (5.22) instead of the local HCl gas flow rate, due to the absence of the gas-phase mass balance. In the present form, eq. (5.22) is a monotonically increasing function, but in reality, the mass transfer rate decreases from the inlet towards the outlet, due to the disappearance of the gas bubbles. Anyhow, eq. (5.22) can be considered a reasonable alternative to take the gas flow rate effect on the mass transfer into account.

As discussed in Section 5.4.5, the Péclet number estimated by the RTD experiments could be assumed virtually constant for all the experimental temperatures, gas flow rates, liquid flow rates and catalyst concentrations investigated. Thus, the liquid dispersion was calculated as from eq. (5.23),

$$D_L = \frac{\mathrm{L}}{A\overline{Pe}}\dot{V}^0_L \tag{5.23}$$

where $\overline{Pe} = 4.28$ is the average Péclet number for all experiments.

The kinetic parameters (Tables 3.1 and 3.3), the HCl distribution coefficient, eq. (3.14), and the HCl saturation concentration $C^{sat}_{HCl,L}$ were obtained from the glycerol hydrochlorination study in semi-batch reactor (Chapter 3). The parameter *b,* which correlates the increase in liquid volumetric flow rate ($\dot{V}_L$) with the total concentration of compounds, was estimated separately for each experiment according

to equation (5.9), based on the concentrations of compounds at the outlet. Thus, the only parameters estimated by the model equation (5.18) were ε_L, ω_0, ω_1 and ω_2.

The finite differences method was applied in order to discretize the length coordinate in 22 equidistant node points, which yielded a set of stiff ODE system. The software Modest [60] was used to solve the underlying differential equations in the parameter estimation subroutine. The combination of the Levenberg-Marquardt and Simplex algorithms were used to find the minimum of the objective function (Q), defined as

$$Q = \sum_i \left(C_{L,i_{exp}} - C_{L,i} \right)^2 \tag{5.24}$$

in which i=glycerol, α-MCP, β-MCP, αγ-DCP and HCl. $C_{L,i_{exp}}$ is the experimental concentration of compound i at the reactor outlet and $C_{L,i}$ is the concentration at the outlet calculated by the model. The degree of explanation of the parameter estimation (R^2) was calculated with the formula

$$R^2 = 1 - \frac{\sum_i \left(C_{L,i_{exp}} - C_{L,i} \right)^2}{\sum_i \left(C_{L,i_{exp}} - \overline{C_{L,i_{exp}}} \right)^2} \tag{5.25}$$

where $\overline{C_{L,i_{exp}}}$ is an average value of the experimentally measured concentrations.

5.6. Modelling results

Based on experimental observations and the images captured by the high-speed camera, it is presumed that the experiments conducted at 0.4, 0.6 and 0.8 L/min of the HCL flow rates have approximately similar conditions concerning the fluid dynamics. Therefore, they should have the same values of ε_L and $\overline{Pe}$. On the other hand, the mass transfer is highly dependent on the gas flow rate; thus, $k_G a$ should be different at different gas flow rates. The experiments performed using gas flow rate of 1.0 L/min are excluded from the parameter estimation because they already constitute a transitioning fluid dynamic regime to slug flow; therefore, they have different mass transfer characteristics, as evidenced by Figure 5.3. Figure 5.12 presents the fit of the transient model for the glycerol hydrochlorination experiments performed at the HCl flow rate of 0.4-0.8 L/min.

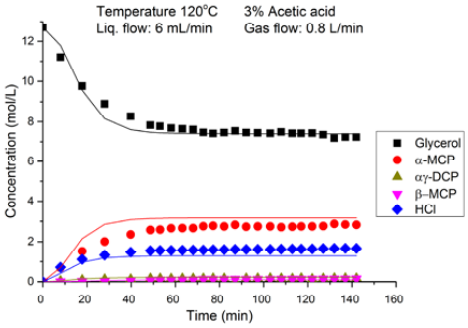
Temperature 120°C 3% Acetic acid
Liq. flow: 6 mL/min Gas flow: 0.8 L/min
Concentration (mol/L)
Time (min)
Glycerol
α-MCP
αγ-DCP
β–MCP
HCl

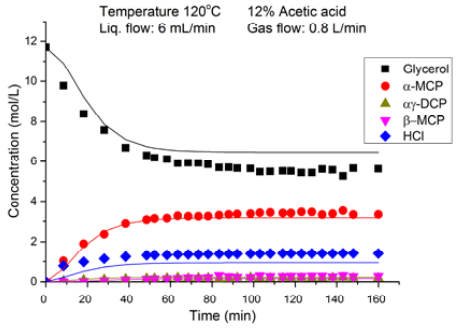
Temperature 120°C 12% Acetic acid
Liq. flow: 6 mL/min Gas flow: 0.8 L/min
Concentration (mol/L)
Time (min)
Glycerol
α-MCP
αγ-DCP
β–MCP
HCl

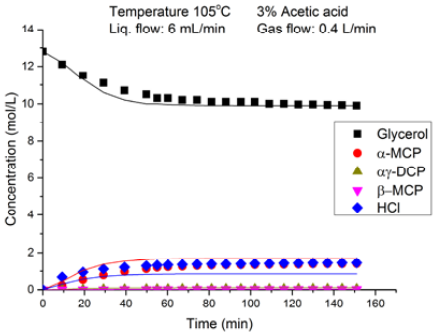
Temperature 105°C 3% Acetic acid
Liq. flow: 6 mL/min Gas flow: 0.4 L/min
Concentration (mol/L)
Time (min)
Glycerol
α-MCP
αγ-DCP
β–MCP
HCl

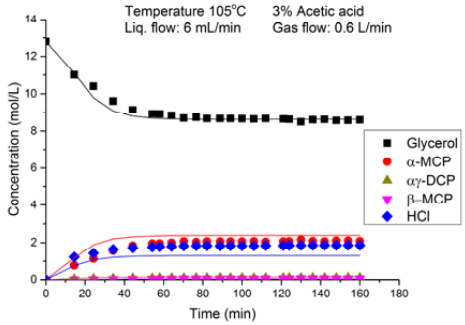
Temperature 105°C 3% Acetic acid
Liq. flow: 6 mL/min Gas flow: 0.6 L/min
Concentration (mol/L)
Time (min)
Glycerol
α-MCP
αγ-DCP
β–MCP
HCl

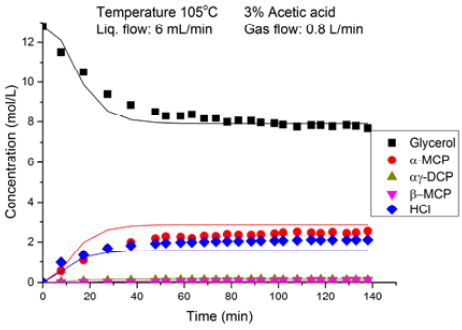
Temperature 105°C 3% Acetic acid
Liq. flow: 6 mL/min Gas flow: 0.8 L/min
Concentration (mol/L)
Time (min)
Glycerol
α-MCP
αγ-DCP
β–MCP
HCl

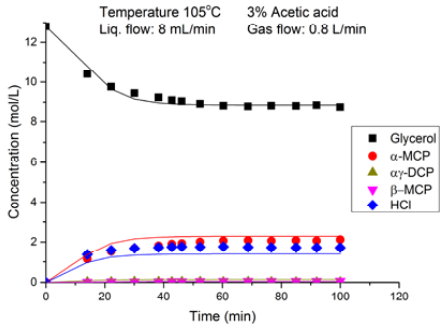
Temperature 105°C 3% Acetic acid
Liq. flow: 8 mL/min Gas flow: 0.8 L/min
Concentration (mol/L)
Time (min)
Glycerol
α-MCP
αγ-DCP
β–MCP
HCl

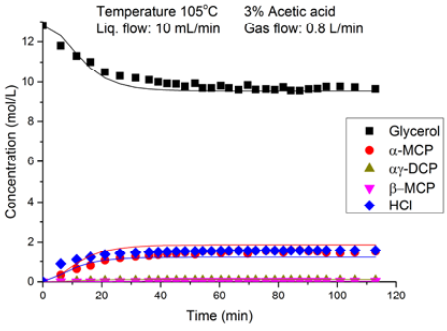
Temperature 105°C 3% Acetic acid
Liq. flow: 10 mL/min Gas flow: 0.8 L/min
Concentration (mol/L)
Time (min)
Glycerol
α-MCP
αγ-DCP
β–MCP
HCl

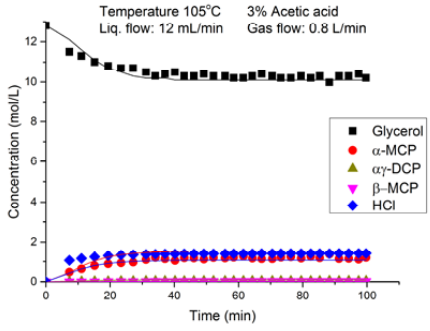
Temperature 105°C 3% Acetic acid
Liq. flow: 12 mL/min Gas flow: 0.8 L/min
Concentration (mol/L)
Time (min)
Glycerol
α-MCP
αγ-DCP
β–MCP
HCl

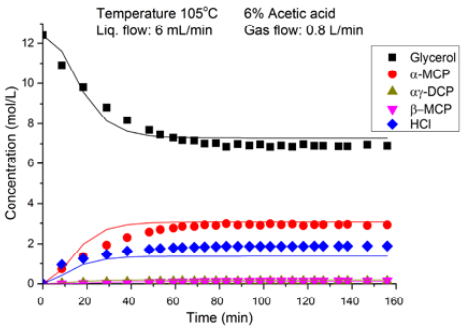
Temperature 105°C 6% Acetic acid
Liq. flow: 6 mL/min Gas flow: 0.8 L/min
Glycerol
α-MCP
αγ-DCP
β–MCP
HCl
Concentration (mol/L)
Time (min)

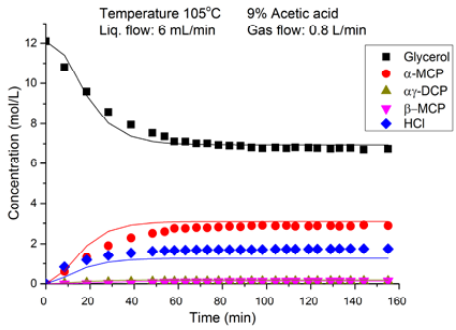
Temperature 105°C 9% Acetic acid
Liq. flow: 6 mL/min Gas flow: 0.8 L/min
Glycerol
α-MCP
αγ-DCP
β–MCP
HCl
Concentration (mol/L)
Time (min)

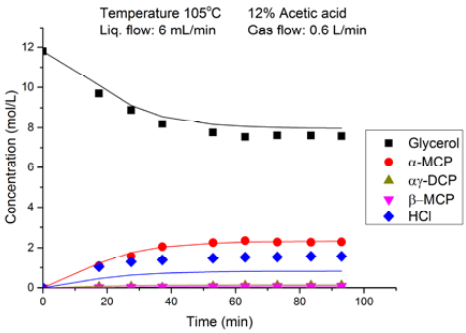
Temperature 105°C 12% Acetic acid
Liq. flow: 6 mL/min Gas flow: 0.6 L/min
Glycerol
α-MCP
αγ-DCP
β–MCP
HCl
Concentration (mol/L)
Time (min)

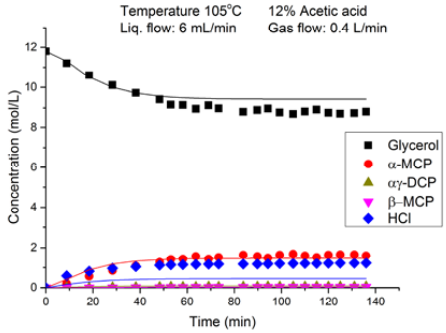
Temperature 105°C 12% Acetic acid
Liq. flow: 6 mL/min Gas flow: 0.4 L/min
Glycerol
α-MCP
αγ-DCP
β–MCP
HCl
Concentration (mol/L)
Time (min)

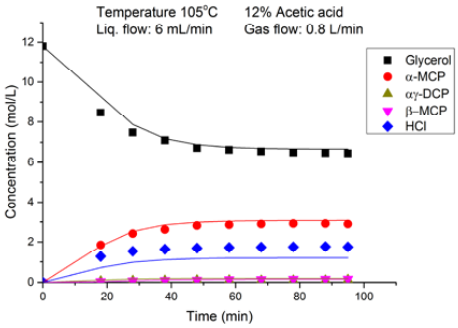
Temperature 105°C 12% Acetic acid
Liq. flow: 6 mL/min Gas flow: 0.8 L/min
Glycerol
α-MCP
αγ-DCP
β–MCP
HCl
Concentration (mol/L)
Time (min)

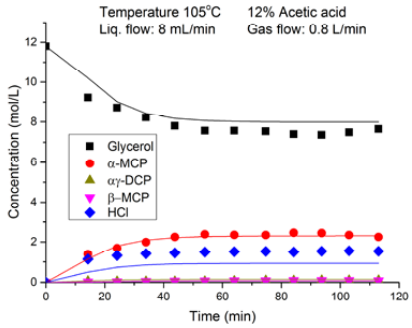
Temperature 105°C 12% Acetic acid
Liq. flow: 8 mL/min Gas flow: 0.8 L/min
Glycerol
α-MCP
αγ-DCP
β–MCP
HCl
Concentration (mol/L)
Time (min)

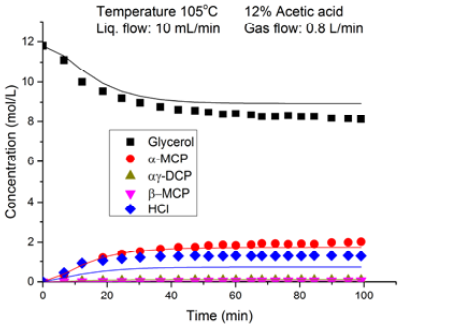
Temperature 105°C 12% Acetic acid
Liq. flow: 10 mL/min Gas flow: 0.8 L/min
Glycerol
α-MCP
αγ-DCP
β–MCP
HCl
Concentration (mol/L)
Time (min)

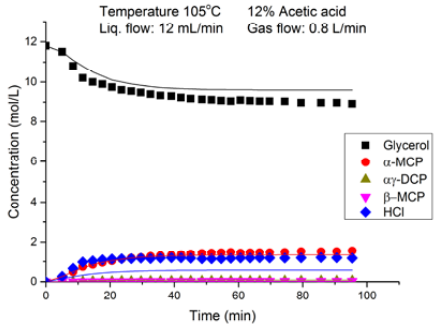
Temperature 105°C 12% Acetic acid
Liq. flow: 12 mL/min Gas flow: 0.8 L/min
Glycerol
α-MCP
αγ-DCP
β–MCP
HCl
Concentration (mol/L)
Time (min)

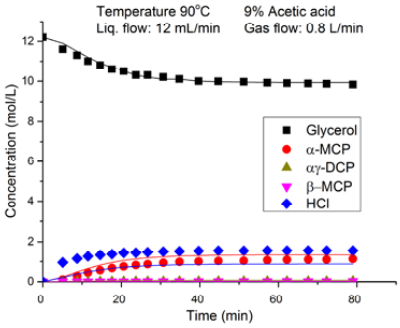
Temperature 90°C
Liq. flow: 12 mL/min
9% Acetic acid
Gas flow: 0.8 L/min
Concentration (mol/L)
Time (min)
Glycerol
α-MCP
αγ-DCP
β–MCP
HCl

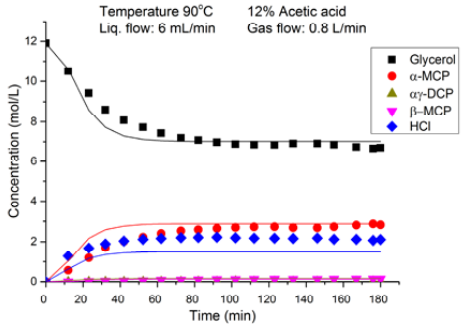
Temperature 90°C
Liq. flow: 6 mL/min
12% Acetic acid
Gas flow: 0.8 L/min
Concentration (mol/L)
Time (min)
Glycerol
α-MCP
αγ-DCP
β–MCP
HCl

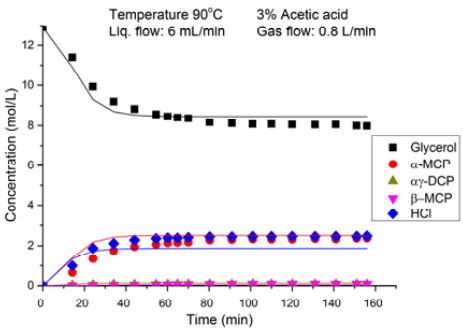
Temperature 90°C
Liq. flow: 6 mL/min
3% Acetic acid
Gas flow: 0.8 L/min
Concentration (mol/L)
Time (min)
Glycerol
α-MCP
αγ-DCP
β–MCP
HCl

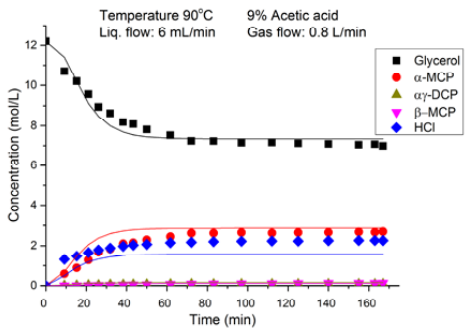
Temperature 90°C
Liq. flow: 6 mL/min
9% Acetic acid
Gas flow: 0.8 L/min
Concentration (mol/L)
Time (min)
Glycerol
α-MCP
αγ-DCP
β–MCP
HCl

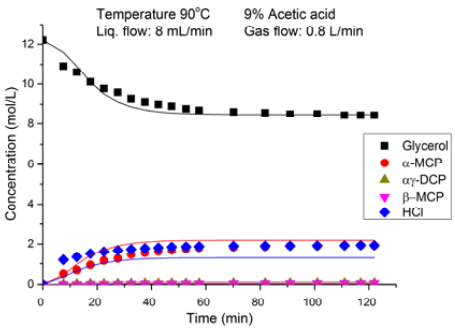
Temperature 90°C
Liq. flow: 8 mL/min
9% Acetic acid
Gas flow: 0.8 L/min
Concentration (mol/L)
Time (min)
Glycerol
α-MCP
αγ-DCP
β–MCP
HCl

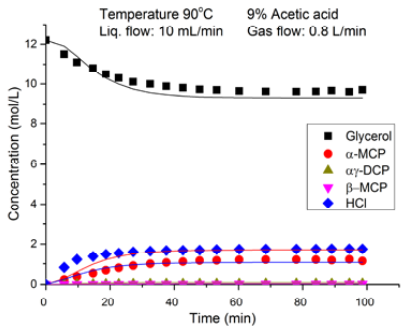
Temperature 90°C
Liq. flow: 10 mL/min
9% Acetic acid
Gas flow: 0.8 L/min
Concentration (mol/L)
Time (min)
Glycerol
α-MCP
αγ-DCP
β–MCP
HCl

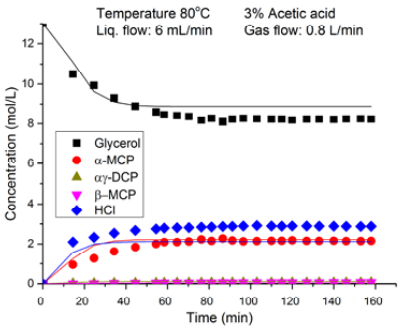
Temperature 80°C
Liq. flow: 6 mL/min
3% Acetic acid
Gas flow: 0.8 L/min
Concentration (mol/L)
Time (min)
Glycerol
α-MCP
αγ-DCP
β–MCP
HCl

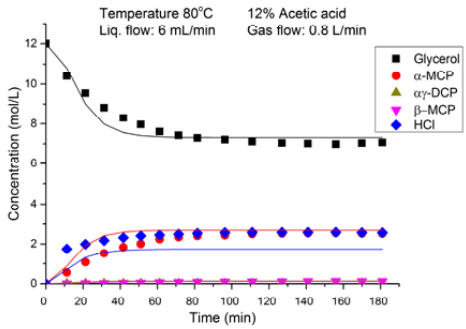
Temperature 80°C
Liq. flow: 6 mL/min
12% Acetic acid
Gas flow: 0.8 L/min
Concentration (mol/L)
Time (min)
Glycerol
α-MCP
αγ-DCP
β–MCP
HCl

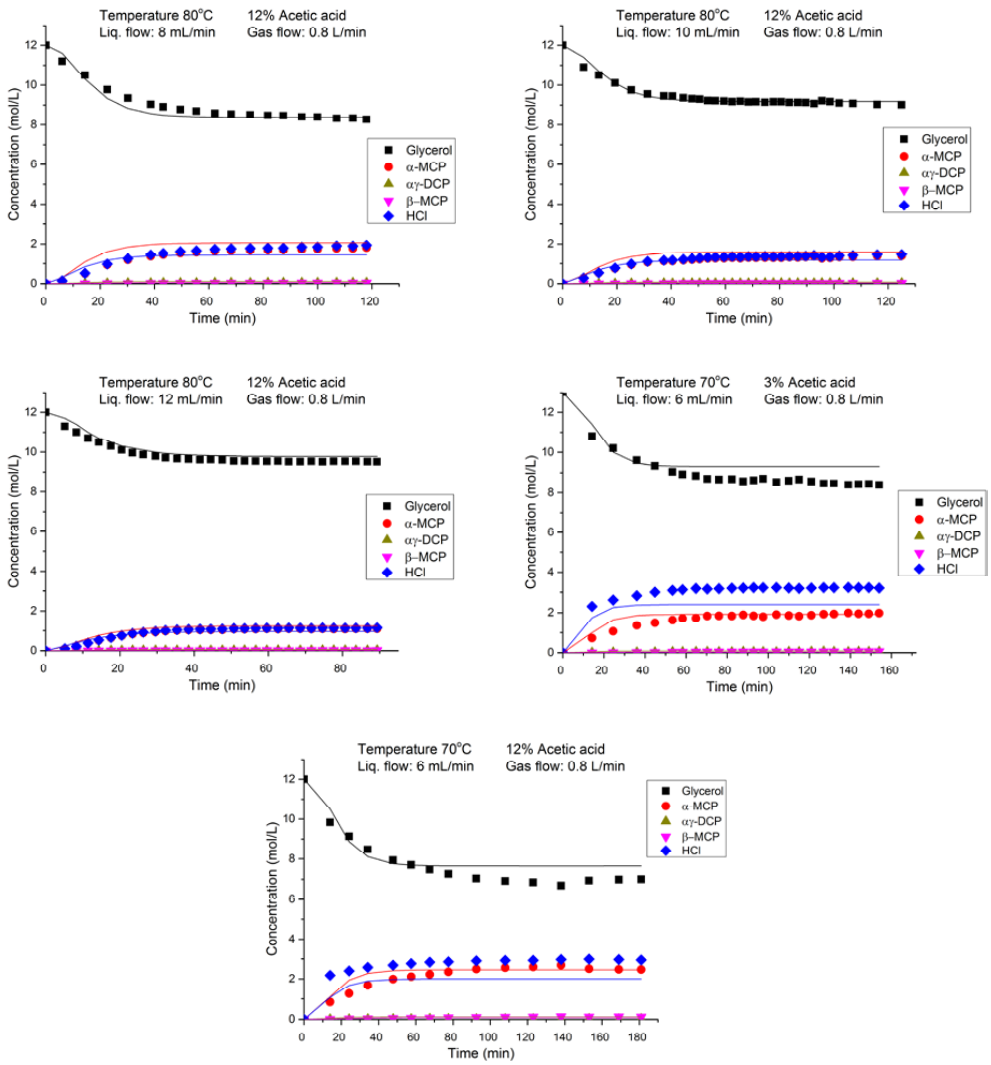

Figure 5.12. Fit of the dynamic model for glycerol hydrochlorination in bubble column at gas flow rates of 0.4, 0.6 and 0.8 L/min of HCl. The dots represent the experimental data and the lines represent the values predicted by the model. R^2=99.22%.

The model was able to explain satisfactorily the effect of different temperatures, catalyst concentrations and liquid flow rates on the solvent-free glycerol hydrochlorination product distribution. The HCl concentration in the liquid phase was, for most experiments, underestimated; which is attributed to the lack of a rigorous description of the gas phase in the model. Furthermore, the majority of the experiments were carried out at 105ºC, which causes the estimated parameters to be more heavily weighted to that temperature. For this reason, one can see a more pronounced deviation of the model at lower temperatures of 70, 80 and 90ºC. Nevertheless, a reasonable fit was obtained for the curves depicted in Figure 5.12. The overall degree of explanation (R^2) for the 29 experiments used in the numerical regression was 99.22%, which is very high. The results obtained from the parameter estimation are depicted in Table 5.2

Table 5.2. Fluid dynamic and mass transfer parameters estimated for the experiments performed at 0.4-0.8 L/min of HCl.

$HCl\ flow$: 0.4, 0.6 *and* 0.8 L/min		
$Parameter$	$Value$	$Error$ (%)
ε_L	0.965	1.3
ω_0	1.11 min^{-1}	4.6
ω_1	45.6	0.6
ω_2	0.93	2.5

As revealed from Table 5.2, the averaged liquid holdup is quite high, which is evidence that the gas phase dissolves very rapidly into the liquid. The mass transfer parameter, $k_G a$, varied within the range of $6 - 37\ min^{-1}$, which is a very high value when compared to the values reported by Charpentier [84] for general bubble columns and by Grund et al. [89] for organic liquids bubble columns. Even though eq. (5.22) satisfactorily correlated $k_G a$ values with the reaction conditions, a more rigorous approach should be given to this equation once a reliable gas-phase mass balance is developed; implying that, the local gas flow rate should considered instead of the inlet gas flow rate.

It is remarkable that the kinetic and solubility data obtained in the semi-batch reactor could be directly applied to the present system. Analogously, the Péclet number was also calculated apart from the model, leaving it only with the task to estimate the liquid holdup and mass transfer parameters. Overall, the proposed model was successful in explaining the experimental data obtained with the laboratory scale column reactor.

Although the present bubble column reactor was not effective on producing αγ-DCP, it was rather selective on the conversion of α-MCP. Due to fluid dynamic limitations related to the absorption of HCl in the liquid phase, the conversion level was severely compromised. In this sense, it may be suggested that, for a bubble column reactor with several HCl injection points along the tube (Figure 5.13), such a hydrodynamic limitation may be circumvented, giving rise to an effective reactor for continuous production of dichlorohydrins.

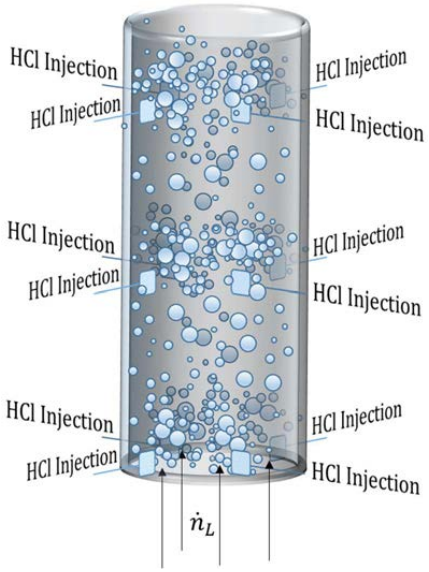

Figure 5.13. General representation of an efficient design for the glycerol hydrochlorination in bubble columns.

In fact, the more injection points are placed along the reactor length, the continuous bubble column reactor behaviour approaches to that of a semi batch process, with the advantage that the bubble column may be less energy consuming than a classic semi batch reactor. Naturally, more investigations should be carried out to optimize the distance between the gas injection points and the gas flow rate for each position; however, it is reasonable to assume that such a design should be effective on a large scale.

6. Conclusions

The present thesis contributes significantly to expanding the knowledge on the solvent-free glycerol hydrochlorination process. In essence, a kinetic model based on molecular mechanism was created and verified; a more rigorous approach was given to the description of such a dynamic gas-liquid reaction system, which revealed itself more complex than described previously in the literature.

The most reasonable reaction mechanism available in the literature was revisited and a more formal treatment was given to the derivation of the kinetic equations. The model was successfully tested with data available in the literature and with data of our own.

The literature lacked a proper study of the effects of reaction conditions on the solvent-free glycerol hydrochlorination. Therefore, semi-batch experiments were carried out covering a wide range of temperatures, catalyst concentrations, HCl partial pressures and stirring speeds. Furthermore, non-catalytic experiments were conducted at several temperatures. For the first time, the influence of HCl absorption on increasing the liquid phase volume was described and quantified; the volume increase is an important phenomenon which affects significantly the concentration of compounds, as was demonstrated. An important novelty of this work was that the non-catalytic reaction pathway was included in the reaction mechanism, yielding a more complete kinetic model for the reaction. A proper description of the HCl solubility as a function of partial pressure and reaction temperature was presented for semi-batch experiments. A classical semi-batch mass balance was coupled with the newly derived kinetic model, providing an excellent description of the experimental data. Kinetic and mass transfer parameters were successfully estimated. A new dimensionless parameter, called Catalyst Modulus, was introduced and tested with the experimental data, which corroborated the validity of the kinetic model.

Most literature sources have had a very simplistic approach toward the role of water in the solvent-free glycerol hydrochlorination system. Due to few experimental evidences, it has been commonly accepted that water removal would enhance the reaction rate, even though this assumption was never properly tested. In this sense, catalytic and non-catalytic reactive flash distillation experiments were performed and compared with semi-batch experiments. As it turned out, water has an important effect on the HCl absorption and dissociation in the liquid phase, causing the reactive flash distillation experiments to have a lesser performance compared to semi-batch ones. Only at the highest temperature of 120ºC and 12% catalyst, the reactive flash distillation mode was able to surpass the performance of the semi-batch reactor. These experiments brought into discussion the role of solvents in the glycerol hydrochlorination process. Therefore, further semi-batch experiments were carried out in which initial amounts of water and αγ-DCP were added to the mixture of glycerol and catalyst. These experiments revealed that αγ-DCP is a potential ideal solvent for hydrochlorination. As αγ-

DCP was added, the glycerol conversion was improved and the HCl liquid uptake was diminished considerably. It means that the reaction mixture was able to achieve a faster conversion spending less HCl gas. Furthermore, αγ-DCP is constantly generated by the reaction and do not require any extra separation unit downstream. Therefore, the cost of implementing such an efficient approach to an existing αγ-DCP production plant should be very low.

A co-current bubble column reactor was used to test the feasibility of glycerol hydrochlorination in a continuous apparatus. A thorough investigation of the reaction performance over a wide range of temperatures, catalyst concentration, liquid flow rates and gas flow rates was conducted. Remarkably, the bubble column has a fluid dynamic behaviour similar to a vertical tubular absorber, due to the high solubility of HCl in the liquid phase. High-speed camera images were collected at three different positions along the reactor tube at four gas flow conditions, depicting different fluid dynamic regimes. In fact, due to the limitations in fluid dynamics, the conversions of αγ-DCP remained very low for all reaction conditions; however, α-MCP was formed with an extraordinary high selectivity. Step response residence time distribution experiments were conducted at various conditions, in which the degree of dispersion of the liquid phase (Péclet number) was estimated. Axial dispersion model was used to describe the liquid-phase flow inside the bubble column. Due to the lack of information from literature about this complex gas-liquid system and the numerical challenges imposed by the steep gradients which appear in the vicinity of the reactor inlet, the gas-phase mass balance was not considered. Kinetic and solubility data obtained from the semi-batch experiments and the Péclet estimated by the RTD were utilized in solving the transient model for bubble column. The model described satisfactorily the dynamic behaviour of the studied conditions, with a degree of explanation exceeding 99% for all 29 experiments regressed. Mass transfer and fluid dynamic parameters were successfully estimated by the model. Due to the fluid dynamics limitations imposed by the HCl absorption in the liquid phase, it is suggested that several HCl injection points along the reactor length shall increase the efficiency of the bubble column apparatus towards the production of αγ-DCP. In fact, by doing so, the bubble column behaviour approaches the behaviour of a classic semi-batch reactor, however, spending less energy than the other. It is also highly suggested that αγ-DCP is fed to the reactor, due to its effect of enhancing the reaction rate. Based on these consideration brought by the discoveries made in the present thesis, a more efficient continuous reactor for glycerol hydrochlorination can be designed.

7. Appendix

Table 7.1 lists few selected physical properties of the compounds discussed in the present thesis.

Table 7.1. List of selected physical properties of the compounds discussed in the present thesis.

	$CAS\ Number$	$Density$ (@ 25℃)	$Visc.$ (@ 25℃)	$Boil.point$ (@ 1 bar)
$Glycerol$	$58-81-5$	1.26 g/mL [66]	749.3 cP [66]	290℃ [62]
$\alpha - MCP$	$96-24-2$	1.32 g/mL [61]	*	213℃ [34]
$\beta - MCP$	$497-04-1$	1.32 g/mL [61]	*	213℃ [62]
$\alpha\gamma - DCP$	$96-23-1$	1.35 g/mL [61]	12.1 cP [90]	174℃ [62]
$\alpha\beta - DCP$	$616-23-9$	1.35 g/mL [61]	12.1 cP [90]	174℃ [90]
$Water$	$7732-18-5$	0.997 g/mL [66]	0.89 cP [66]	100℃ [62]
$Acetic\ acid$	$64-19-7$	1.05 g/mL [66]	1.22 cP [66]	117℃ [62]
$Adipic\ acid$	$124-04-9$	1.36 g/mL [66]	**	338℃ [62]
HCl	$7647-01-0$	**	**	−85℃ [62]

*** Not found in the literature**
**** Does not apply**

The properties presented in Table 7.1 were measured at atmospheric pressure. Remind that, at 1 bar and 25ºC, adipic acid is solid and hydrogen chloride is gaseous.

8. Notation

8.1. Nomenclature

a	$Catalyst\ Modulus\ fitting\ parameter$
a	$merged\ constant\ in\ the\ derivation\ of\ rate\ equations$
a	$ratio\ between\ the\ gas - liquid\ interfacial\ area\ and\ reactor\ volume\ [m^{-1}]$
A	$pre-exponential\ factor\ [depends\ on\ rate\ equation]$
A	$cross-sectional\ area\ [m^2]$
A_{GL}	$gas-liquid\ interfacial\ area\ [m^2]$
b	$fitting\ parameter\ eq.(5.9)\ \ [L^2 mol^{-1} min^{-1}]$
C	$concentration\ [mol \cdot L^{-1}]$
D	$dispersion\ coefficient\ [m^2 s^{-1}]$
E_a	$activation\ energy, [kJ \cdot mol^{-1}\ ]$
k	$mass\ transfer\ coefficient\ \ [m \cdot s^{-1}]$
k, k', k''	$reaction\ rate\ constant\ [depends\ on\ kinetics]$
K	$equilibrium\ constant\ [depends\ on\ stoichiometry]$
K	$distribution\ coefficient\ [-]$
$\dot{m}$	$mass\ flow\ rate\ [g \cdot s^{-1}]$
m	$mass\ [g]$
M	$molar\ mass\ of\ compound\ [g\ \cdot mol^{-1}]$
n	$amount\ of\ substance\ [mol]$
$\dot{n}$	$flow\ of\ amount\ of\ substance\ [mol \cdot s^{-1}]$
N	$molar\ flux\ [mol \cdot m^{-2} \cdot s^{-1}]$
N	$stoichiometric\ number\ of\ a\ reaction\ route$
P	$pressure\ [bar]$
Pe	$Péclet\ number\ [-]$
Q	$objective\ function$
r	$reaction\ rate\ [mol \cdot L^{-1} \cdot s^{-1}]$
R	$ideal\ gas\ constant\ [8.3143\ J\ \cdot mol^{-1} \cdot K^{-1}]$
R^2	$degree\ of\ explanation\ [-]$
t	$time\ [s]$
$\bar{t}$	$mean\ residence\ time\ [min]$
T	$temperature\ [K]$
u	$fluid\ velocity\ [dm \cdot min^{-1}]$
w	$mass\ fraction\ in\ the\ liquid-phase\ [-]$
$\dot{V}$	$volumetric\ flow\ rate\ [m^3 \cdot s^{-1}]$
V	$volume\ [m^3]$
x	$molar\ fraction$

$\alpha, \alpha', \mathrm{K}, \mathrm{K}'$	$merged\ parameters\ in\ rate\ equations$
ε	$holdup\ [-]$
ρ	$density, [g \cdot m^{-3}]$
σ^2	$variance\ of\ E(t)\ curve\ [min^2]$
Ψ	$Catalyst\ Modulus$
$\omega_0, \omega_1, \omega_2$	$fitting\ parameters\ eq.\ (5.22)$

8.2. Subscripts and superscripts

G	$gas\ phase$
GL	$gas - liquid\ interface$
i	$component\ index$
L	$liquid\ phase$
0	$initial\ condition\ or\ standard\ ambient\ temperature\ or\ pressure$
∞	$limit\ value$
exp	$experimental\ value$

8.3. Abbreviations

A	$glycerol$
E	$ester\ intermediate$
I^+	$epoxide\ cation\ intermediate$
α, α-MCP	$3 - chloro - 1{,}2 - propanediol$
β, β-MCP	$2 - chloro - 1{,}3 - propanediol$
$\alpha\gamma, \alpha\gamma$-DCP	$1{,}3 - dichloro - 2 - propanol$
$\alpha\beta, \alpha\beta$-DCP	$1{,}2 - dichloro - 3 - propanol$
GCD	$glycerol\ and\ chlorinated\ derivatives, formed\ from\ glycerol, \alpha, \beta, \alpha\gamma\ and\ \alpha\beta$

9. References

[1] S. Naik, V. V. Goud, P. K. Rout and A. K. Dalai, "Production of first and second generation biofuels: A comprehensive review," *Renewable and Sustainable Energy Reviews ,* vol. 14, no. 2, pp. 578-597, 2010.

[2] D. Y. Leung, X. Wu and M. Leung, "A review on biodiesel production using catalyzed transesterification," *Applied Energy,* vol. 87, no. 4, pp. 1083-1095, 2010.

[3] H. Tan, A. A. Aziz and M. Aroua, "Glycerol production and its applications as a raw material: A review," *Renewable and Sustainable Energy Reviews,* vol. 27, pp. 118-127, 2013.

[4] S. S. Yazdani and R. Gonzalez, "Anaerobic fermentation of glycerol: a path to economic viability for the biofuels industry," *Current Opinion in Biotechnology ,* vol. 18, no. 3, pp. 213-219, 2007.

[5] M. MCCoy, "Glycerin Surplus," *Chemical & Engineering News Archive,* vol. 84, no. 6, p. 7, 2006.

[6] M. Ayoub and A. Z. Abdullah, "Critical review on the current scenario and significance of crude glycerol resulting from biodiesel industry towards more sustainable renewable energy industry," *Renewable and Sustainable Energy Reviews,* vol. 16, no. 5, pp. 2671-2686, 2012.

[7] M. O. Guerrero-Pérez, J. M. Rosas, J. Bedia, J. Rodríguez-Mirasol and T. Cordero, "Recent inventions in glycerol transformations and processing," *Recent Patents on Chemical Engineering,* vol. 2, no. 1, pp. 11-21, 2009.

[8] R. Karinen and A. Krause, "New biocomponents from glycerol," *Applied Catalysis A: General,* vol. 306, pp. 128-133, 2006.

[9] M. D. Bohon, B. A. Metzger, W. P. Linak, C. J. King and W. L. Roberts, "Glycerol combustion and emissions," *Proceedings of the Combustion Institute,* vol. 33, no. 2, pp. 2717-2724, 2011.

[10] J. Albarelli, D. Santos and M. Holanda, "Energetic and economic evaluation of waste glycerol cogeneration in Brazil," *Brazilian Journal of Chemical Engineering,* vol. 28, no. 4, pp. 691-698, 2011.

[11] C. O. Tuck, E. Pérez, I. T. Horváth, R. A. Sheldon and M. Poliakoff, "Valorization of Biomass: Deriving More Value from Waste," *Science,* vol. 337, no. 6095, pp. 695-699, 2012.

[12] M. Pagliaro, R. Ciriminna, H. Kimura, M. Rossi and C. Della Pina, "From Glycerol to Value-Added Products," *Angewandte Chemie International Edition,* vol. 46, no. 24, pp. 4434-4440, 2007.

[13] Z. Y. Zakaria, J. Linnekoski and N. Amin, "Catalyst screening for conversion of glycerol to light olefins," *Chemical Engineering Journal,* vol. 207, pp. 803-813, 2012.

[14] B. Katryniok, S. Paul, M. Capron and F. Dumeignil, "Towards the Sustainable Production of Acrolein by Glycerol Dehydration," *ChemSusChem,* vol. 2, no. 8, pp. 719-730, 2009.

[15] Y. Gu, A. Azzouzi, Y. Pouilloux, F. Jérôme and J. Barrault, "Heterogeneously catalyzed etherification of glycerol: new pathways for transformation of glycerol to more valuable chemicals," *Green Chemistry,* vol. 10, no. 2, pp. 164-167, 2008.

[16] W. K. Teng, G. C. Ngoh, R. Yusoff and M. K. Aroua, "A review on the performance of glycerol carbonate production via catalytic transesterification: Effects of influencing parameters," *Energy Conversion and Management,* vol. 88, pp. 484-497, 2014.

[17] T. Hirai, N. Ikenaga, T. Miyake and T. Suzuki, "Production of hydrogen by steam reforming of glycerin on ruthenium catalyst," *Energy & Fuels,* vol. 19, no. 4, pp. 1761-1762, 2005.

[18] E. Markočič, B. Kramberger, J. G. van Bennekom, H. J. Heeres, J. Vos and Ž. Knez, "Glycerol reforming in supercritical water; a short review," *Renewable and Sustainable Energy Reviews,* vol. 23, pp. 40-48, 2013.

[19] G. Wen, Y. Xu, H. Ma, Z. Xu and Z. Tian, "Production of hydrogen by aqueous-phase reforming of glycerol," *International Journal of Hydrogen Energy,* vol. 33, no. 22, pp. 6657-6666, 2008.

[20] S. Adhikari, S. D. Fernando and A. Haryanto, "Hydrogen production from glycerol: An update," *Energy Conversion and Management,* vol. 50, no. 10, pp. 2600-2604, 2009.

[21] S. Abad and X. Turon, "Valorization of biodiesel derived glycerol as a carbon source to obtain added-value metabolites: Focus on polyunsaturated fatty acids," *Biotechnology Advances,* vol. 30, no. 3, pp. 733-741, 2012.

[22] Y. Liang, N. Sarkany, Y. Cui and J. W. Blackburn, "Batch stage study of lipid production from crude glycerol derived from yellow grease or animal fats through microalgal fermentation," *Bioresource Technology,* vol. 101, no. 17, pp. 6745-6750, 2010.

[23] M. A. Dasari, P.-P. Kiatsimkul, W. R. Sutterlin and G. J. Suppes, "Low-pressure hydrogenolysis of glycerol to propylene glycol," *Applied Catalysis A: General,* vol. 281, no. 1-2, pp. 225-231, 2005.

[24] C. Rabello, M. Gomes, B. Siqueira, R. de Menezes, W. Huziwara, T. Yamada, L. de Oliveira and G. de Carvalho Oliveira, "Production of propylene glycol from glycerine". US Patent 8,492,597, 23 July 2013.

[25] C. E. Nakamura and G. M. Whited, "Metabolic engineering for the microbial production of 1,3-propanediol," *Current Opinion in Biotechnology,* vol. 14, no. 5, pp. 454-459, 2003.

[26] S. Hirschmann, K. Baganz, I. Koschik and K. Vorlop, "Development of an integrated bioconversion process for the production of 1,3-propanediol from raw glycerol waters," *Landbauforschung Völkenrode,* vol. 55, no. 4, pp. 261-267, 2005.

[27] S. Carrà, E. Santacesaria, M. Morbidelli, P. Schwarz and C. Divo, "Synthesis of epichlorohydrin by elimination of hydrogen chloride from chlorohydrins. 1. Kinetic aspects of the process," *Industrial & Engineering Chemistry Process Design and Development,* vol. 18, no. 3, pp. 424-427, 1979.

[28] B. M. Bell, J. R. Briggs, R. M. Campbell, S. M. Chambers, P. D. Gaarenstroom, J. G. Hippler, B. D. Hook, K. Kearns, J. M. Kenney, W. J. Kruper and others, "Glycerin as a renewable feedstock for epichlorohydrin production. The GTE process," *CLEAN,* vol. 36, no. 8, pp. 657-661, 2008.

[29] E. Santacesaria, R. Tesser, M. D. Serio, L. Casale and D. Verde, "New Process for Producing Epichlorohydrin via Glycerol Chlorination," *Industrial & Engineering Chemistry Research,* vol. 49, no. 3, pp. 964-970, 2010.

[30] E. Santacesaria, R. Vitiello, R. Tesser, V. Russo, R. Turco and M. Di Serio, "Chemical and technical aspects of the synthesis of chlorohydrins from glycerol," *Industrial & Engineering Chemistry Research,* vol. 53, no. 22, pp. 8939-8962, 2014.

[31] F. Ullmann, W. Gerhartz, Y. Yamamoto, F. Campbell, R. Pfefferkorn and J. Rounsaville, Ullmann's Encyclopedia of Industrial Chemistry, New Jersey: VCH, 1995.

[32] P. T. Anastas and J. C. Warner, Green chemistry: Theory and practice, New York: Oxford University Press, 1998.

[33] L. Ma, J. Zhu, X. Yuan and Q. Yue, "Synthesis of epichlorohydrin from dichloropropanols: Kinetic aspects of the process," *Chemical Engineering Research and Design,* vol. 85, no. 12, pp. 1580-1585, 2007.

[34] S. Carrà, E. Santacesaria, M. Morbidelli, P. Schwarz and C. Divo, "Synthesis of epichlorohydrin by elimination of hydrogen chloride from chlorohydrins. 2. Simulation of the reaction unit," *Industrial & Engineering Chemistry Process Design and Development,* vol. 18, no. 3, pp. 428-433, 1979.

[35] R. Tesser, E. Santacesaria, M. Di Serio, G. Di Nuzzi and V. Fiandra, "Kinetics of Glycerol Chlorination with Hydrochloric Acid: A New Route to alfa,gamma-Dichlorohydrin," *Industrial & Engineering Chemistry Research,* vol. 46, no. 20, pp. 6456-6465, 2007.

[36] C. A. de Araujo Filho, T. Salmi, A. Bernas and J.-P. Mikkola, "Kinetic model for homogeneously catalyzed halogenation of glycerol," *Industrial & Engineering Chemistry Research,* vol. 52, no. 4, pp. 1523-1530, 2013.

[37] C. A. de Araujo Filho, K. Eränen, J.-P. Mikkola and T. Salmi, "A comprehensive study on the kinetics, mass transfer and reaction engineering aspects of solvent-free glycerol hydrochlorination," *Chemical Engineering Science,* vol. 120, pp. 88-104, 2014.

[38] T. H. Rider and A. J. Hill, "Studies of glycidol I. Preparation from glycerol monochlorohydrin," *Journal of the American Chemical Society,* vol. 52, no. 4, pp. 1521-1527, 1930.

[39] E. Britton and H. Slagh, "Glycerol dichlorohydrin". US Patent 2,198,600, 30 April 1940.

[40] J. B. Conant and O. R. Quayle, "Glycerol alfa-gamma-dichlorohydrin," *Organic Synthesis,* vol. 1, p. 292, 1941.

[41] J. Conant and O. R. Quayle, "Glycerol alfa-monochlorohydrin," *Organic Synthesis,* vol. 1, p. 294, 1941.

[42] R. Vitiello, V. Russo, R. Turco, R. Tesser, M. D. Serio and E. Santacesaria, "Glycerol chlorination in a gas-liquid semibatch reactor: New catalysts for chlorohydrin production," *Chinese Journal of Catalysis ,* vol. 35, no. 5, pp. 663-669, 2014.

[43] R. Tesser, M. Di Serio, R. Vitiello, V. Russo, E. Ranieri, E. Speranza and E. Santacesaria, "Glycerol Chlorination in Gas-Liquid Semibatch Reactor: An Alternative Route for Chlorohydrins Production," *Industrial & Engineering Chemistry Research,* vol. 51, no. 26, pp. 8768-8776, 2011.

[44] S. H. Lee, D. R. Park, H. Kim, J. Lee, J. C. Jung, S. Y. Woo, W. S. Song, M. S. Kwon and I. K. Song, "Direct preparation of dichloropropanol (DCP) from glycerol using heteropolyacid (HPA) catalysts: A catalyst screen study," *Catalysis Communications,* vol. 9, no. 9, pp. 1920-1923, 2008.

[45] L. Carius, "Über die Sulfide der Alkoholradicale.," *Justus Liebigs Annalen der Chemie,* vol. 122, no. 1, pp. 71-77, 1862.

[46] Z.-H. Luo, X.-Z. You and H.-R. Li, "Direct Preparation Kinetics of 1,3-Dichloro-2-propanol from Glycerol Using Acetic Acid Catalyst," *Industrial & Engineering Chemistry Research,* vol. 48, no. 1, pp. 446-452, 2009.

[47] Z.-H. Luo, X.-Z. You and H.-R. Li, "A kinetic model for glycerol chlorination in the presence of acetic acid catalyst," *Korean Journal of Chemical Engineering,* vol. 27, no. 1, pp. 66-72, 2010.

[48] S. H. Lee, S. H. Song, D. R. Park, J. C. Jung, J. H. Song, S. Y. Woo, W. S. Song, M. S. Kwon and I. K. Song, "Solvent-free direct preparation of dichloropropanol from glycerol and hydrochloric acid gas in the presence of H3PMo12-xWxO40 catalyst and/or water absorbent," *Catalysis Communications,* vol. 10, no. 2, pp. 160-164, 2008.

[49] S. Dmitriev and N. Zanaveskin, "Synthesis of epichlorohydrin from glycerol. Hydrochlorination of glycerol," *Chemical Engineering Transactions,* vol. 24, pp. 43-48, 2011.

[50] E. C. Britton and R. L. Heindel, "Preparation of glycerol dichlorohydrin". US Patent 2,144,162, 24 January 1939.

[51] W. Gerrard, Solubility of Gases and Liquids: A Graphic Approach, New York: Plenum Press, 1976.

[52] E. D. Hughes, "Mechanism and kinetics of substitution at a saturated carbon atom," *Transactions of Faraday Society,* vol. 37, pp. 603-631, 1941.

[53] E. D. Hughes and C. K. Ingold, "Mechanism of substitution at a saturated carbon atom. Part IV. A discussion of constitutional and solvent effects on the mechanism, kinetics, velocity and orientation of substitution," *Journal of Chemical Society ,* pp. 244-255, 1935.

[54] J. Lehtonen, T. Salmi, T. Harju, K. Immonen, E. Paatero and P. Nyholm, "Dynamic modelling of simultaneous reaction and distillation in a semibatch reactor system," *Chemical Engineering Science,* vol. 53, no. 1, pp. 113-121, 1998.

[55] T. Salmi, E. Paatero, J. Lehtonen, P. Nyholm, T. Harju, K. Immonen and H. Haario, "Polyesterification kinetics of complex mixtures in semibatch reactors," *Chemical Engineering Science,* vol. 56, no. 4, pp. 1293-1298, 2001.

[56] D. Y. Murzin and T. Salmi, Catalytic Kinetics, Amsterdam: Elsevier, 2005.

[57] L. Arnaut, S. Formosinho and H. Burrows, Chemical Kinetics: From Molecular Structure to Chemical Reactivity, Amsterdam: Elsevier Science, 2006.

[58] M. Smith and J. March, March's Advanced Organic Chemistry: Reactions, Mechanisms, and Structure, New Jersey: Wiley, 2001.

[59] T. Salmi, J.-P. Mikkola and J. Wärnå, Chemical Reaction Engineering and Reactor Technology, Boca Raton: Taylor & Francis, 2011.

[60] H. Haario, MODEST - User's Guide, Helsinki: Profmath Oy, 2007.

[61] E. Huntress, The Preparation, Properties, Chemical Behavior and Identification of Organic Chlorine Compounds: Tables of Data on Selected Compounds of Order III., New York: J. Wiley, 1948.

[62] C. Yaws, Chemical Properties Handbook: Physical, Thermodynamics, Environmental Transport, Safety & Health Related Properties for Organic & Inorganic chemicals, New York: McGraw-Hill Education, 1999.

[63] R. Reid, J. Prausnitz and T. Sherwood, The properties of gases and liquids, New York: McGraw-Hill, 1977.

[64] D. Murzin, Engineering Catalysis, Göttingen: De Gruyter, 2013.

[65] P. Fogg and W. Gerrard, Solubility of Gases in Liquids: A Critical Evaluation of Gas/Liquid Systems in Theory and Practice, Chichester: John Wiley & Sons, 1991.

[66] D. Green and R. Perry, Perry's Chemical Engineers' Handbook, Eighth Edition, New York: McGraw-Hill Education, 2007.

[67] W. Gerrard and E. MacKlen, "Solubility of hydrogen halides in organic compounds containing oxygen. I. Solubility of hydrogen chloride in alcohols, carboxylic acids and esters," *Journal of Applied Chemistry,* vol. 6, no. 6, pp. 241-244, 1956.

[68] W. Gerrard, A. M. A. Mincer and P. L. Wyvill, "Solubility of hydrogen halides in organic compounds containing oxygen. III. Solubility of hydrogen chloride in alcohols and certain esters at low temperatures," *Journal of Applied Chemistry,* vol. 9, no. 2, pp. 89-93, 1959.

[69] G. J. Janz and S. S. Danyluk, "Conductances of Hydrogen Halides in Anhydrous Polar Organic Solvents.," *Chemical Reviews,* vol. 60, no. 2, pp. 209-234, 1960.

[70] P. Ballinger and F. A. Long, "Acid ionization constants of alcohols. II. Acidities of some substituted methanols and related compounds," *Journal of the American Chemical Society,* vol. 82, no. 4, pp. 795-798, 1959.

[71] D. van Velzen, R. L. Cardozo and H. Langenkamp, "A Liquid Viscosity-Temperature-Chemical Constitution Relation for Organic Compounds," *Industrial & Engineering Chemistry Fundamentals,* vol. 11, no. 1, pp. 20-25, 1972.

[72] C. Reichardt and T. Welton, Solvents and Solvent Effects in Organic Chemistry, Weinheim: Wiley-VCH, 2006.

[73] E. S. Amis, Solvent effects on reaction rates and mechanisms, New York: Academic Press, 1966.

[74] C. I. Ferreira, "Vertical tubular absorbers for ammonia-salt absorption refrigeration," Doctoral Thesis, 1985.

[75] J. Fernández-Seara, J. Sieres, C. Rodríguez and M. Vázquez, "Ammonia--water absorption in vertical tubular absorbers," *International Journal of Thermal Sciences,* vol. 44, no. 3, pp. 277-288, 2005.

[76] Y. Taitel, D. Bornea and A. Dukler, "Modelling flow pattern transitions for steady upward gas-liquid flow in vertical tubes," *AIChE Journal,* vol. 26, no. 3, pp. 345-354, 1980.

[77] J. Rennie and W. Smith, "A photographyc study of the formation and properties of large gas bubbles and their brake down into froths," in *A.I.Ch.E.-I.Ch.E. Joint Meeting*, London, 1965.

[78] P. Calderbank, M. Moo-Young and R. Bibby, "Coalescence in bubble reactors and absorbers," in *Proc. Third European Symposium on Chemical Reaction Engineering*, 1964.

[79] F. H. H. Valentin, Absorption in gas-liquid dispersions: some aspects of bubble technology, London: Spon, 1967.

[80] O. Levenspiel, Chemical Reaction Engineering, New York: Wiley, 1999.

[81] G. F. Froment , K. B. Bischoff and J. de Wilde, Chemical reactor analysis and design, Hoboken: Wiley, 2011.

[82] S. H. Eissa and K. Schügerl, "Holdup and backmixing investigations in cocurrent and countercurrent bubble columns," *Chemical Engineering Science,* vol. 30, no. 10, pp. 1251-1256, 1975.

[83] J. Zahradník, M. Fialová, M. Růžička, J. Drahoš, F. Kaštánek and H. N. Thomas, "Duality of the gas-liquid flow regimes in bubble column reactors," *Chemical Engineering Science,* vol. 52, no. 21-22, pp. 3811-3826, 1997.

[84] J. C. Charpentier, "What's new in absorption with chemical reaction?," *Transactions Review Paper,* vol. 60, pp. 131-156, 1982.

[85] P. V. Danckwerts, "Continuous Flow Systems: Distribution of residence times," *Chemical Engineering Science ,* vol. 2, no. 1, pp. 1-13, 1953.

[86] J. H. Lee and N. R. Foster, "Measurement of gas-liquid mass transfer in multi-phase reactors," *Applied Catalysis ,* vol. 63, pp. 1-36, 1990.

[87] N. Kantarci, F. Borak and K. O. Ulgen, "Bubble column reactors," *Process Biochemistry,* vol. 40, pp. 2263-2283, 2005.

[88] C. P. Ribeiro Jr. and D. Mewes, "The influence of electrolytes on gas hold-up and regime transition in bubble columns," *Chemical Engineering Science,* vol. 62, pp. 4501-4509, 2007.

[89] G. Grund, A. Schumpe and W.-D. Deckwer, "Gas-liquid mass transfer in a bubble column with organic liquids," *Chemical Engineering Science,* vol. 47, pp. 3509-3516, 1992.

[90] L. A. Oshin, Y. A. Treger, G. V. Motsarev, E. V. Sonin, E. V. Sergeev, M. B. Skibinskaya and E. A. Golfand, Organochloride Industrial Products (in Russian), Moscow: Chemistry, 1978.

ISBN 978-952-12-3369-2
Painosalama Oy – Turku, Finland 2016